2015

Depletion of the Chromatin Remodeler CHD4 Sensitizes AML Blasts to Genotoxic Agents and Reduces Tumor Formation

Justin Sperlazza
sperlazzajr@vcu.edu

Depletion of the Chromatin Remodeler CHD4 Sensitizes AML Blasts to Genotoxic Agents and Reduces Tumor Formation

A dissertation submitted in partial fulfillment of the requirements for the degree of Doctor of Philosophy at Virginia Commonwealth University.

by

Justin Robert Sperlazza
Bachelor of Science, University of North Carolina, Chapel Hill, NC. 2009

Advisor: Gordon D. Ginder, M.D.
Director of Massey Cancer Center
Professor of Internal Medicine, Human and Molecular Genetics,
Microbiology and Immunology

Virginia Commonwealth University
Richmond, Virginia
October 12, 2015

Acknowledgements

I would like to recognize several people for their support, knowledge, and friendship that made this work possible.

First and foremost, I would like to thank my advisor Dr. Gordon Ginder for being an exceptional mentor. Thank you for supporting me throughout this entire project, especially as it twisted and turned outside of the expertise of our lab. Thank you for always providing a guiding hand in righting the ship when experiments went astray. Finally, thank you for being an exceptional role model, whom I respect and look up to as physician scientist.

This work would also not have been possible without the full support of the Massey Cancer Center. Thank you to all of the other researchers who lent their time and expertise, especially Drs. Steven Grant, Mohamed Rahmani, Kristoffer Valerie, Catherine Dumur, and Richard Moran. Without your unique perspectives, we would not have been able to make a complete story out of our observations. Additionally, a HUGE thank you to all of the research support staff that provided the technical expertise to make our experiments possible, especially Shou Zhen Wang, Sheng Zu Zhu, Mandy Aust, Elisa Hawkings, and Julie Farnsworth.

Thank you to my advisory committee of Drs. Joyce Lloyd, Shirley Taylor, Joseph Landry, and David Williams. Additionally, I am extremely grateful to Dr. Gordon Archer and the MD/PhD program.

During my time here at VCU, I have had the privilege to work with an exceptional group of people. Thank you to my lab mates Maria Amaya and Megha Desai for your experience and friendship. Thank you to my fellow MD/PhD students, especially Jason Beckta, Asim Alam, Matthew Baer, Junghoon Ha, and Mohammed Mamdani. A special thank you to Mike Greer for always being a great friend.

Finally, I need to express my gratitude for the many friends and family who have offered me inspiration and encouragement. In particular, I would like to recognize my parents and siblings, Jeremy, Sabrina, and Alyssa. Lastly, I thank my wife, Jet, who consistently shared in both my successes and failures. You are my source of inspiration and with your enduring support, this work was possible.

Table of Contents

Abbreviations

5mC	5-methylCytosine
7AAD	7-AminoActinomycin D
AML	Acute Myeloid Leukemia
ara-C	Cytarabine
ATM	Ataxia Telangiectasia Mutated
CD	ChromoDomain
CHD4	Chromodomain Helicase DNA-binding protein 4
Chk2	Checkpoint kinase 2
CLP	Common Lymphoid Progenitor
CMP	Common Myeloid Progenitor
CpG	Cytosine-Guanine Dinucleotide
CR	Complete Remission
DNR	Daunorubicin
DSB	DNA Double Stranded Break
FDR	False Discovery Rate
GMP	Granulocyte-Macrophage Progenitors
HAT	Histone Acetyl-Transferases
HDAC	Histone Deacetylases
HR	Homologous Recombination
HSC	Hematopoietic Stem Cell
IPA	Ingenuity Pathway Analysis
MBD	Methyl CpG Binding Domain
MEP	Megakaryocyte-Erythroid Progenitors
MPP	Multipotent Progenitor
NFR	Nucleosome Free Region
NHEJ	Non-Homologous End Joining
NMR	Nuclear magnetic resonance
NuRD	Nucleosome Remodeling and Deacetylase
PARP	Poly ADP Ribose Polymerase
PHD	Plant HomeoDomain
PI	Propidium Iodide
PTM	Post-Translational covalent Modifications
SAHA	Suberanilohydroxamic Acid
shRNA	short hairpin RNA
TIC	Tumor-Initiating Cells
TSS	Transcription Start Site

Abstract

Chromodomain Helicase DNA-Binding Protein 4 (CHD4) is an ATPase that alters the phasing of nucleosomes on DNA and has recently been implicated in DNA double stranded break (DSB) repair. Here, we show that depletion of CHD4 in Acute Myeloid Leukemia (AML) blasts induces a global relaxation of chromatin that renders cells more susceptible to DSB formation, while concurrently impeding their repair. Furthermore, CHD4 depletion renders AML blasts more sensitive both *in vitro* and *in vivo* to genotoxic agents used in clinical therapy: daunorubicin (DNR) and cytarabine (ara-C). Sensitization to DNR and ara-C is mediated in part by activation of the ATM pathway, which is preliminarily activated by a Tip60-dependent mechanism in response to chromatin relaxation and further activated by genotoxic-agent induced DSBs. This sensitization preferentially affects AML cells, as CHD4 depletion in normal $CD34^+$ hematopoetic progenitors does not increase their susceptibility to DNR or ara-C. Unexpectedly, we found that CHD4 is necessary for maintaining the tumor formatting behavior of AML cells, as CHD4 depletion severely restricted the ability of AML cells to form xenografts in mice and colonies in soft agar. Taken together, these results provide evidence for CHD4 as a novel therapeutic target whose inhibition has the potential to enhance the effectiveness of genotoxic agents used in AML therapy.

Chapter 1: Introduction

Part 1: Background

Hematopoiesis

Blood is among the most highly regenerative tissues in the human body, with an average adult generating approximately one trillion ($1x10^{12}$) new cells in the bone marrow each day. At the core of this regenerative capacity is a common hematopoietic stem cell (HSC). In humans, HSCs are extremely rare, an estimated 1 in 10^6 cells in the bone marrow, and often reside in a quiescent state, doubling an estimated once every 175-300 days.[1] These cells are defined by their unique ability for self-renewal and capacity to differentiate into all of the mature blood cell types. During self-renewal, the HSCs replicate and create additional identical daughter HSCs. Conversely, HSCs can differentiate to give rise to a complex cellular hierarchy of progenitor intermediates that become increasingly more restricted in their fated lineages and ultimately assume mature blood cell identities.

Once committed to differentiation, a human HSC first becomes a multipotent progenitor (MPP). MPPs are similar to HSCs in that they are capable of differentiating into any mature blood cell, but differ in that they are not capable of self-renewal.[2] Upon further differentiation, MPPs experience the first major lineage commitment: the myelo-lymphoid split. An MPP can differentiate into either a Common Myeloid Progenitor (CMP), which is committed to a myeloid lineage, or a Common Lymphoid Progenitor (CLP). CMPs undergo further commitments to become either Granulocyte-Macrophage Progenitors (GMPs) which give rise to basophils, eosinophils, monocytes, and neutrophils, or megakaryocyte-erythroid progenitors (MEPs) which give rise to megakaryocytes and erythrocytes. CLPs also undergo further commitments to give rise to T, B, and NK-cells.

The balance between self-renewal and differentiation is tightly regulated in order to maintain self-sustainable pools of HSCs and adequate production of mature blood cells. At the molecular level, this balance is driven largely by gene expression alterations of transcription factors induced by epigenetic changes in gene regulatory regions of the genome. For instance, increasing the expression of the transcription factors HoxB4, Bmi1, HLF, and HES1 have been shown to tilt the balance towards self-renewal and expands the pool of HSCs[1]. Conversely, upregulation of MYC and IKZF1 are associated with increasing the differentiation of HSCs into MPPs.[3] Disruptions in the balance between self-renewal and differentiation are associated with hematopoietic failure and leukemic transformation.

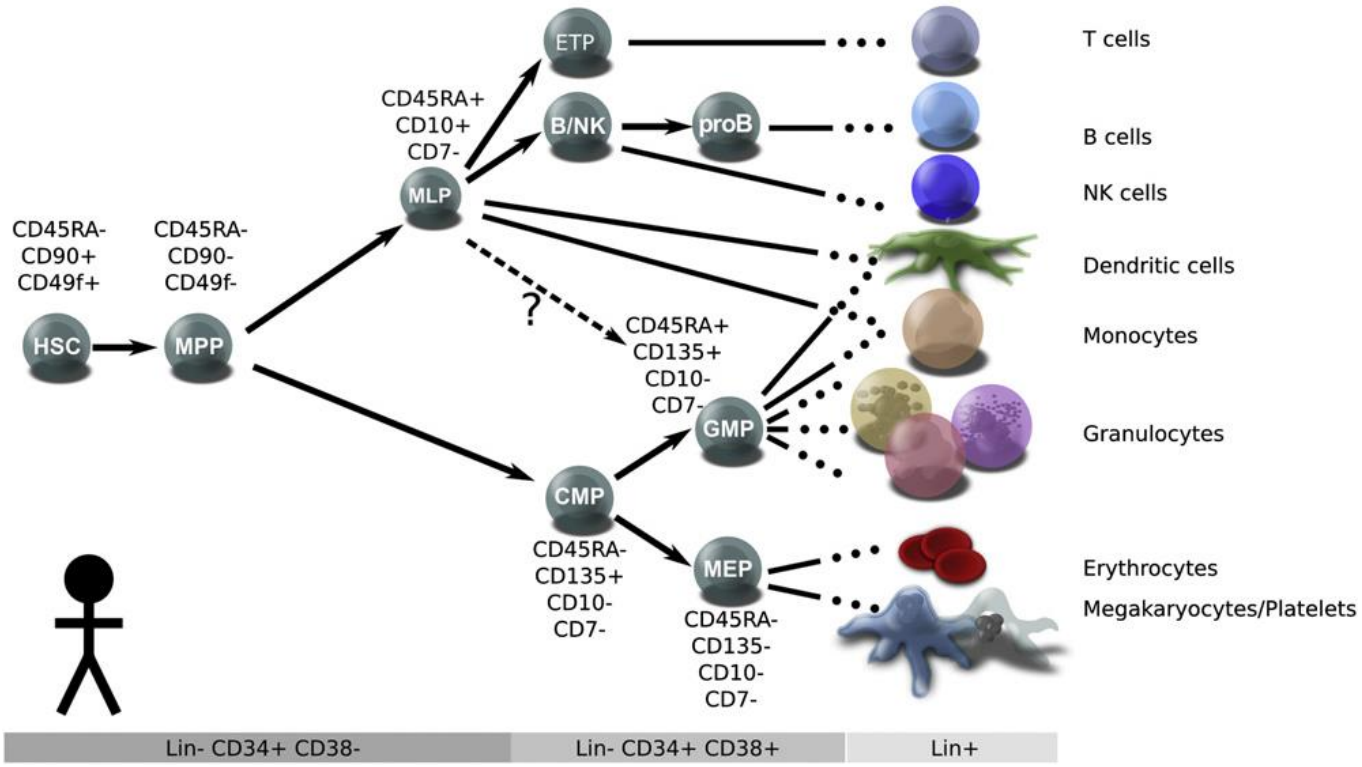

Figure 1. Current Model of Human Hematopoiesis. Model illustrating the differentiation of hematopoietic stem cells (HSC) into terminally differentiated blood cells. Note that the first major lineage commitment occurs at the multipotent progenitor (MPP), at which point the cells become committed to a myeloid or lymphoid lineage. Image used with license from Doulatov et al. *Cell Stem Cell* (2012)

Acute Myeloid Leukemia

Acute Myeloid Leukemia (AML) is a malignancy that arises when myeloid committed progenitors acquire oncogenic mutations that impede their normal differentiation. Unable to properly differentiate, these immature myeloid progenitors, termed blasts, clonally proliferate within the marrow and suppress the function of the other normal HSCs and progenitors, thus leading to complications associated with bone marrow failure, including: anemia, thrombocytopenia, and neutropenia. Although AML can occur at any age, this is typically a disease of older people, with a median age of diagnosis of 67. In 2015, it is estimated that 21,000 new diagnoses of AML will be made and an estimated 10,500 will die of the disease. Due to low remission and high relapse rates in older patients and those with complex tumor genotypes, the over-all 5 year survival is only 24%.[4]

By comparison to other malignancies, AML cells harbor relatively few genetic abnormalities (Fig 2). A recent study of 200 patients with de novo AML identified an average of 13 coding mutations in each genome, of which only 5 were recurrently mutated in AML. This study identified at least one potential driver mutation in nearly every AML sample with mutations commonly occurring in signaling genes (59% of cases), DNA-methylation related genes (44%), chromatin-modifying genes (30%), the gene NPM1 (27%), myeloid transcription-factor genes (22%), transcription-factor fusions (18%), tumor-suppressor genes (16%), spliceosome-complex genes (14%), and cohesion-complex genes (13%). The individual genes most commonly found to be mutated included: FLT3 (28%), NPM1 (27%), DNMT3A (26%), IDH1 or IDH2 (20%), NRAS or KRAS (12%), RUNX1 (10%), TET2 (8%), and TP53 (8%).[5]

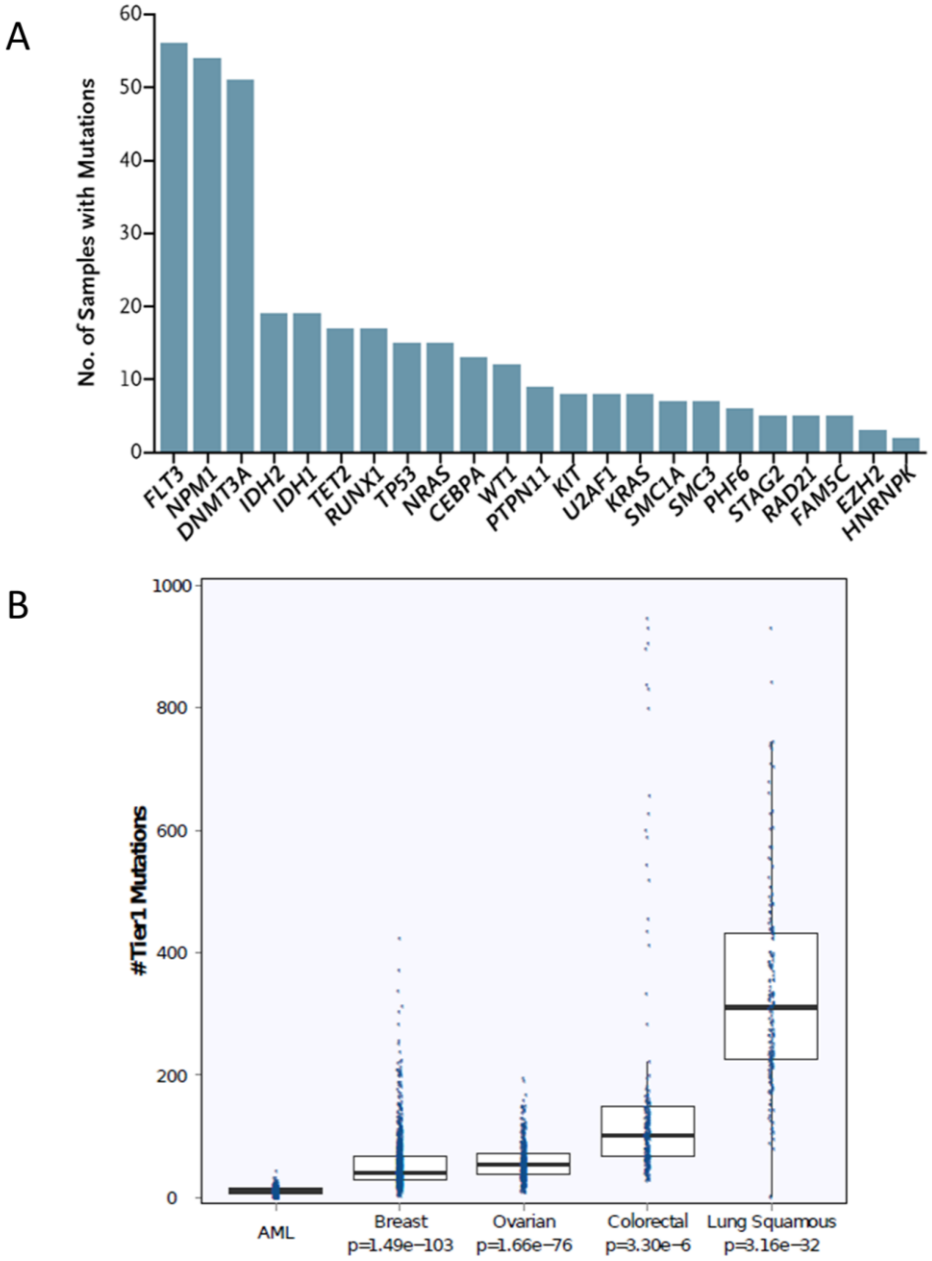

Figure 2. Genetics of AML. (A) Significantly mutated genes found in an analysis of 200 *de novo* AML patients. (B) Comparison of tier 1 (coding) mutations found in 5 tumor types published in The Cancer Genome Atlas. Note that AML has significantly less coding mutations than any of the other cancer types analyzed. Images are reproduced with permission from Cancer Genome Atlas Research Network *N. Engl. J. Med.* (2013), Copyright Massachusetts Medical Society

Management of AML

Current AML management begins with an initial course of highly intensive chemotherapy to induce a complete clinical remission. This so called "remission induction therapy" generally consists of cytarabine (ara-C), supplemented with an anthracycline, such as daunorubicin (DNR). Combined DNR/ara-C regimens are highly toxic, primarily to the hematopoietic and gastrointestinal systems, but effective, achieving complete remission (CR) rates of approximately 53-58%.[6] Despite numerous attempts at improvement, this combination therapy has been relatively unchanged since its inception in the mid-1980s;[6] however, a recent set of trials suggest that increasing the DNR dose may yield tangible benefits to the CR rates and survival of a subset of patients.[7,8] It should be noted, however, that the maximum lifetime dose of any anthracycline, including DNR, is severely limited by a cumulative, dose-dependent cardiotoxicity.[9] Thus, strategies for further improvement based on additional increases to the dose of DNR are not viable.

Once a CR is achieved, additional post-remission therapy is needed to maintain the remission since nearly every patient will relapse within a median of four to eight months without additional therapy.[10] This second round of therapy is targeted at the blasts that survived the initial induction therapy, but are undetectable by standard clinical tests. These post-remission therapies consist mainly of either additional high dose cytarabine or hematopoietic cell transplantation (autologous or allogeneic).

Approximately 10-40% of patients present with primary refractory disease, meaning that they are unable to achieve a CR with 1-2 rounds of standard induction therapy.[11] Additionally, the majority of patients who achieve a CR will recur within 3 years of diagnosis.[12] Both patients with primary refractory and relapsed disease have

significantly poorer prognoses and are best treated with an allogeneic hematopoietic cell transplant. Prior to transplant, these patients are often treated with additional chemotherapy to reduce the tumor burden. Regimens containing various combinations of anthracyclines and high-dose ara-C form the foundation of these salvage therapies, including ICE (idarabucin, high-dose cytarabine, etoposide) and FLAG-IDA (fludarabine, high-dose cytabine, idarubicin, granulocyte colony-stimulating factor) .[13,14]

Thus, in the clinical management of AML, combinations of anthracyclines and cytarabine form the core of chemotherapy regiments utilized in induction, consolidation, and salvage therapies.

DNA damage and repair

The anthracycline DNR is a topoisomerase inhibitor that induces DNA double-stranded breaks (DSB), which are highly cytotoxic.[15] Similarly, the nucleoside analog ara-C also induces DNA damage, including DSBs, during DNA synthesis through inhibition of DNA polymerase and incorporation into DNA.[16,17] Both normal and leukemic cells can evade cell death following chemotherapy-induced DSBs by repairing damage through numerous repair mechanisms, including homologous recombination (HR) or non-homologous end joining (NHEJ). However, malignant cells tend to be more susceptible to DSB insults due to their rapid proliferation, deregulated cell cycle checkpoints, and inactive DNA repair machinery.[18] For HR, DSBs are first identified by the human single-stranded binding protein 1 (hSSB1), which recruits MRN (Mre-11-Rad50-NBS1) complex. The MRN complex resects the ends of the DNA and then recruits and activates the Ataxia telangiectasia mutated (ATM) protein. The ATM kinase begins a complex cell-signaling cascade that

results in the triggering of cell-cycle checkpoints, phosphorylation of downstream targets, and in some cases apoptosis. Final repair of the DNA is mediated by the DNA recombinase Rad51, which allows for the strand invasion of the sister chromatid. In NHEJ, the Ku60/70 heterodimer binds to the DSB and recruits DNA-PKcs. The DNA-PKcs regulate processing of the DNA ends such that the DNA ligase IV-XRCC4-XLF complex can physically rejoin the ends.[18]

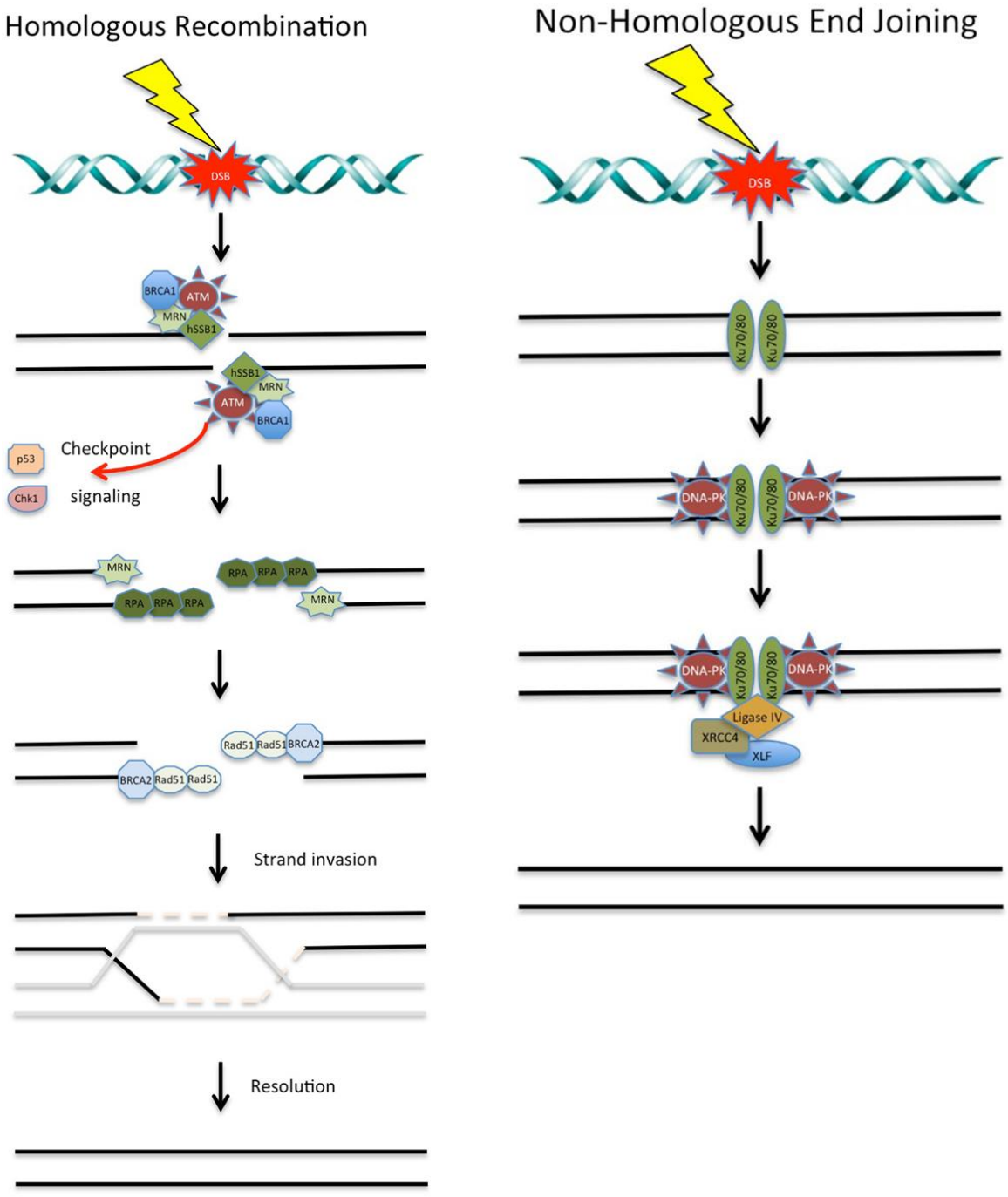

Figure 3. DSB Repair. (A) Schematic of Homologous Recombination. (B) Schematic of Non-Homologous End Joining. Image adapted with permission from Jekimovs et al. *Font. Oncol.* (2014).

Part 2. Epigenetics

Overview

Although every cell within an organism contains exactly the same genomic DNA sequence, multicellular organisms are comprised of numerous distinct cell types and tissues that perform a variety of specialized functions and contain substantially different gene expression profiles that are maintained in each somatic tissue. Epigenetics, officially defined as the heritable changes in genome function that occur without alterations to the DNA sequence,[19,20] provides numerous mechanisms to account for this broad diversity, including: DNA methylation, small interfering RNAs, histone variants, histone post-translational modifications, chromatin remodeling, and nucleosome positioning.

Chromatin

In eukaryotes, genomic DNA is organized into highly complex and dynamic structures termed chromatin. This organization allows the DNA, all 1.8 linear meters, to be packaged into a more compact form in order to fit into each cell nucleus and protects the DNA from damage. The nucleosome is the most basic unit of chromatin, comprised of 145-147 base pairs of DNA wrapped around a histone octamer core, which itself is comprised of two copies of the histone proteins H2A, H2B, H3, and H4. Each nucleosome is linked to its adjacent nucleosome by short DNA linker to form nucleosome arrays. Short range interactions between arrays provide further organization to create 30nm fibers, which in turn are then capable of organizing into higher-order structures.[21]

Local chromatin structures inhibit access to the underlying DNA and hence have profound effects on almost all DNA-related processes.[22] In terms of transcription,

nucleosomes form a strong barrier to transcription factor binding and Pol II transcription initiation. Thus, sites of active transcription tend to occur within regions of chromatin that are less condensed, termed euchromatin, and DNA sites that are refectory to transcription initiation tend to occur within regions of chromatin that are more compact, termed heterochromatin. Similarly, the chromatin structure surrounding DNA damage has emerged as a key determinant of the kinetics and mechanism of repair since the compact nature of chromatin within regions of heterochromatin impairs the activation of the DNA repair machinery.[23–26] Therefore, enzymes capable of altering local chromatin environments can have large impacts on transcription, recombination, DNA repair, and replication.[19,27–30]

DNA Methylation

The most prominent epigenetic mark is the methylation of the 5th position carbon in cytosines (5mC) found in cytosine-guanine (CpG) dinucleotides, with approximately 4% of all cytosines in the human genome being methylated.[31] Importantly, DNA methylation is a stable source of epigenetic information, as it is heritably maintained during replication. This heritability is attributed to the preference of methylation to occur symmetrically over a CpG dinucleotide, meaning that both strands of DNA contain the methylation mark. Following DNA replication, daughter strands of DNA are hemimethylated at CpGs, where the enzyme DNA (Cytosine-5)-Methyltransferase 1 (DNMT 1) methylates the nascent strands. However, DNA methylation is not an entirely static epigenetic mark, as new methylation patterns can be established by the DNMT3 class of enzymes during development and differentiation.

The distribution of CpG dinucleotides is not homogenous throughout the genome; rather, they tend to cluster into small regions of DNA, termed "CpG islands", generally found within the promoters at 5' regulatory regions of genes.[32] An estimated 60% of genes transcribed by RNA polymerase II contain CpG islands within their promoter.[33] In normal cells, 80 percent of CpGs found outside of CpG islands are heavily methylated; however, the majority found within CpG islands are unmethylated, especially if the island is within a gene's promoter region.[20] Methylation of gene promotor CpG islands is classically considered to be incompatible with active transcription, as 5mC itself can prevent the binding of transcription factors or act as a docking site for co-repressor complexes.[31,34] In contrast, certain CpG islands are regularly methylated and are utilized for the transcriptional silencing associated with gene imprinting, X-chromosome inactivation, and repetitive elements.[35]

Histones

The histones are a family of highly basic proteins that, as previously mentioned, form the core of the nucleosome. In terms of epigenetics, these proteins are interesting because some (H3 and H4) contain basic N-terminal "tails" that protrude from the nucleosome and are prone to a wide variety of post-translational covalent modifications (PTMs), including: methylation, acetylation, phosphorylation, and ubiquination. These PTMs are hypothesized to create a "histone code" that is readable by other proteins to bring about specific down-stream events, including the regulation of gene expression.[36] This histone code is highly dynamic, with numerous enzymes capable of adding new modifications ("writers") and removing modifications ("erasers").[37]

Acetylation of the lysine residues on histones was the first identified PTM.[38] This process is highly dynamic and regulated by two opposing classes of enzymes, the Histone Acetyl-Transferases (HATs) and the Histone Deacetylases (HDACs). There are numerous lysines on the histones that have the potential to be acetylated, including: Histone H3 Lysine 9 (H3K9), H3K14, H3K18, H4K5, H4K8, H4K12, and H4K16. Acetylation of the lysine residues is thought to reduce the effective positive charge of the histones, thereby loosening the electrostatic interaction between the histone and the DNA in order to grant other proteins access to the DNA.[37] Thus, histone acetylation is generally associated with euchromatin environments and transcriptionally active regions of the genome.

In contrast to histone acetylation which is always associated with transcriptional activation, histone methylation is more complex and can be associated with transcriptional silencing or activation, depending on the specific residue that is being methylated.[39] Histone methylation occurs on lysine and arginine residues and 1-3 methyl groups can be added to form mono-, di-, or tri-methylation. Since methylation does not alter the electrostatic interaction between the DNA and the histones, the resulting effect of the methylation is directly related to the "reader" protein that is capable of binding to the methylated histone tail. For example, the H3K9me3 mark is bound by HP1, which forms one of the key structural components of repressive heterochromatin. Alternatively, the H3K4me3 mark is associated with actively transcribed chromatin since it is bound by the ING family of proteins, which are themselves associated with HAT proteins.[37]

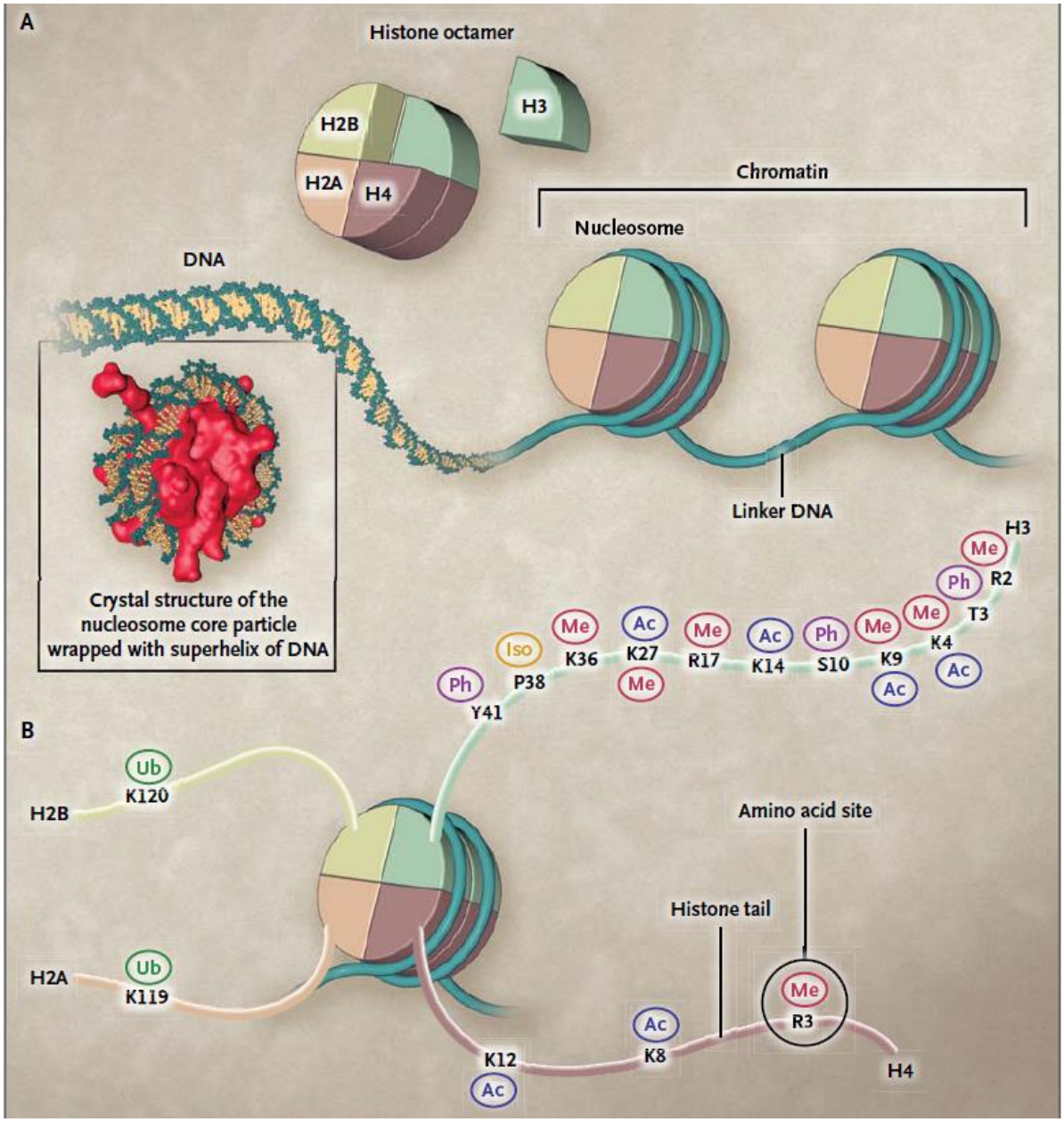

Figure 4. The Nucleosome. (A) The basic unit of chromatin is the nucleosome, which is comprised of a histone octamer wrapped in DNA. (B) The tails of histone proteins are subjected to a variety of post-translational modifications that make up the "histone code". Image is reproduced with permission from Dawson et al. *N. Engl. J. Med.* (2012), Copyright Massachusetts Medical Society.

Epigenetics in Cancer

Classically, cancer has been viewed as a disease that results from the successive accumulation of mutations in tumor suppressor genes and oncogenes, leading to uncontrolled growth and survival. However, epigenetic studies of numerous cancer types are challenging this traditional view by indicating that an intricate interplay exists between classical genetic mutations and aberrant epigenetic mechanisms that induce and promote carcinogenesis.[39]

Since the early 1980s, researchers have known that malignant cells contain abnormal patterns of DNA methylation compared to their normal counterparts.[40] These profiles are characterized by a seemingly paradoxical global hypomethylation of a malignant cell's genome in conjunction with hypermethylation of CpG islands located in gene promoter regions. Hypomethylation of the malignant genome is hypothesized to relax the transcriptional repression of viral genes, repetitive elements, and imprinted genes, all of which are normally silenced through DNA methylation. Additionally, hypomethylation is thought to contribute to the genomic instability in transforming cells, as hypomethylation can promote the formation of deletions, translocations, and chromosomal rearrangements. Interestingly, the degree of hypomethylation of genomic DNA has been found to increase as a tumor progresses from a benign lesion to a malignant cancer.[41] Paradoxically, within the background of global hypomethylation, the CpG islands located within tumor-suppressor genes' promoters tend to be hypermethylated. This abnormal promoter hypermethylation is associated with transcriptional silencing and can provide a mechanism for malignant cells to inactivate tumor-suppressor genes. It is not uncommon for hypermethylation to provide the "second hit" in the Knudson's two-hit model of cancer development, with a

coding-region mutation providing the "first-hit". Classic tumor suppressor genes such as Rb, VHL, $p16^{INK4a}$, hMLH1, and BRCA1 have all been shown to be inactivated by hypermethylation.[42] However, hypermethylation appears to be specific to a cancer type and specific mechanisms to explain why certain genes are hypermethylated in one cancer type, but are not hypermethylated in another type have yet to be elucidated.

In addition to DNA methylation alterations, the epigenetic profiles of cancer cells are characterized by the hypoacetlyation of histones. Hypoacetylation occurs early in the process of transformation and occurs predominantly on H4K16 and H4K20.[43] This hypoacetylation is catalyzed by the Histone Deacetylase (HDAC) class of enzymes, which are often overexpressed in many tumor types.[44–46] Hypoacetylation is thought to work in cooperation with aberrant DNA hypermethylation to repress the transcription of tumor-suppressor genes.

In contrast to genetic mutations, epigenetic changes are readily reversible and have the potential for profound antitumor effects through the re-expression of tumor-suppressor genes. Two classes of epigenetically modulating drugs are currently used in the clinic: DNA-demethylating drugs and HDAC inhibitors. DNA-demethylating drugs such as 5-azacytidine and decitabine are cytosine analogs that have a modified 5-carbon position that are unable to be methylated. These drugs incorporate into a replicating genome and inhibit the DNMT enzymes, thus leading to a loss of methylation and the restored expression of silenced genes. Currently, these drugs are approved for the treatment of myelodysplastic syndrome and leukemia, but their use is greatly limited due to systemic toxicities including myelosuppressoin, potentially due to non-specific effects. HDAC inhibitors have been demonstrated to be effective at inducing differentiation, cell-cycle arrest, and apoptosis in

vitro.[42] In contrast to the DNA demethylating agents, HDAC inhibitors are associated with a lower incidence of severe side-effects. However, the effectiveness of HDAC inhibition appears to be secondary to DNA demethylation, as inhibition of HDACs only restores the expression of genes that do not possess a hypermethylated promoter.[20,47] Given that epigenetics regulate a wide range of genes in malignant cells, targeting the epigenome could produce unintended consequences, such as promoting the growth of tumors. Therefore, recent research has been directed towards targeting more specific transcription factors and machinery involved in the regulation of the epigenome in malignant cells.

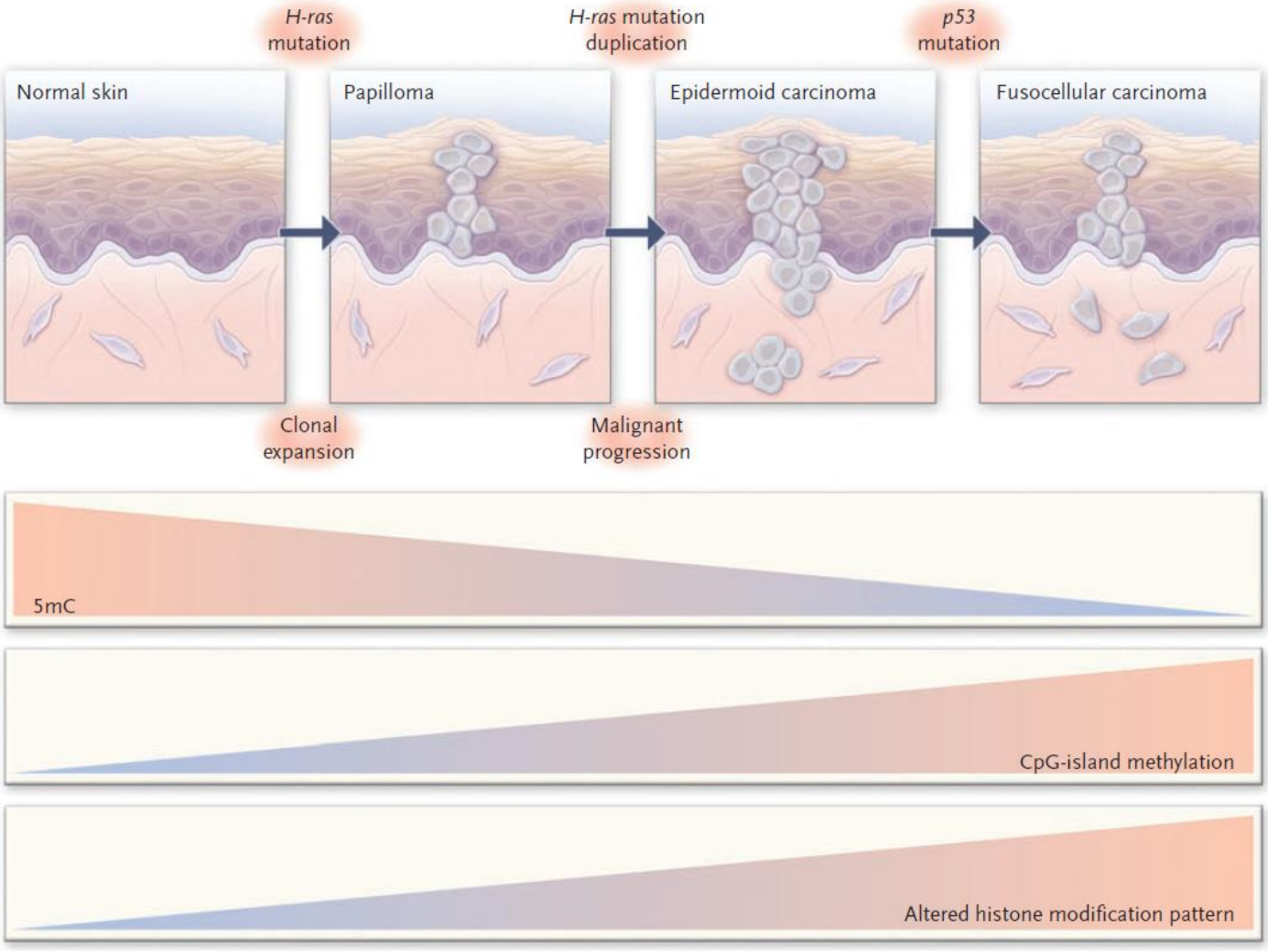

Figure 5. Epigenetic Alterations in Tumor Progression. During the development of a tumor, several changes occur to the epigenetic profile of the transforming cells. First, the net DNA methylation of the cells decreases. Most of this demethylation occurs in the regions of DNA outside of CpG islands. Paradoxically, CpG islands become more methylated as the tumor progresses. Additionally, the histone code becomes more deregulated as the tumor progresses. Image is reproduced with permission from Esteller et al. *N. Engl. J. Med.* (2008), Copyright Massachusetts Medical Society.

Part 3. Methyl-CpG Binding Domain proteins and the Nucleosome Remodeling and Deacetylase Complex

Methyl-CpG Binding Domain proteins

Methylated CpG islands serve as binding targets for the Methyl-CpG-Binding Domain (MBD) family of proteins, which are widely thought to translate the DNA methylation signal into transcriptional silencing through their interactions with chromatin remodeling enzymes.[20,48–51]

These enzymes alter chromatin structure through repositioning, ejecting, or covalently modifying histones or modifying the composition of the nucleosome with substitution of various histone variants.[23] For most genes, the chromatin near the transcription start site (TSS) of a gene is organized in a regular pattern: an unusually large ~140 bp linker region known as the nucleosome free region (NFR) precedes the TSS and is flanked by two well positioned (phased) nucleosomes labeled +1 and -1. This NFR provides various transcription factors access to the DNA and assembly of the transcription machinery.[29] Additionally, the amino-terminal histone 'tails' that protrude past the DNA are subject to covalent modifications as previously mentioned. Modifications to the positioning of nucleosomes surrounding the TSS or to the histone tails regulate the accessibility of the chromatin structure to transcriptional machinery and hence provide a clear mechanism of epigenetic control on gene expression.[20,29]

Members of the MBD family of proteins include MeCP2 and MBD1 through MBD4 and share a common ~60 amino acid methyl-CpG binding fold. Within this MBD family, only MeCP2, MBD1, and MBD2 are capable of repressing transcription of genes with methylated promoters, since they each contain a transcription repression domain that associates with a co-repressor complex.[52,53] MBD2 is unique among the other MBD proteins in that it binds to methylated CpGs with the greatest affinity.[54,55]

The Nucleosome Remodeling and Deacetylase Complex

The Nucleosome Remodeling and Deacetylase (NuRD) complex is an abundant co-repressor complex with a variable subunit composition that comprises of at least one copy of six core proteins: a MBD (MBD2 or MBD3), a retinoblastoma-associated protein (RBBP4 or 7), a Chromodomain Helicase DNA Binding Protein (CHD3, 4, or 5), a p66 (α or β), a histone deacetylase (HDAC 1 or 2), and a metastasis associated protein (MTA 1-3). Traditionally, NuRD has been associated with transcriptional repression.[24] However, given the wide variability in NuRD complex components and the combinatorial assembly of the complex, different NuRD complexes are capable of performing various functions within a cell. For instance, since MBD3 cannot bind to methylated DNA[55], only NuRD complexes containing MBD2 are thought to play a role in methylation-dependent transcriptional silencing. CHD4-containing NuRD complexes have been shown to facilitate DSB DNA repair[56–58], whereas CHD3-containg NuRD complexes have been shown to hinder repair.[59] Only MTA3 containing complexes have been shown to repress the expression of plasma cell-specific genes in germinal centers.[60] Therefore, it is not surprising that NuRD has been implicated in a wide variety of cell functions, including transcription regulation, chromatin assembly, cell cycle progression, and genomic stability.[48]

Among chromatin-remodeling complexes, the NuRD complex is unique since it contains two subunits with enzymatic activity capable of modifying chromatin structure: CHD3/4 and HDAC 1/2. As described below, CHD4 is an ATPase that is capable of rearranging the position of histone octamers[61,62], whereas HDAC 1 and 2 are enzymes capable of deacetylating histone tails.[63] Therefore, NuRD has two enzymatic activities that

promote the formation of heterochromatin and repress transcription. Previous work has shown that depletion of NuRD components alters gene expression in cells. For instance, depletion of MBD2 was shown to re-express methylated tumor suppressor genes in various cancers.[42,49,64–66] Additionally, depletion of CHD4 and MBD2 resulted in the restored expression of methylated fetal ϒ-globin in erythroid lineage cells.[67–69]

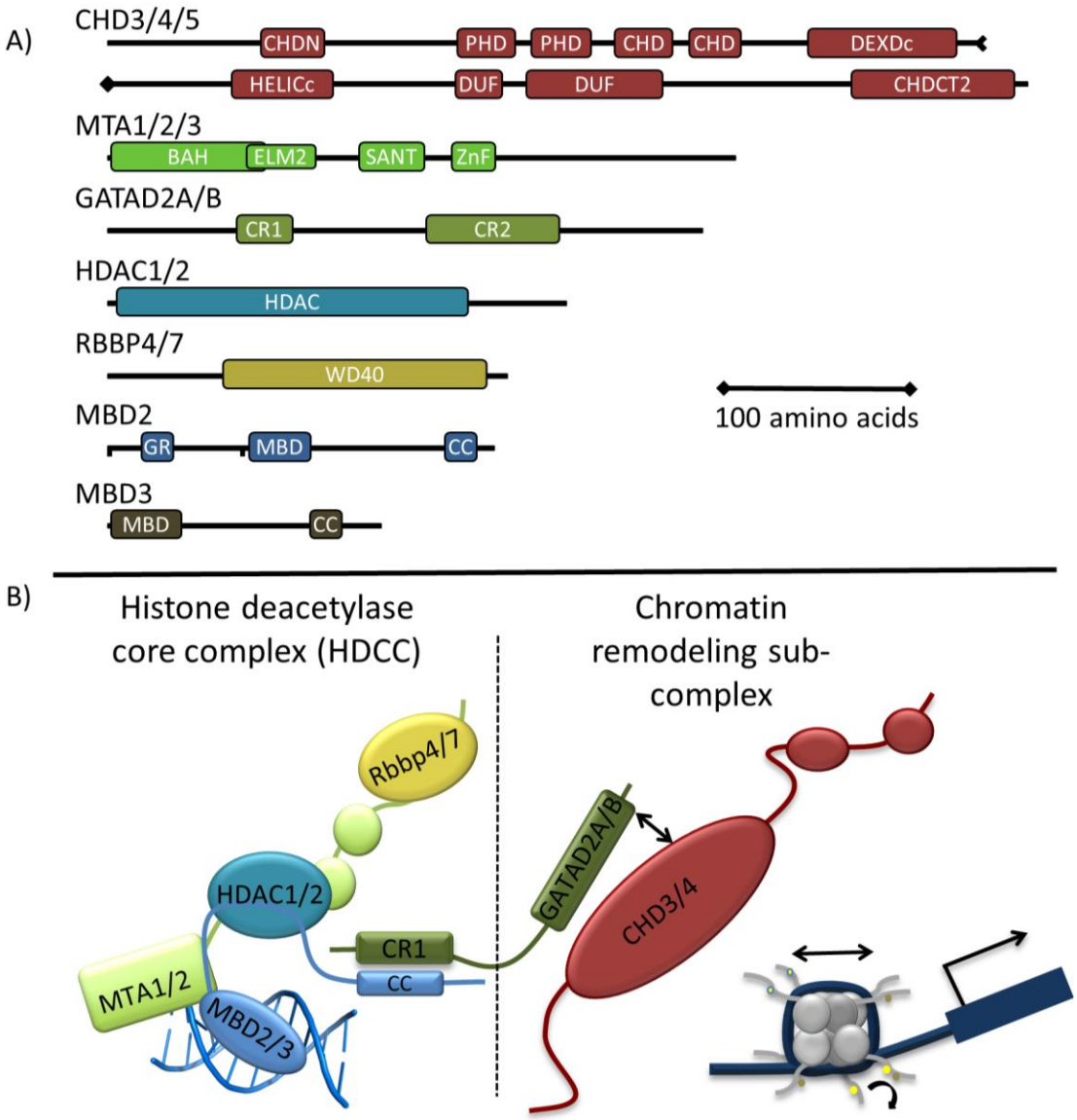

Figure 6. Model of the Nucleosome Remodeling and Deacetylase Complex (NuRD). (A) Diagram of identified domains in NuRD subunits. (B) Current model of the assembly of NuRD. Note that the complex can be split into a HDAC core complex that contains HDAC enzymatic activity and a chromatin remodeling sub-complex that contains the nucleosome repositioning activity. Image courtesy of David Williams.

Chromodomain Helicase DNA Binding Protein 4

Chromodomain Helicase DNA Binding Protein 4 (CHD4) was originally identified as an autoantigen in patients with the connective-tissue disorder dermatomyositis.[48] CHD4 is a widely conserved (among plant and animal kingdoms, but absent in yeast[24]) member of the SNF2 superfamily of chromatin remodeling ATPases that is capable of altering the phasing of nucleosomes on DNA.[70–74] This protein is comprised of several highly-conserved domains (Figure 6A): two tandem plant homeodomain (PHD) fingers, two chromodomains (CDs), a SWI2/SNF2-type ATPase/helicase domain, two domains of unknown function (DUFs), and a C-terminal domain (CTD).[62] The PHD finger domains distinguish CHD3 and CHD4 from the rest of the CHD family and have been shown to bind to the tails of histone H3, with a strong preference for those containing an unmodified or methylated H3K4 modification, but an inability to bind acetylated H3K4.[75] Interestingly, a short ~70Å linker exists in between the tandem PHD domains has been hypothesized to allow both PHD fingers from a single CHD4 protein to bind to both H3 tails in a nucleosome octamer simultaneously.[76] In contrast, the CDs of CHD4 are thought to both bind to DNA[77] and form a large interface with ATPase/helicase domain of CHD4. This interface has been suggested to form a regulatory mechanism for CHD4 enzymatic activity through the CDs sterically blocking access of DNA and ATP to the ATPase/helicase domain until the PHD and CD release the ATPase/helicase domain by binding to histone tails and DNA, respectively.[78] The ATPase/helicase domain, as its name implies, couples the energy from the hydrolysis of ATP to mechanically slide or displace nucleosomes. Given the intricate nature of the regulation of the ATPase/helicase domain, both PHD and both CD domains are required for the function of the enzyme, as an inactivating mutation in any one of these domains can

disrupt the enzymatic activity of CHD4 and the ability of CHD4-containing NuRD complex to repress transcription.[62] The CTD is not necessary for the interaction of CHD4 with chromatin, but is necessary for transcriptional repression of NuRD complexes. Thus, the CTD is hypothesized to bind to co-repressors and/or other NuRD components.[62]

Although CHD3 and CHD4 are both widely expressed, CHD4 forms the predominant Chromodomain Helicase DNA Binding Protein component of the NuRD complex.[75] However, recent studies have hinted that CHD4 may possess roles outside of the NuRD complex.[67,79,80] For instance, one study described a possible new chromatin remodeling complex that consisted of CHD4 interacting with the histone acetyltransferase p300 and the E box binding protein HEB to regulate the expression of CD4 in T-cell development.[79]

In addition to its role in transcriptional regulation, recent studies have implicated CHD4 in the DNA Double Stranded Break (DSB) repair response.[56–58,81,82] As mentioned previously, compact chromatin is refractory to the initiation of the DSB repair process and significant evidence implicates the role of chromatin remodeling complexes in relieving this inhibition.[23,24] Multiple studies have demonstrated that CHD4 is rapidly recruited to sites of DSB through two distinct mechanisms of recruitment.[56,58] First, CHD4 was described to be recruited to sites of DSBs through a Poly(ADP-Ribose) Polymerase PARP-dependent mechanism, in which CHD4 directly bound the PAR-chains.[56] Alternatively, CHD4 has been described to be recruited to sites of DSBs through an interaction with the E3 ubiquitin ligase RING finger protein (RNF) 8.[58] Once recruited to a DSB site, CHD4 is hypothesized to relax the chromatin in order to facilitate the recruitment of other repair proteins, such as BRCA1, BRCA2, RAD51, and RPA, thus leading to the efficient repair of the break.[58,83] Highlighting its importance in the DSB repair pathway, depletion of CHD4 has

been shown to sensitize U2OS cells to ionizing radiation.[57,81] Additionally, depletion of CHD4 leads to increased loads of spontaneous DNA damage, indicating that CHD4 may also play a role in genomic maintenance.[82,84]

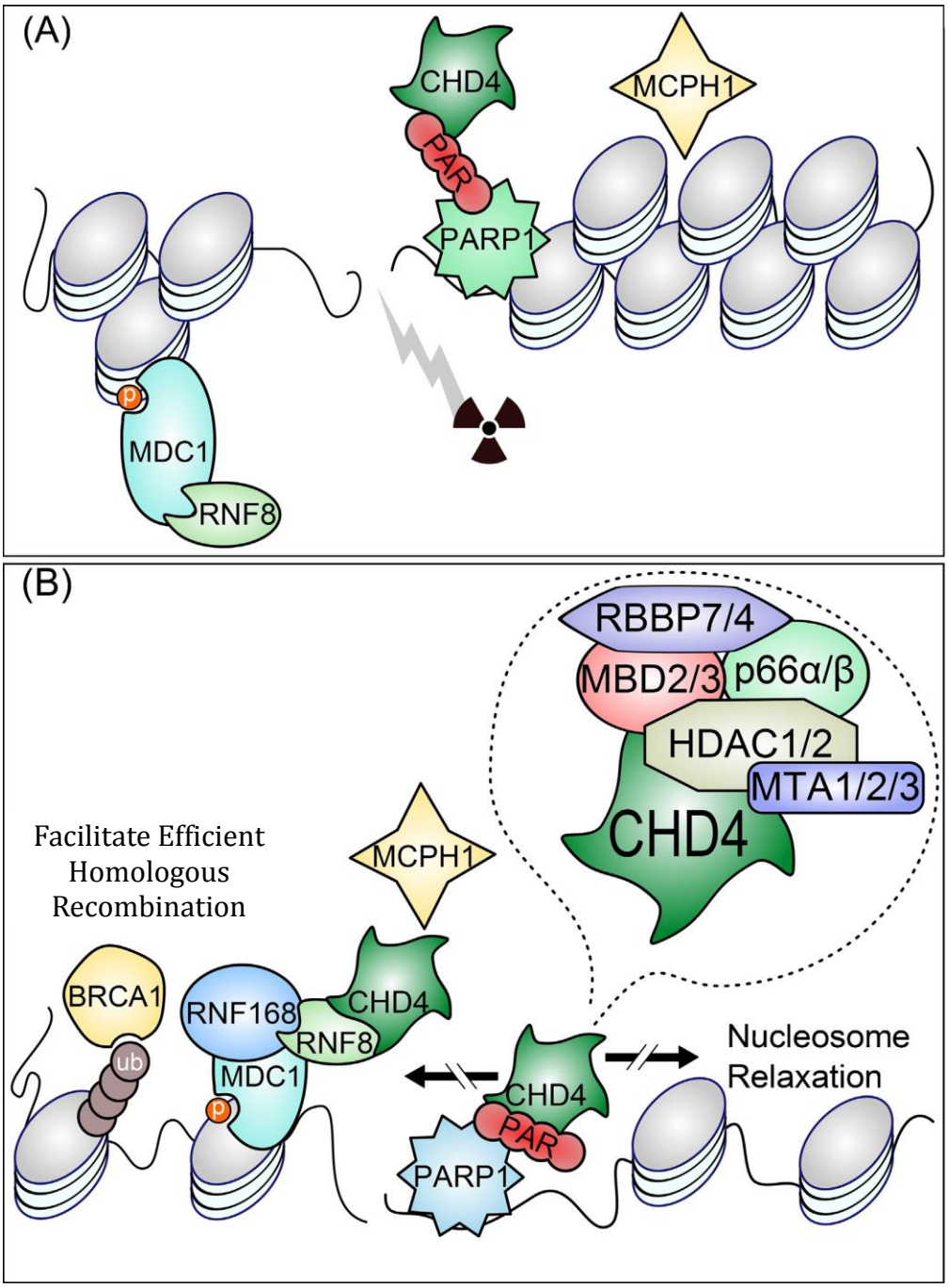

Figure 7. Model of CHD4 in the repair of DNA double strand breaks (DSB). (A) The first model indicates that CHD4 is recruited to DSB sites by PAR chains created by the enzyme PARP. (B) The second model indicates that CHD4 is recruited to sites of DSBs by the ubiquitin ligase RNF8. In both models, CHD4 and its associated NuRD complex alter the chromatin environment surrounding the break to promote the recruitment of other repair factors including MCPH1 and BRCA1. Image used with license from Stanley et al. *Mutat. Res.* 2013.

Interestingly, the most current studies on CHD4 have implicated it in the maintenance of cancer stem cells.[85,86] The first study to make this observation found that the transcription factor ZFHX4 utilizes CHD4/NuRD to alter gene expression programs required for the maintenance of the self-renewing, multipotent tumor-initiating cells (TICs) in glioblastoma. Furthermore, they demonstrated that depletion of CHD4 and other NuRD components resulted in the differentiation of glioblastoma TICs.[85] The second study found that CHD4 expression was significantly upregulated in EpCAM+ hepatocellular carcinoma stem cells and that high levels of CHD4 expression in patient samples of HCC correlated with a poorly differentiated morphology, a larger tumor size, increased marks of hepatocellular carcinoma stem cells, and worse survival compared to patients with low levels of CHD4 expression. [86]

Given its diverse roles in transcription regulation, DSB repair, and maintenance of cancer stem cells, CHD4 has been suggested as a drug target for various solid cancer types. [83,85,86] In this dissertation, I will discuss the functionality of CHD4 within the context of AML. My data shows that CHD4 is necessary for the efficient repair of DSBs within AML cells and that AML cells partially depleted of CHD4 are more susceptible to clinically used DNA damaging agents, such as DNR and ara-C, both *in vitro* and *in vivo*. Additionally, I will demonstrate that the depletion of CHD4 in AML cells reduces their potential to form mouse xenografts and markedly inhibits their ability to generate colonies. Both of these phenotypes are consistent with gene expression alterations resulting from CHD4 depletion. Importantly, all of these events occur preferentially in AML cells, as similar depletion of CHD4 in normal CD34+ hematopoietic progenitor cells does not result in similar

phenotypes. Taken together, the present findings from our studies highlight for the first time the therapeutic potential of targeting CHD4 in AML.

Chapter 2: Depletion of CHD4 sensitizes AML cells but not normal CD34+ progenitors to genotoxic agents by relaxing chromatin and impairing DSB repair.

Rationale

CHD4 is a chromatin remodeling ATPase that has been previously shown to play a significant role in the repair of DNA DSBs. As the foundation of standard AML therapy is based upon agents that derive their therapeutic potential from the induction of DSBs, we hypothesized that inhibition of CHD4 could sensitize AML cells to genotoxic agents used in standard therapy.

Results

CHD4 is necessary for maintaining heterochromatin in AML blasts. As CHD4 is a chromatin-remodeling ATPase,[70–73] we investigated the effect of CHD4 depletion on the overall chromatin structure of AML cells. Integration of a CHD4-targeting short-hairpin RNA (shCHD4-1) into the AML cell lines U937, MV4-11, and AML-3 by a lentiviral vector resulted in the robust depletion of the CHD4 protein (Figure 8).

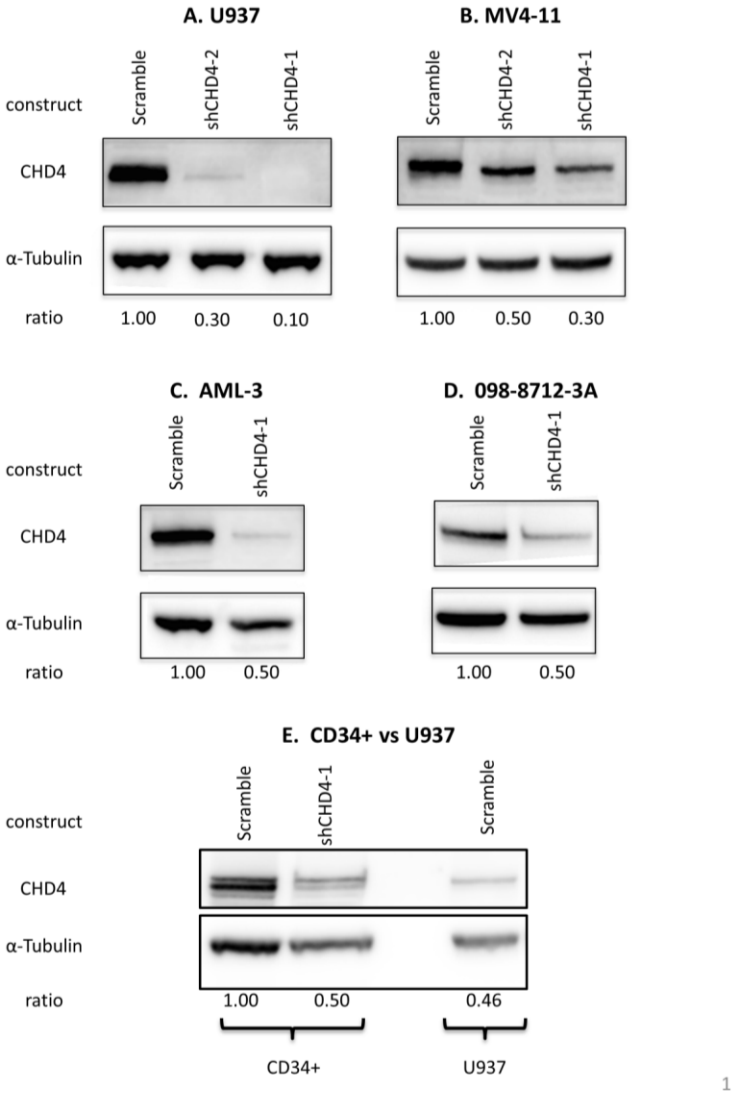

Figure 8. Depletion of CHD4. Western blot analysis to determine the extent of CHD4 protein depletion in response to shRNA expression in the human AML cell lines (A) U937, (B) MV4-11, (C) AML-3, (D) the primary AML sample 098-8712-3A, and (E) normal CD34+ hematopoietic progenitors. U937 was added to the CD34+ blot to highlight the difference in endogenous CHD4 between normal CD34+ cells and AML blasts. Scramble is the non-targeting control construct. shCHD4-1/2 are the independent CHD4-targeting constructs. Densitometry was used to quantify each band and α-Tubulin was used to normalize.

When compared to control cells in which a scrambled, non-targeting shRNA was integrated, cells depleted of CHD4 were found to have a global increase in the euchromatin-associated acetylation of Histone H3 Lysine 9 and Histone H4 Lysine 8 (Figure 9A) and disruption of heterochromatin-associated trimethyl-Histone H3 Lysine 9 foci (Figure 9B). These results indicate that inhibition of CHD4 function induces a global relaxation of the chromatin structure in AML blasts.

Depletion of CHD4 renders AML blasts more sensitive to DSB damage and impairs the repair of DSBs. Because chromatin remodeling enzymes have been found to play key roles in mediating the repair of DSBs,[23,26] we investigated if CHD4 is involved in DSB repair in AML blasts. We subjected U937 cells to 6Gy of radiation and detected DSBs using a neutral comet assay over a 4-hour time course (Figure 9C). CHD4-depleted cells demonstrated significantly more evidence of DSBs 1 hour after radiation exposure, suggesting that inhibition of CHD4 rendered the cells more susceptible to the formation of DSBs. The tail moment of control cells returned to baseline after just 2 hours, indicating that cells expressing wild-type levels of CHD4 are capable of rapidly repairing radiation-induced DSBs to levels below the detection limits of the assay (~50 DSBs per cell). However, the tail moment of the CHD4 depleted cells remained elevated throughout the 4-hour course of the experiment, indicating that CHD4 is required for the efficient repair of DSBs in AML cells.

To confirm our observations from the neutral comet assay, we performed immunostaining for γH2A.X foci, a histone marker of DSBs, over the 4-hour time course

(Figure 9D and9E). Cells depleted of CHD4 contained a significant increase in γH2A.X foci at 0.5 hours post radiation exposure and the number of foci remained elevated above that in control cells over the 4-hour time course. Similar results were obtained for MV4-11 and AML-3 (Figure 10).

We then confirmed that the DSBs observed over the 4-hour time course were not the result of apoptosis, as PARP or caspase-3 cleavage did not occur throughout the 4-hour time course (Figure 11). Thus, in AML cells, inhibition of CHD4 impedes the repair of DSBs and increases susceptibility to their formation.

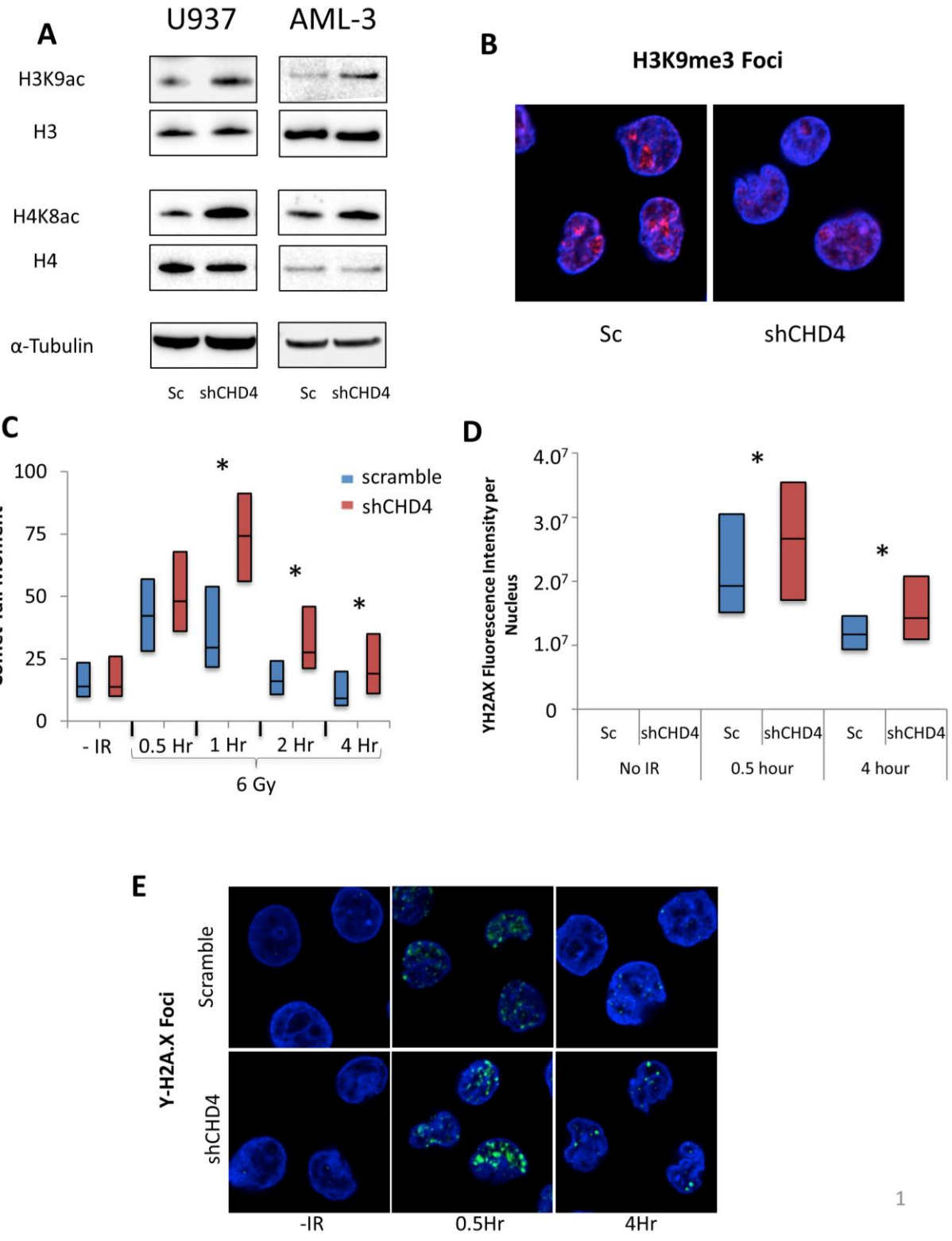
A
U937
AML-3
H3K9ac
H3
H4K8ac
H4
α-Tubulin
Sc
shCHD4
Sc
shCHD4
B
H3K9me3 Foci
Sc
shCHD4
C
Comet Tail Moment
100
75
50
25
0
scramble
shCHD4
*
*
*
- IR
0.5 Hr
1 Hr
2 Hr
4 Hr
6 Gy
D
YH2AX Fluorescence Intensity per Nucleus
4.0^7
3.0^7
2.0^7
1.0^7
0
*
*
Sc
shCHD4
Sc
shCHD4
Sc
shCHD4
No IR
0.5 hour
4 hour
E
Y-H2A.X Foci
Scramble
shCHD4
-IR
0.5Hr
4Hr

1

Figure 9. CHD4 is necessary for the maintenance of heterochromatin and the efficient repair of DNA DSBs in AML blasts. AML cell lines were infected by lentivirus to integrate either a non-targeting, scrambled (Sc) shRNA or a CHD4-targeting shRNA. (A) Depletion of CHD4 leads to a global increase in euchromatin-associated histone H3K9 and H4K8 acetylation. (B) Depletion of CHD4 also results in a disruption of heterochromatin-associated Histone H3K9me3 foci in U937 cells as shown by staining with anti-H3K9me3 antibody. (C) U937 cells were exposed to 6 Gy of radiation to induce DNA DSBs. DSB formation and repair was monitored over a 4-hour time course using a neutral comet assay. CHD4-depleted cells displayed significantly more evidence of DSBs and were delayed in their repair. (n>50 comets) (D) The results of the comet assay were confirmed by staining for ϒ-H2A.X foci and calculating the fluorescent intensity per nucleus. (n>60 cells per time point) (E) Representative images of the ϒ-H2A.X stain. * indicates $p<0.05$

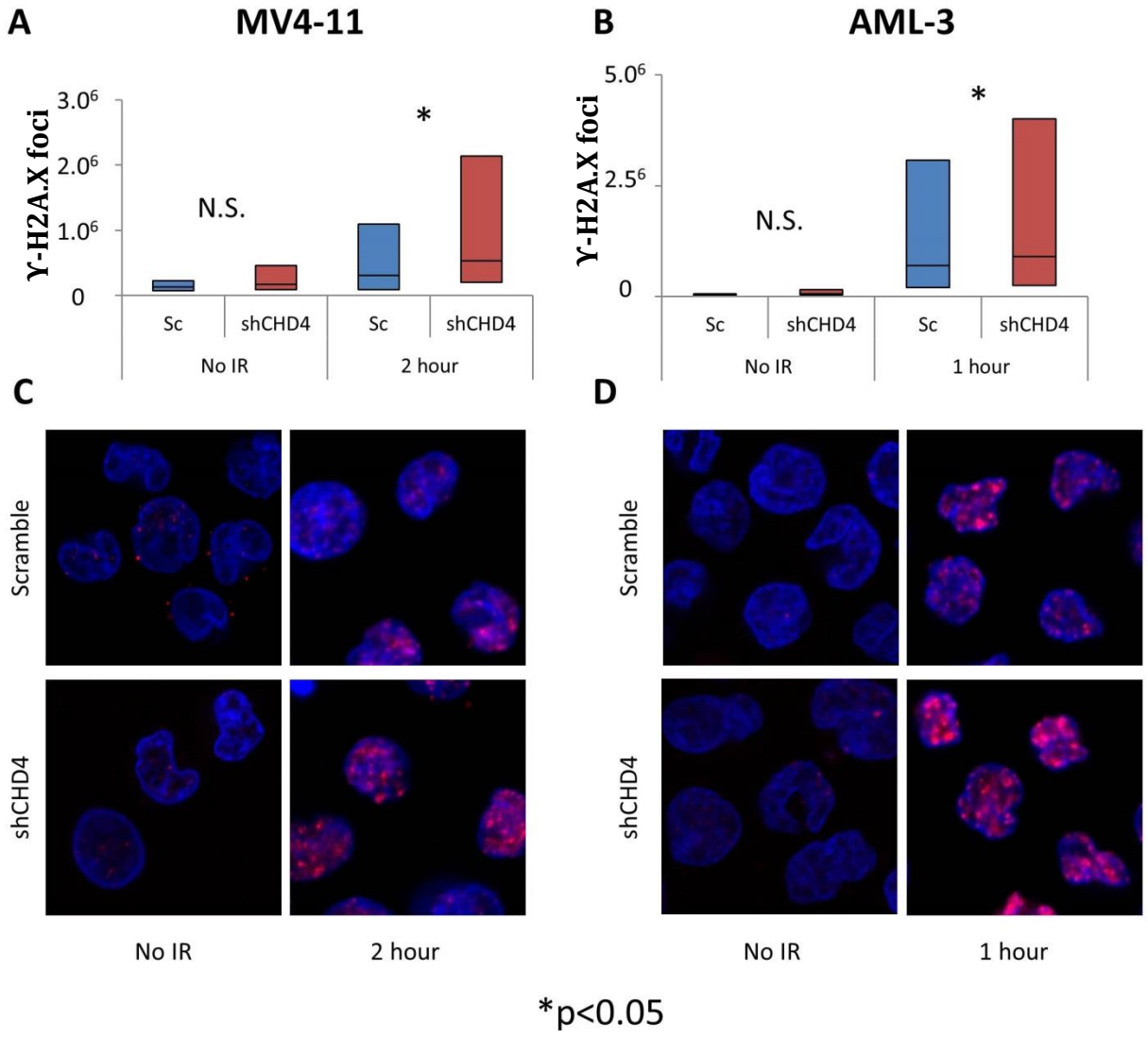

Figure 10. CHD4 is necessary for the efficient repair of DNA DSBs in AML blasts.

Similar to the U937 cells in Figure 1, MV4-11 (A) and AML-3 (B) cell lines were exposed to 6 Gy of radiation to induce DNA DSBs. DSB formation was detected by staining for Υ-H2A.X foci and calculating the fluorescent intensity per nucleus (n>60 cells per time point). Cells depleted of CHD4 displayed significantly elevated evidence of DSB formation (* indicates $p<0.05$). Representative images of the Υ-H2A.X stain for MV4-11 (C) and AML-3 (D).

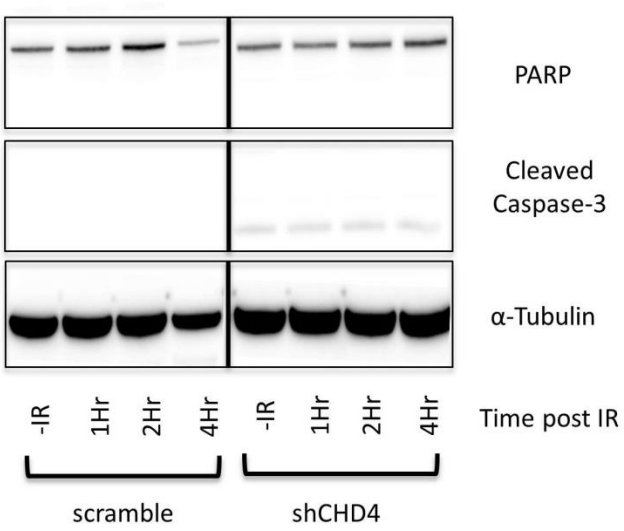

Figure 11. Lack of increased markers of apoptosis shortly following radiation exposure. No evidence of PARP or caspase-3 cleavage was found during the 4-hour time course upon exposing U937 cells to 6 Gy of radiation as described in Figures 1C and 1D. This confirms that the increased evidence of DSBs in the comet assay and the γH2A.X stain was not due to induction of apoptotic mechanisms.

Inhibition of CHD4 renders AML blasts more sensitive to DNR and ara-C *in vitro*.

Having determined that CHD4 affects the formation and repair of DSB in AML cells, we hypothesized that AML cells depleted of CHD4 would be more sensitive to the DSB-inducing agents DNR and ara-C. To test this hypothesis, we incubated the AML cells for 24 hours with clinically relevant concentrations of either DNR (Figure 12A) or ara-C (Figure 12B) and the assessed their viability with 7AAD (7-Aminoactinomycin D) staining. At all DNR and ara-C concentrations tested, significantly more cell death was observed in the AML cells depleted of CHD4, with some concentrations resulting in as much as a 5-fold increase in cell death. Similar results were obtained when we depleted CHD4 in a primary AML sample (098-8712-3A).

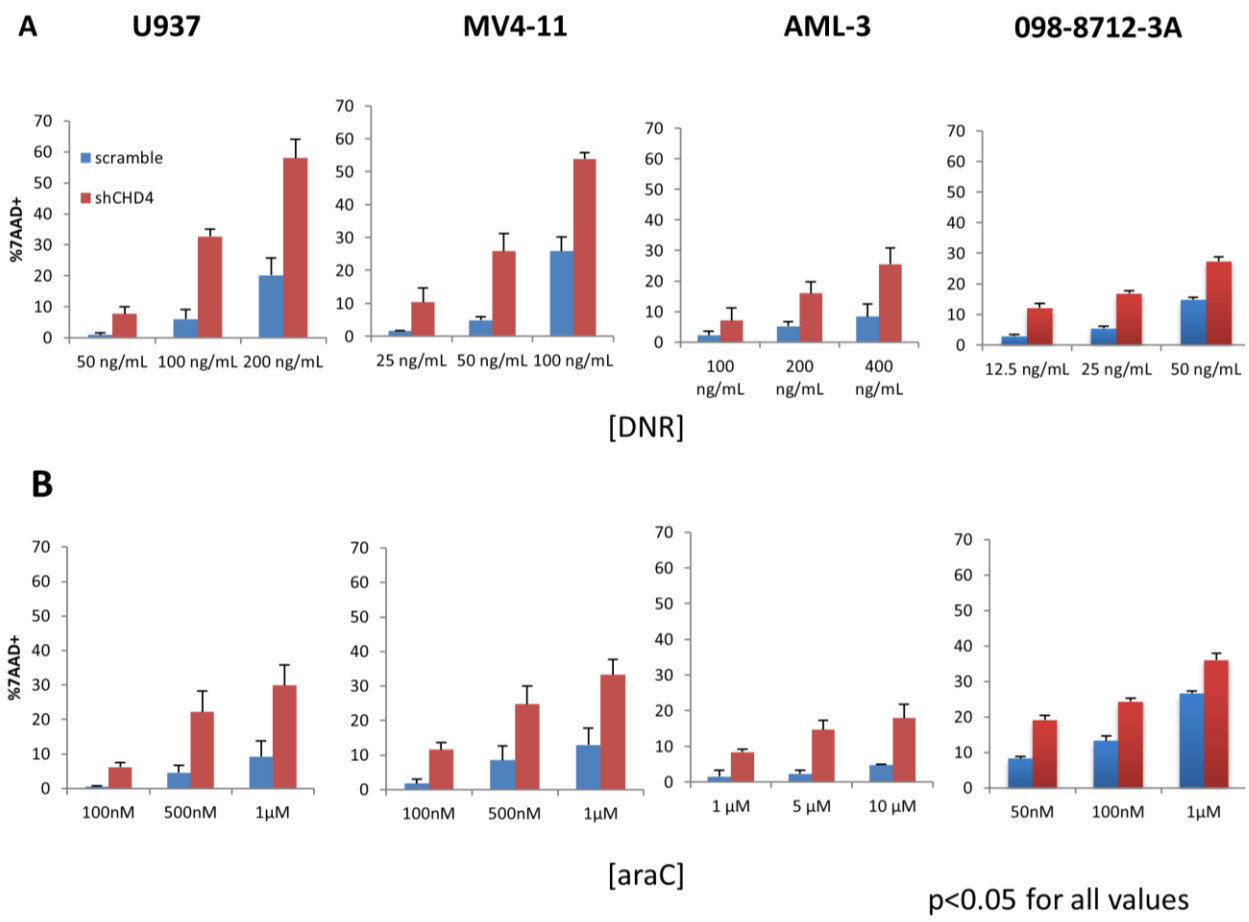

Figure 12. Inhibition of CHD4 renders AML blasts more sensitive to DNR and ara-C *in vitro*. U937, MV4-11, and AML-3 human AML cell lines and a primary AML sample were incubated with various concentrations of (A) DNR or (B) ara-C for 24 hours *in vitro*. Cell viability was assayed using a 7AAD stain and quantified by flow cytometry. For all AML cells and concentrations of DNR/ara-C tested, AML cells depleted of CHD4 displayed significantly more cell death compared to controls. $p<0.05$ for every data point tested. n=3 biological replicates for each data point.

To confirm that the increase in sensitivity to DNR and ara-C was not the result of an off-target effect of the shRNA construct used, a second CHD4-targeted shRNA construct (shCHD4-2, Figure 8) was tested and induced a similar increase in sensitivity to DNR (Figure 13). Thus, knockdown of CHD4 with two independent shRNA constructs enhanced the *in vitro* sensitivity of AML cells to DNR and ara-C.

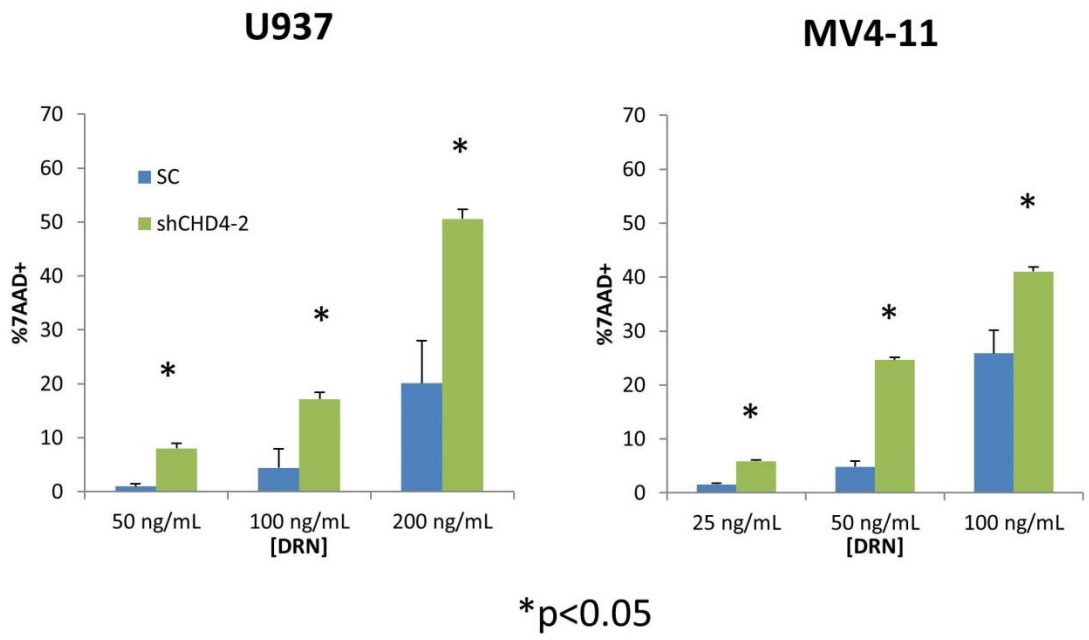

Figure 13. Depletion of CHD4 with a second shRNA construct renders AML blasts more sensitive to DNR. To confirm that the observations found in Figure 2 was not the result of off-target effects of shRNA construct 1, we depleted CHD4 using a second shRNA (shCHD4-2). Upon incubation with DNR for 24 hours, we observed a similar increase in both (A) U937 and (B) MV4-11 cell sensitivity as the result of CHD4 depletion. (n = 3 biological repeats, * indicates $p<0.05$)

As DNR is a fluorescent intercalating agent[87] and CHD4 depletion induces a global relaxation of chromatin in AML blasts, we tested whether CHD4-depleted cells were more susceptible to DNR intercalation. Incubation of U937 cells for 2 hours with 200 ng/mL of DNR resulted in significantly more DNR fluorescent signal inside the nuclei of CHD4-depleted cells (Figure 14). This finding is consistent with increased DNR intercalation within CHD4 depleted cells.

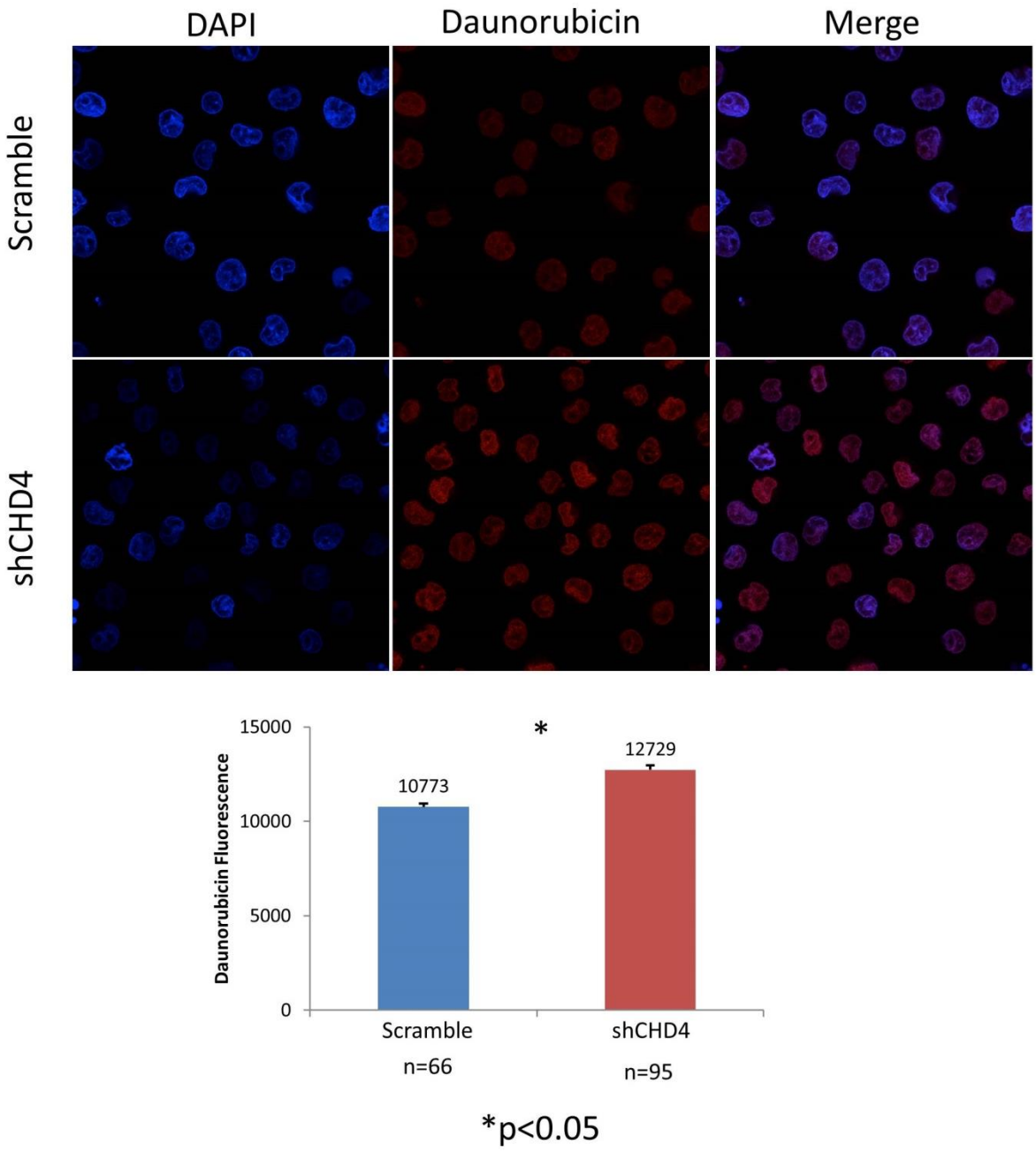

Figure 14. CHD4 depletion increases the intercalation of DNR. U937 cells were incubated with 200 ng/mL of DNR for 2 hours. DNR fluorescence within the cells was detected by measuring the emissions at 580 nm. The increased DNR fluorescent signal in CHD4-depleted cells is consistent with increased DNR intercalation. (* indicates $p<0.01$)

To gain insight into what cell cycle checkpoints the DNR-induced DNA damage was activating, we performed a cell cycle analysis using propidium iodide (PI) stain on treated U937 cells. Based on this analysis, we saw that DNR induces an intra-S phase checkpoint as the percentage of cells in S phase increased in a DNR dose-dependent manner (Figure 15). Interestingly, we found that cells depleted of CHD4 activated the checkpoint at lower doses of DNR than control cells, as evident at the 50 ng/mL concentration. This finding is consistent with CHD4 depleted cells being more prone to the induction of DNA DSBs due to treatment with DNR.

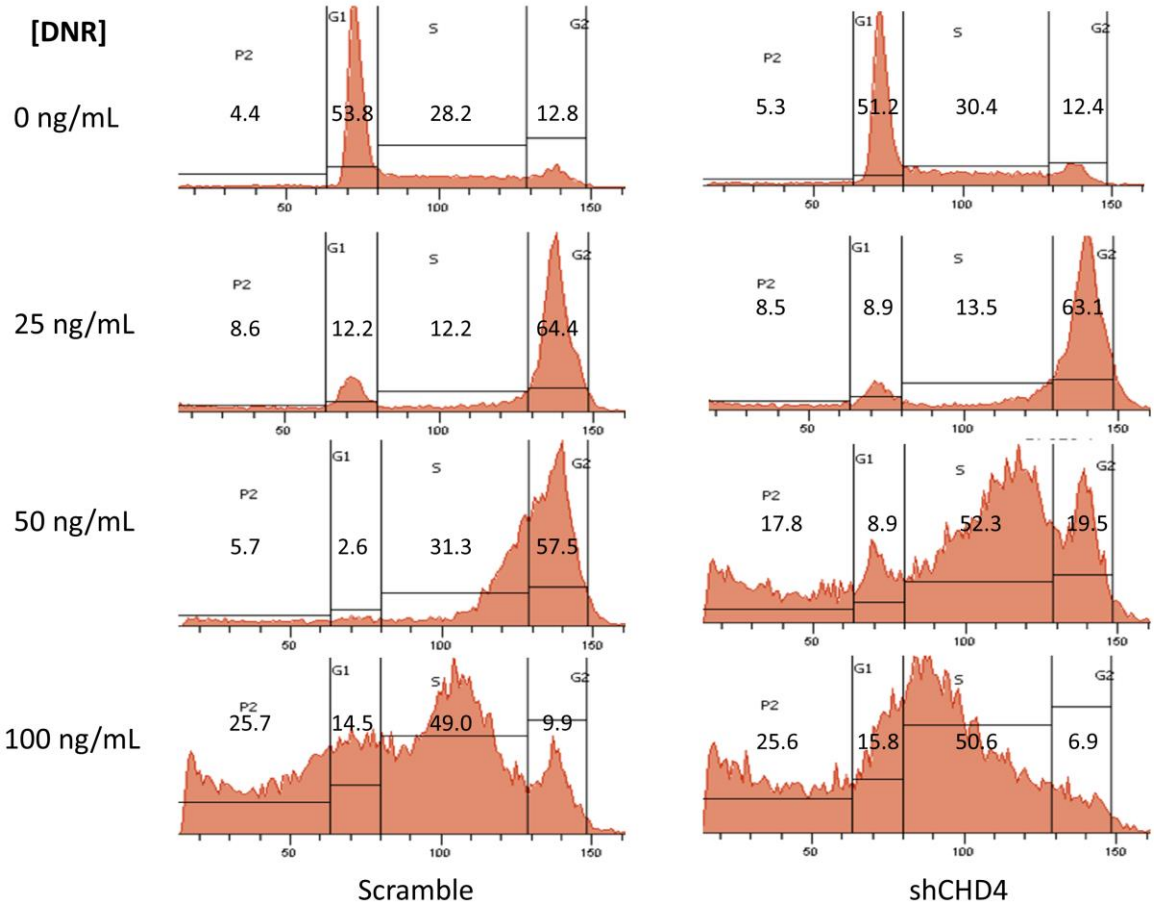

Figure 15. CHD4 depleted cells are more prone to DNR-induced S-phase checkpoint activation. U937 cells were treated with the indicated doses of DNR for 24 hours. Cell cycle was analyzed using a PI stain. DNR was found to activate an S-phase cell cycle checkpoint and activated the checkpoint more readily in CHD4 depleted cells at lower concentrations of DNR. Note that cells found in the "P2" category are apoptotic.

Inhibition of CHD4 does not sensitize normal CD34+ progenitor cells to DNR and ara-C. We next investigated if the increased sensitivity to DNR and ara-C induced by CHD4 inhibition occurs preferentially in AML blasts. We depleted CHD4 in CD34+ hematopoietic progenitor cells isolated from the mobilized blood of 3 normal donors (Figure 8E). Following incubation for 24 hours with DNR and ara-C, CD34+ cells did not display a significant increase in sensitivity to DNR (Figure 16A) or ara-C (Figure 16B).

To gain insight into how CHD4 depletion might preferentially sensitize leukemic cells, we compared the total endogenous CHD4 protein levels in CD34+ cells from the 3 normal donors to that in 3 AML cell lines (U937, MV4-11, AML-3) and blasts isolated from the bone marrow of 3 different AML patients whose marrow contained >90% blasts. AML cell lines and primary AML blasts contained on average ~50% less CHD4 total protein than CD34+ cells (Figure 8E and 16C). Surprisingly, AML cell lines and primary AML samples did not have significantly different amounts of CHD4 mRNA compared to the normal CD34+ progenitors, suggesting that post-transcriptional alterations could account for the discrepancy in the observed amount of CHD4 protein.

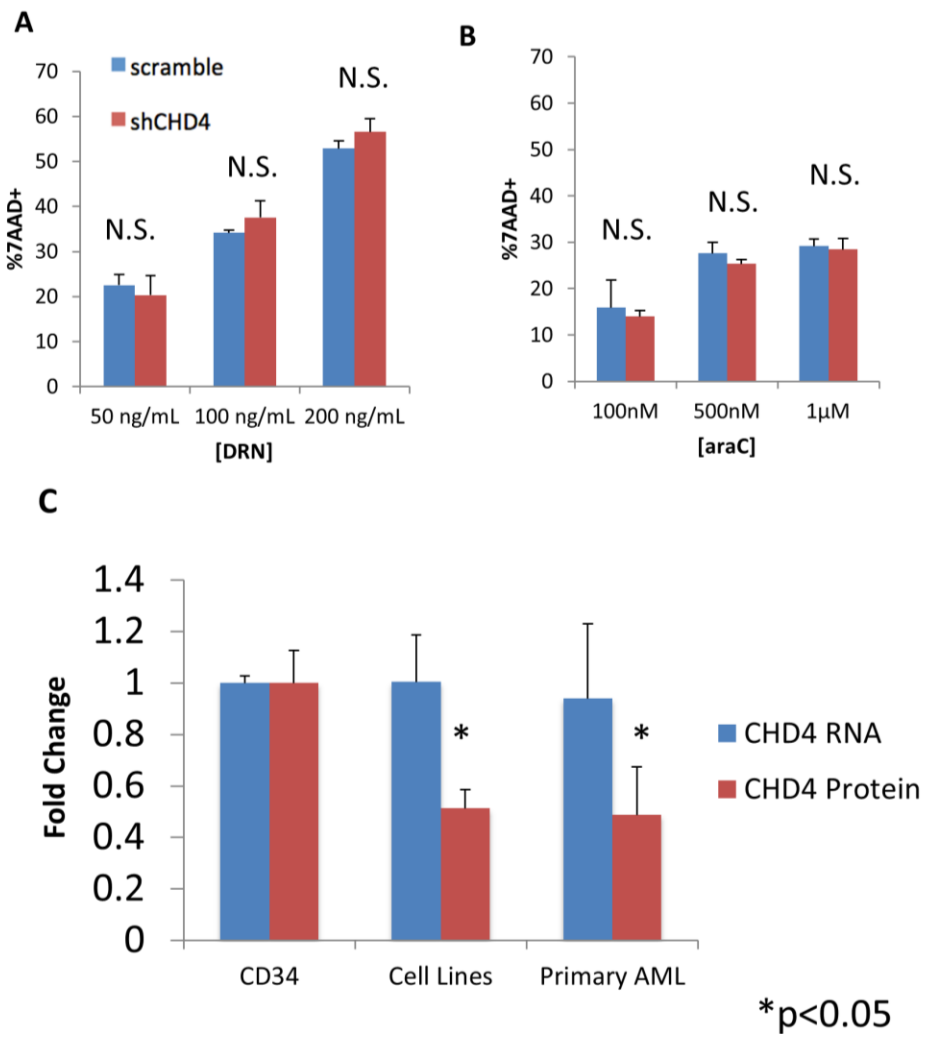

Figure 16. Inhibition of CHD4 does not sensitize normal CD34+ progenitor cells to DNR and ara-C. CD34+ hematopoietic progenitors were isolated from the 3 normal donors. Depletion of CHD4 did not significantly increase the sensitivity of the CD34+ cells to either (A) DNR or (B) ara-C. (C) The CD34+ cells were found to contain significantly more endogenous CHD4 protein than the AML cell lines (U937, MV4-11, AML-3) and primary AML blasts isolated from the bone marrow of 3 patients. Interestingly, there was no difference in CHD4 mRNA between the CD34+ and AML cells. * indicates $p<0.05$ Note: RNA was normalized to GAPDH and protein was normalized to tubulin.

Inhibition of CHD4 sensitizes AML blasts to DNR and ara-C in a xenograft model. Having demonstrated that depletion of CHD4 preferentially increases the sensitivity of AML cells to DNR and ara-C *in vitro*, we tested the effect of CHD4 depletion in AML cells *in vivo*. To this end, we utilized a previously described mouse xenograft model of the human "7+3" induction regimen[88,89] that consists of 5 continuous days of ara-C treatment and doxorubicin co-administered on days 1 through 3. In this model, the anthracycline doxorubicin is substituted for the anthracycline DNR used in humans due to the systemic toxicity of the latter in mice.[88] Luciferase expressing U937 cells were systemically engrafted by tail vein injection into NSG mice (n=3 mice per condition) and disease progression was monitored by total radiance (measured in photons/second/cm^2/sr) generated within each mouse upon subcutaneous administration of luciferin.

The treatment regimen was initiated once a systemic xenograft was confirmed and mice were re-imaged 7 days later, a time we had previously observed to yield the maximum drug-induced anti-tumor effect. Post-treatment, mice engrafted with control cells displayed on average 43% of their total pre-treatment radiance. However, mice engrafted with CHD4 depleted cells displayed only 20% of their pretreatment radiance (Figure 17A), indicating that AML blasts depleted of CHD4 are indeed more sensitive to DNR and ara-C treatment *in vivo*.

Mice were then followed for survival, until a humane endpoint was reached (Figure 17B). Untreated mice engrafted with CHD4 depleted cells survived significantly longer than those engrafted with control cells. The survival of the mice engrafted with CHD4-depleted cells further improved with the addition of the drug regimen. Once the mice reached their humane endpoints, bone marrow was collected and analyzed. In the marrow

of mice that received the shCHD4-depleted cells, the AML cells retained ~75% knockdown of CHD4 mRNA compared to cells from the bone marrow of mice containing the control shRNA (data not shown).

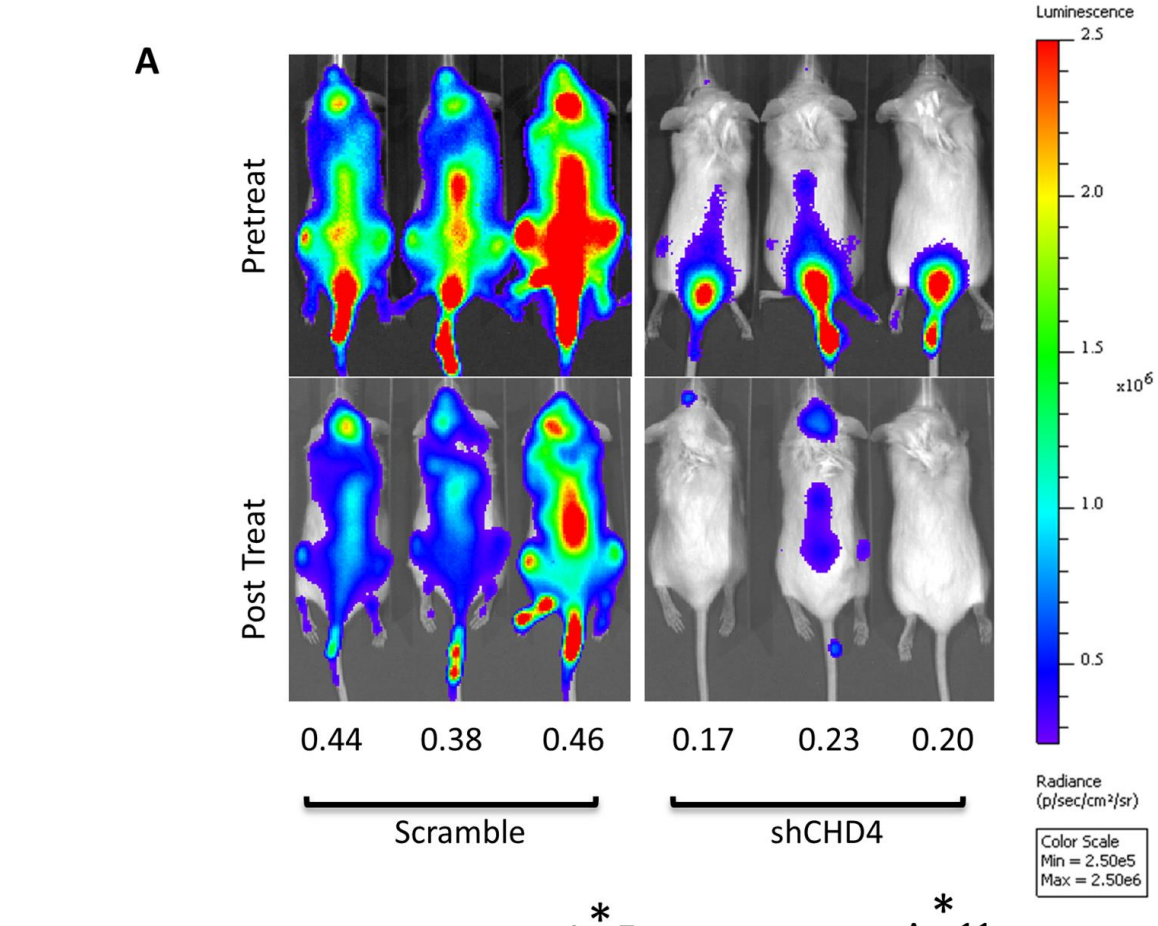
A
Pretreat
Post Treat
Luminescence
2.5
2.0
1.5
x10^6
1.0
0.5
0.44
0.38
0.46
0.17
0.23
0.20
Scramble
shCHD4
Radiance
(p/sec/cm²/sr)
Color Scale
Min = 2.50e5
Max = 2.50e6

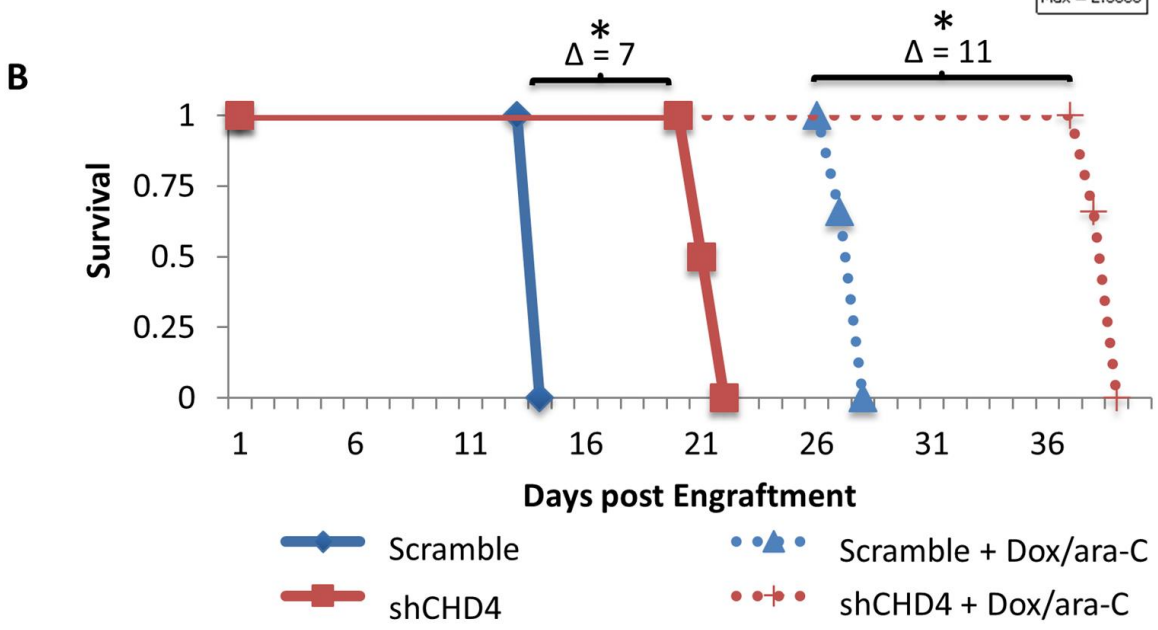
B
*
Δ = 7
*
Δ = 11
Survival
1
0.75
0.5
0.25
0
1
6
11
16
21
26
31
36
Days post Engraftment
Scramble
shCHD4
Scramble + Dox/ara-C
shCHD4 + Dox/ara-C

*p<0.05

Figure 17. Inhibition of CHD4 sensitizes AML blasts to DNR and ara-C in a xenograft model. Equal numbers of luciferase-expressing Scramble and shCHD4 U937 cells were engrafted into NSG mice by tail-vein injection and tumor burden was non-invasively monitored by measuring the total radiance generated upon subcutaneous administration of luciferin. (A) Once a tumor was well established (as seen in the pretreatment panels), the mice were treated with 5 continuous days of ara-C, with concurrent doxorubicin on days 1 through 3. Post-treatment, mice engrafted with control cells were found to possess 43% of their pretreatment radiance, whereas mice engrafted with CHD4-depleted cells possessed 20% ($p<0.001$). (B) The mice were followed for survival. CHD4-depletion alone, resulted in a 7-day improvement in mouse survival. Treatment with Doxorubicin/ara-C improved the survival of the mice engrafted with CHD4-depleted cells by an additional 4 days. * indicates $p<0.05$

Inhibition of CHD4 activates the ATM signaling pathway to induce apoptosis. As AML cells depleted of CHD4 are more sensitive to DSB inducing agents, we investigated the role of the ataxia-telangiectasia mutated (ATM) pathway. The serine/threonine kinase ATM is a master regulator of the DSB repair response and is classically activated by auto-phosphorylation of serine 1981 in response to dsDNA breaks.[18,90] Recently, the protein acetyl-transferase Tip60 was found to activate ATM in response to chromatin relaxation.[91] Because depletion of CHD4 led to a global relaxation of the chromatin structure of AML cells, we hypothesized that depletion of CHD4 would induce a Tip60 dependent activation of ATM. Accordingly, a 10-fold increase in the phosphorylation of S1981 on ATM in U937 cells was observed upon the depletion of CHD4. However, the phosphorylation of ATM remained at control levels upon concomitant depletion of Tip60 in CHD4 depleted cells (Figure 18A). This observation indicates that inhibition of CHD4 does induce a Tip60-dependent activation of ATM.

We next sought to investigate the ATM pathway in AML cells in response to DNR. As expected, ATM is auto-phosphorylated in a dose-dependent manner in both control and shCHD4 cells. However, a significant increase in the amount of phosphorylated-ATM was detected at each DNR concentration tested in CHD4 depleted cells (Figure 18B). Interestingly, depletion of CHD4 also increased the level of total ATM by 3-fold. Once active, ATM induces numerous downstream phosphorylation events that signal for cell survival by initiating the repair of DSBs or it can trigger apoptosis.[18,92] E2F1 is a pro-apoptotic transcription factor that is stabilized by ATM through phosphorylation of Serine-31.[93] E2F1 is stabilized in U937 cells in a DNR dose-dependent manner in control cells; however, significantly more E2F1 is stabilized in response to DNR in cells partially depleted of CHD4.

E2F1 did not undergo a DNR dose-dependent stabilization when the ATM inhibitor KU60019 was added, indicating that the observed dose-dependent stabilization requires ATM (Figure 18C-E). Ultimately, the increased activation of ATM and the subsequently increased downstream pro-apoptotic signaling in response to DNR in CHD4-depleted cells resulted in increased apoptosis compared to control cells (Figure 18F).

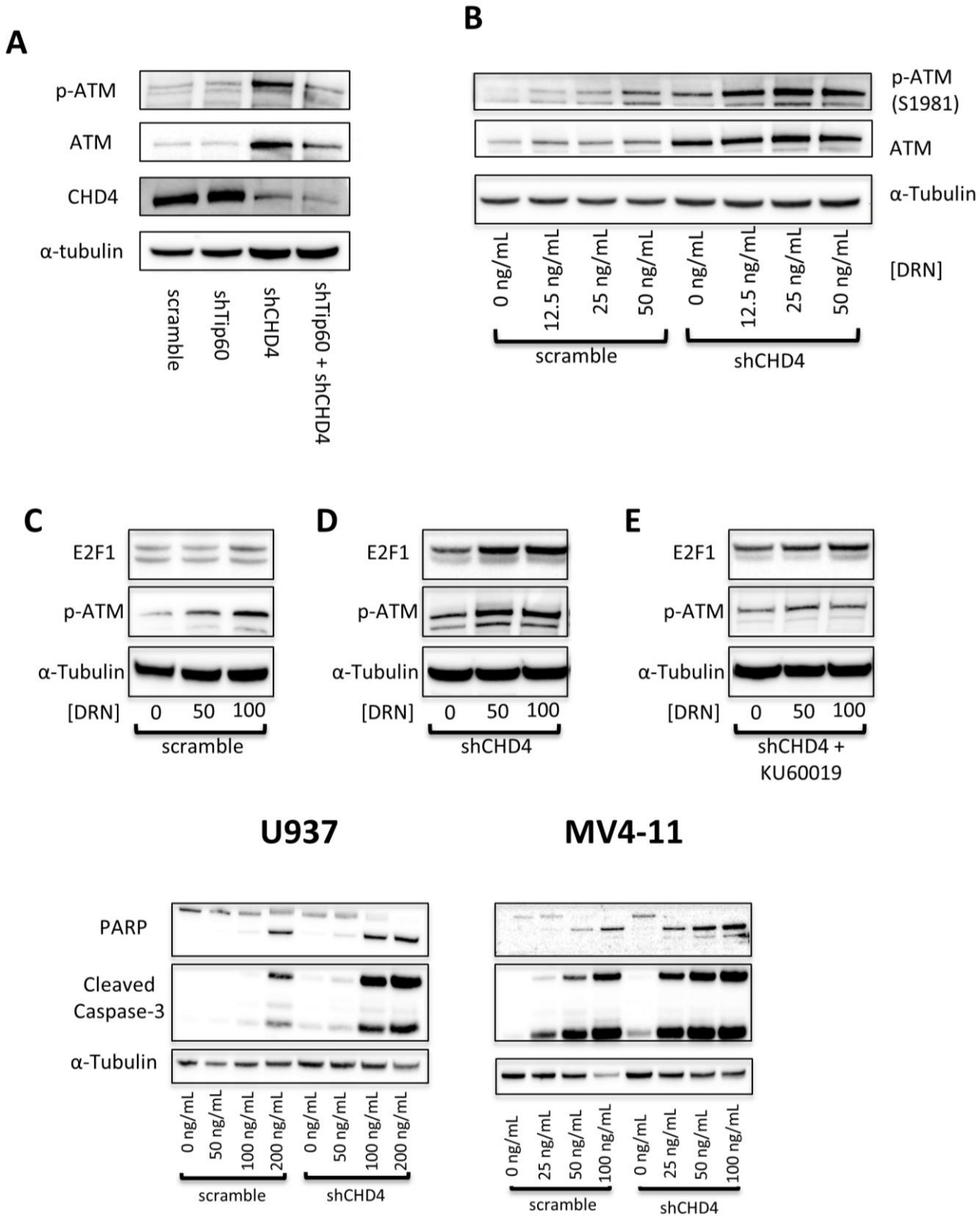
A
p-ATM
ATM
CHD4
α-tubulin
scramble
shTip60
shCHD4
shTip60 + shCHD4
B
p-ATM (S1981)
ATM
α-Tubulin
[DRN]
0 ng/mL
12.5 ng/mL
25 ng/mL
50 ng/mL
scramble
shCHD4
C
E2F1
p-ATM
α-Tubulin
[DRN] 0 50 100
scramble
D
E2F1
p-ATM
α-Tubulin
[DRN] 0 50 100
shCHD4
E
E2F1
p-ATM
α-Tubulin
[DRN] 0 50 100
shCHD4 + KU60019
F
U937
MV4-11
PARP
Cleaved Caspase-3
α-Tubulin
0 ng/mL
50 ng/mL
100 ng/mL
200 ng/mL
25 ng/mL
scramble
shCHD4

Figure 18. Inhibition of CHD4 activates the ATM signaling pathway to induce increased apoptosis. (A) Depletion of CHD4 in U937 cells induces a significant activation of ATM, which is blocked by the concurrent depletion of Tip60. (B) Upon addition of DNR, ATM is activated in a concentration-dependent manner, with significantly more activation in the CHD4-depleted cells. (C) Once active, ATM acts on its downstream targets, including stabilizing the pro-apoptotic transcription factor E2F1. E2F1 is stabilized in a DNR concentration-dependent manner, (D) with significantly more being stabilized in the CHD4-depleted cells. (E) This stabilization is diminished upon the addition of the ATM inhibitor KU60019. (F) Ultimately, in response to the DNR, CHD4-depleted AML cells display elevated markers of apoptosis, including PARP and Caspase-3 cleavage.

Inhibition of CHD4 inactivates the Chk2 pathway. Since we found that DNR induces an S phase checkpoint (Figure 15) and CHD4 depletion activates ATM (Figure 18), we investigated the effect of CHD4 depletion on the Checkpoint kinase (Chk) 2 pathway. Chk2 is a serine/threonine kinase that is phosphorylated on threonine-68 by ATM in reaction to DSBs. Once activated, Chk2 homodimerizes, autophosphorylates on serine-516, and then targets >20 downstream targets for phosphorylation to induce a wide range of responses to the DNA damage, which include cell cycle checkpoint activation and DNA repair, apoptosis, or senescence.[94] Among these substrates are the proteins Cell Division Cycle (Cdc) 25A and 25C. When active, Chk2 phosphorylates CdC25A and Cdc25C to signal for their degradation and results in arrest of the cell cycle. Both p53 and E2F1 are also targets of Chk2 and have the potential to induce apoptosis.

As previously mentioned, DNR-induced DSBs activate ATM (Figure 18B) and lead to the phosphorylation of Chk2 at Threonine-68 (Figure 19). However, U937cells depleted of CHD4 are deficient in their ability to activate Chk2 as seen by the decreased amount of p-Chk2 at serine-516 following phosphorylation by ATM. Interestingly, it appears that cells depleted of CHD4 contain less total Chk2 than control cells, despite roughly equivalent amounts of Chk2 mRNA. Previous reports indicate that Chk2 protein is degraded following the repair of DSBs[95,96], indicating that the decrease in total Chk2 in CHD4 depleted cells may be due to the increased susceptibility of these cells to the formation of DSBs, both spontaneous (as seen in the decreased total Chk2 in untreated cells) and DNR-induced (as seen in the further reduction in treated cells). However, Chk2 degradation is not consistent among all studies[97] and may indicate a cell line/genotoxic agent specific effect. Consistent with an inactive Chk2 pathway, CHD4 depleted cells do not phosphorylate and

subsequently degrade Cdc25A/C. This could lead to a failure to properly activate a cell cycle checkpoint, despite the presence of DNR-induced DSBs, and may result in apoptosis. Additionally, Chk2 does not phosphorylate the proapoptotic transcription factor E2F1 in CHD4 depleted cells. However, total E2F1 is stabilized in CHD4 depleted cells in a DNR-dose dependent manner, possibly due to (as previously seen in Figure 18) phosphorylation of E2F1 by ATM at a second site. Both the failure to activate the cell cycle checkpoint and the stabilization of E2F1 can lead to apoptosis, indicating another potential mechanism for how CHD4 depletion sensitizes AML cells to DNR. Note: p53 was not assessed in these studies due to the $p53^{-/-}$ status of U937.

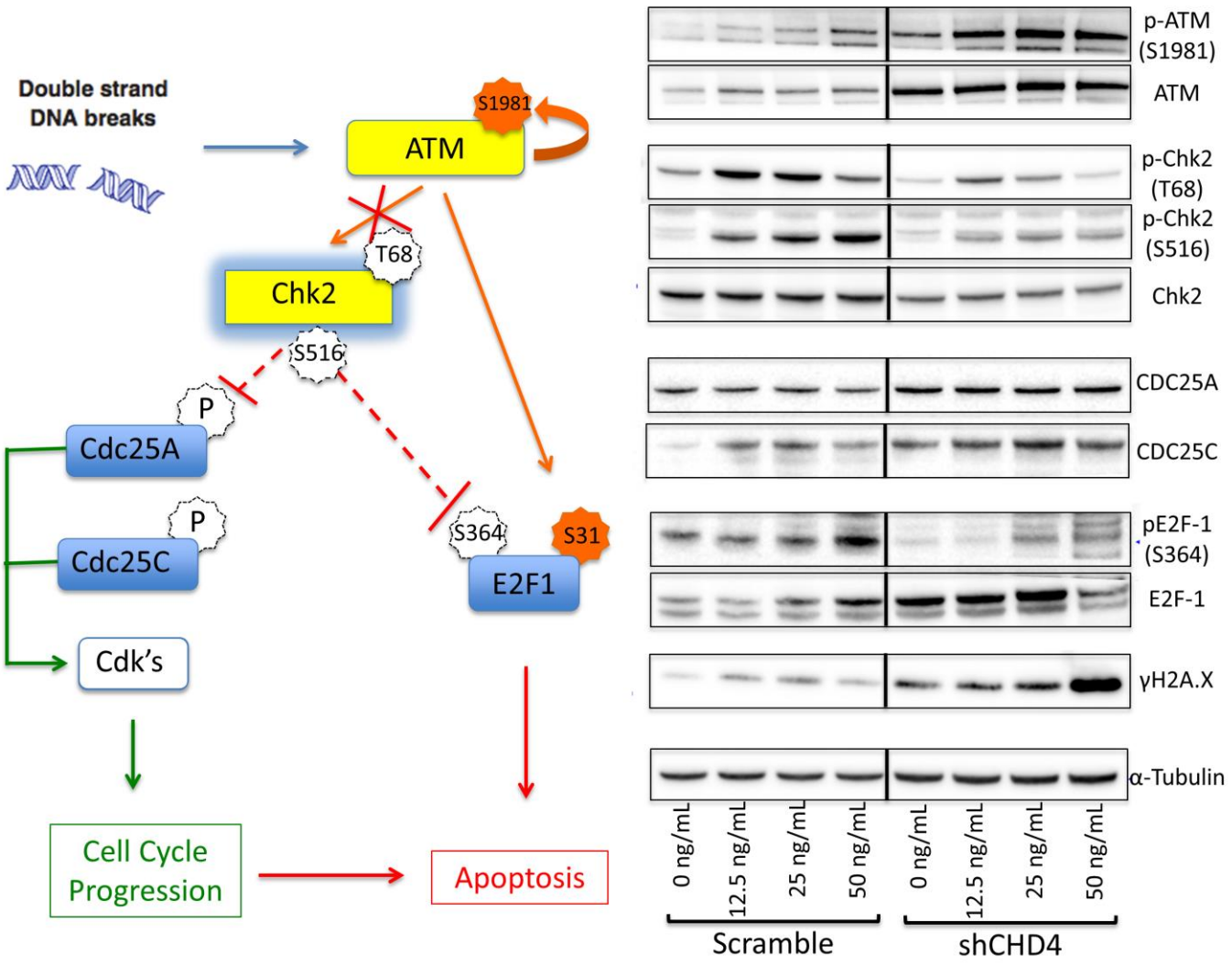
Double strand
DNA breaks
ATM
S1981
T68
Chk2
S516
P
Cdc25A
P
Cdc25C
Cdk's
S364
S31
E2F1
Cell Cycle
Progression
Apoptosis
p-ATM
(S1981)
ATM
p-Chk2
(T68)
p-Chk2
(S516)
Chk2
CDC25A
CDC25C
pE2F-1
(S364)
E2F-1
γH2A.X
α-Tubulin
0 ng/mL
12.5 ng/mL
25 ng/mL
50 ng/mL
0 ng/mL
12.5 ng/mL
25 ng/mL
50 ng/mL
Scramble
shCHD4

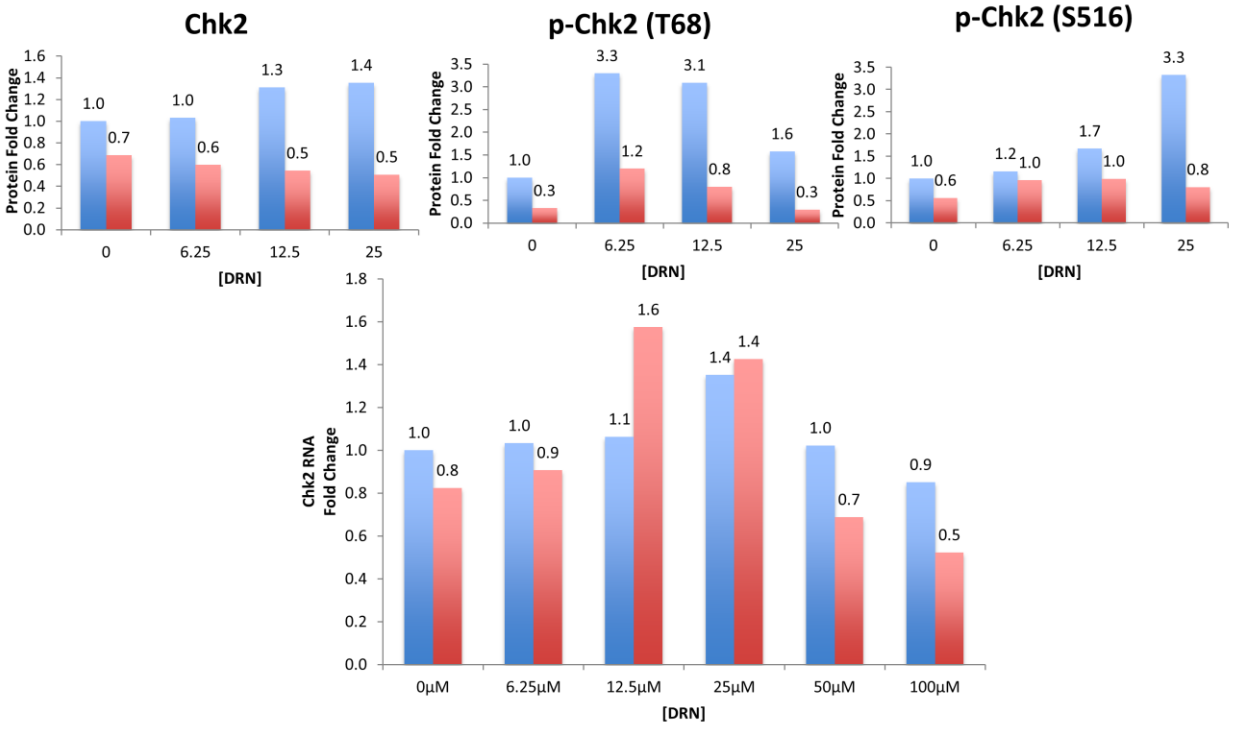
Chk2
Protein Fold Change
1.0
0.7
1.0
0.6
1.3
0.5
1.4
0.5
0
6.25
12.5
25
[DRN]
p-Chk2 (T68)
Protein Fold Change
1.0
0.3
3.3
1.2
3.1
0.8
1.6
0.3
0
6.25
12.5
25
[DRN]
p-Chk2 (S516)
Protein Fold Change
1.0
0.6
1.2
1.0
1.7
1.0
3.3
0.8
0
6.25
12.5
25
[DRN]
Chk2 RNA
Fold Change
1.0
0.8
1.0
0.9
1.1
1.6
1.4
1.4
1.0
0.7
0.9
0.5
0μM
6.25μM
12.5μM
25μM
50μM
100μM
[DRN]

Figure 19. Inhibition of CHD4 inactivates the Chk2 pathway. Depletion of CHD4 leads to an activation of ATM, but inhibits the activation of Chk2. As a result, cells depleted of CHD4 may fail to activate the cell cycle checkpoint, leading to apoptosis. Included is a quantitative comparison of Chk2, pChk2 (T68), and pChk2 (S516) protein based on densitometry analysis of the shown westerns and mRNA differences between scramble U937 cells (blue) and CHD4 depleted cells (red).

CHD4 depletion alters the expression of genes involved in Leukemic Cell Death. Since CHD4/NuRD has best been described as a transcriptional regulation complex, we performed microarrays to investigate if the transcriptional alterations that result from the depletion of CHD4 could contribute to the increased sensitization of the AML cells to the genotoxic agents. Probe sets were considered to be differentially expressed if the false discovery rate (FDR) was less than 0.05, which resulted in 1,320 and 675 differentially expressed genes in U937 and MV4-11, respectively. We then utilized a Downstream Effects Analysis in the Ingenuity Pathway Analysis (IPA) software to interpret the biological implications of gene expression alterations (Figure 20). According to this analysis, CHD4 depletion resulted in a net increase in the expression of genes previously reported to induce cell death of leukemic cells and concomitantly reduced the expression of genes previously reported to prevent cell death of leukemic cells. Taken together, this analysis indicates that the transcriptional alterations associated with CHD4 depletion may contribute to the increased sensitization to genotoxic agents. However, validation by western blots did not result in significant changes to protein concentrations of promising gene targets (Bik, BCL2, ERK, MCL1) found in this analysis.

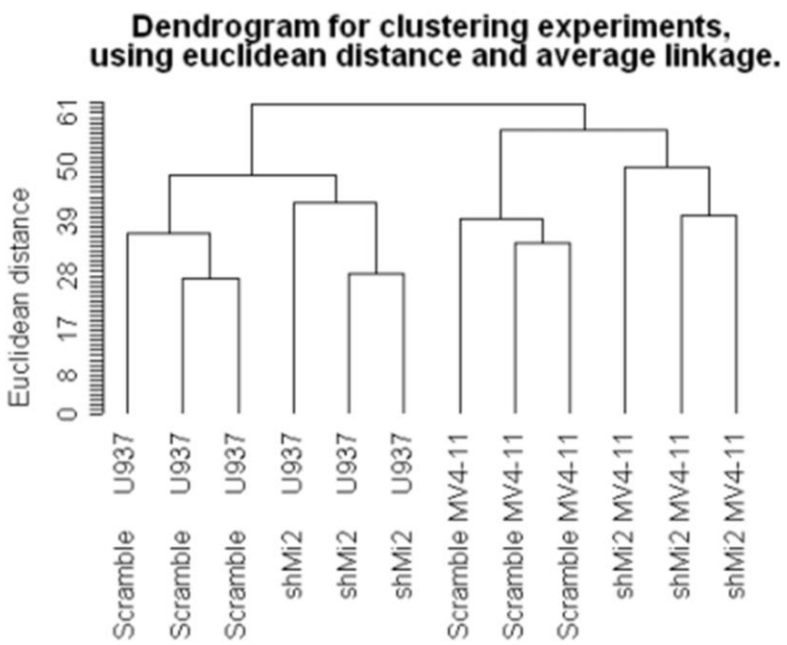

FDR = 0.05

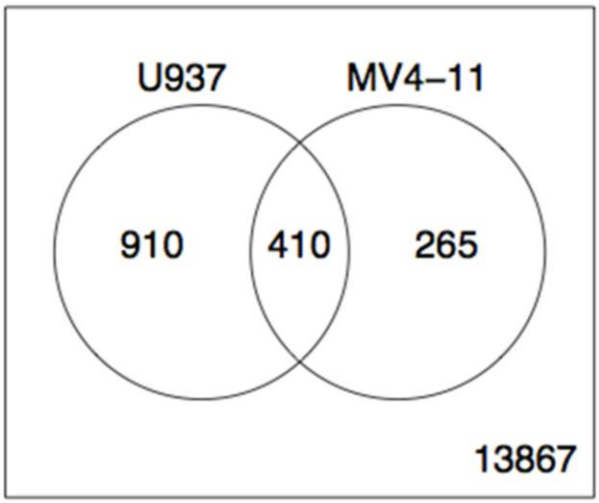

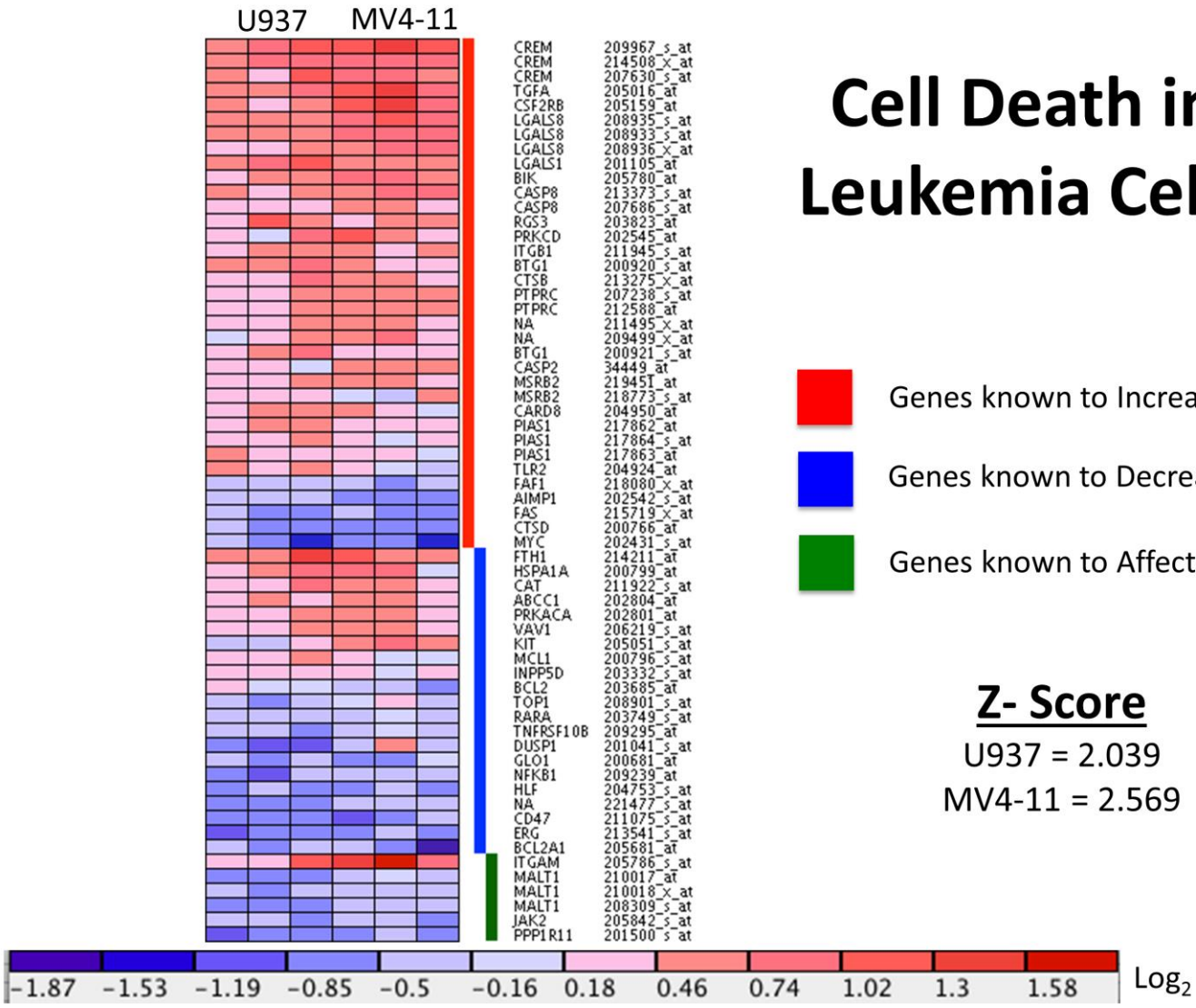

Cell Death in Leukemia Cells

Genes known to Increase

Genes known to Decrease

Genes known to Affect

Z- Score

U937 = 2.039

MV4-11 = 2.569

Figure 20. Depletion of CHD4 may increase cell death in leukemic cells through gene expression alterations. Microarray arrays were performed to determine the gene expression alterations associated with CHD4-depletion. Setting a cutoff of an FDR to less than 0.05 resulted in 1320 significantly differentially expressed genes in U937 and 675 in MV4-11, with 410 overlapping genes. The Ingenuity Pathway Analysis software was used to make biological predictions based on the differentially expressed genes. This analysis predicted a significant increase in cell death of leukemic cells (Activation Z-score of 2.039 and 2.569 for U937 and MV4-11, respectively).

Discussion

CHD4 and its associated NuRD complex have emerged as key mediators of the double-stranded DNA damage repair pathway[23,24] and gene expression, most notably repression of hyper-methylated tumor suppressor genes in cancer.[48,64] Here, we describe the first study that examines the interplay of CHD4's dual functionality in AML. We observed that the partial depletion of CHD4 in AML cells induces a global relaxation of the chromatin structure (Figure 9A-B), which is similar to previous reports in Ramos[84] and HeLa[98] cell lines. CHD4 depleted AML cells were also found to be more susceptible to the formation of DSBs (Figure 9C-E, 10), consistent with evidence that CHD4 protects U2OS osteosarcoma cells from ionizing radiation[56,57,81] and that relaxed chromatin is more susceptible to the formation of DSBs than condensed chromatin[99,100]. In addition, our results show that the DNA of CHD4-depleted cells was more exposed to intercalation by DNR (Figure 14), consistent with the greater capacity of anthracyclines to bind nucleosome-free DNA[101]. CHD4-depleted AML cells also failed to efficiently repair the resulting genotoxic agent-induced DSBs (Figure 9C-E, 10). Probing ATM pathway components in CHD4 depleted AML cells revealed a Tip60-mediated activation of ATM prior to DNA damage as well as an ATM-dependent stabilization of the pro-apoptotic transcription factor E2F1 upon induction of DSBs (Figure 18). Additionally, depletion of CHD4 was found to deregulate the Chk2 pathway (Figure 19) and altered gene expression to induce cell death of leukemic cells (Figure 20). Taken together, these results indicate that targeting CHD4 could increase the sensitivity of AML cells to genotoxic agents commonly used in therapy through a combination of increased susceptibility to the formation of DSBs and inhibition of their repair (Figure 21).

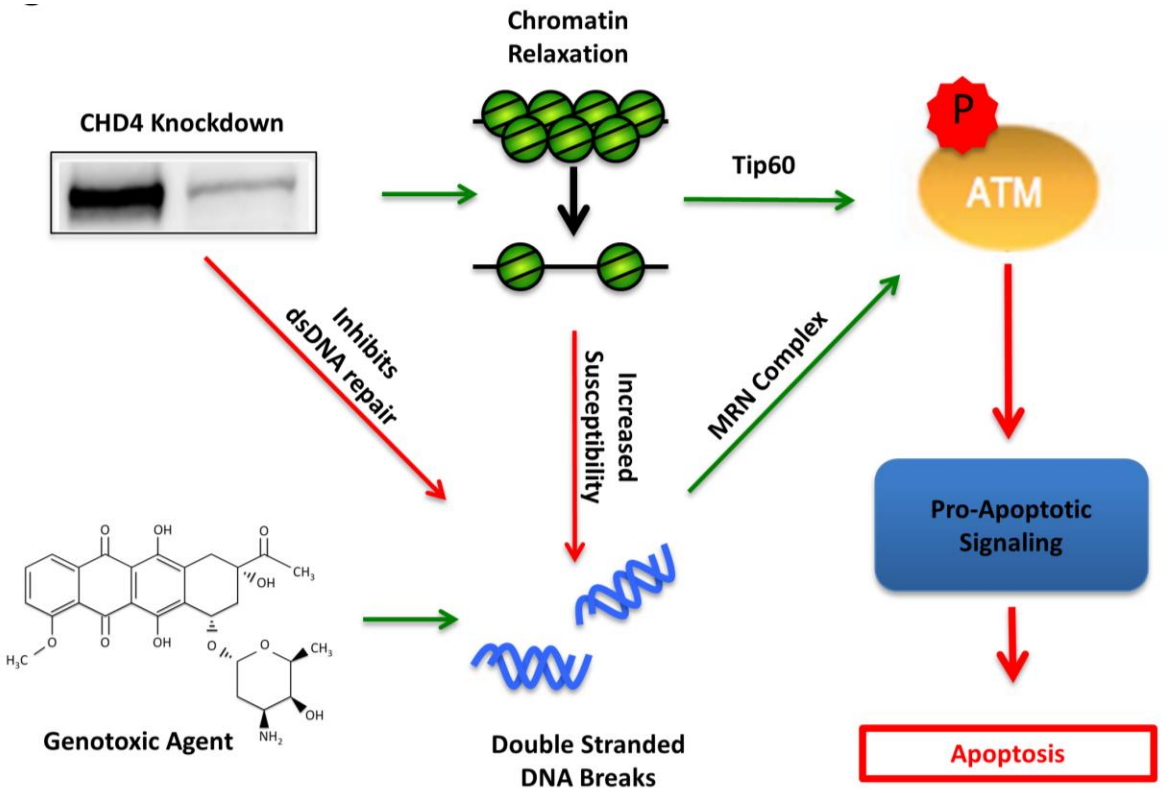

Figure 21. Model of CHD4 enhancement of genotoxic agent-induced apoptosis through DSB repair inhibition and chromatin relaxation. In AML blasts, depletion of CHD4 relaxes the chromatin, resulting in the activation of ATM through Tip60 and thereby primes the cells for apoptotic signaling. Moreover, the relaxed chromatin is more susceptible to genotoxic agent-induced DSBs. Additionally, CHD4 deficient blasts have impaired DSB repair, resulting in the accumulation of more DSBs and further activation of ATM through the classical Mre11, Rad50, NBs1 (MRN) complex. The net activation of ATM in CHD4-depleted cells increases its downstream pro-apoptotic signaling cascade, thereby resulting in apoptotic cell death.

Depletion of CHD4 in three AML cell lines and a primary AML patient sample increased the *in vitro* sensitivity to clinically relevant concentrations of single agent DNR and ara-C (Figure 12,13). Importantly, the increased sensitivity to DNR and ara-C occurred preferentially in AML cells, as normal CD34+ hematopoietic progenitors partially depleted of CHD4 did not demonstrate a similar increase in susceptibility (Figure 16A-B). We hypothesize that the preferential sensitivity of AML cells to CHD4 depletion may reflect disparate levels of endogenous CHD4 between normal CD34+ cells and AML cells, as AML cell lines and primary AML cells appear to contain significantly less total endogenous CHD4 protein compared to normal CD34+ progenitor cells (Figure 16C). It remains uncertain whether the diminished levels of CHD4 protein in AML cells reflects the normal differentiation of myeloid lineage cells or is associated in a yet to be determined way with the tumorigenic capacity of AML. Consistent with our findings, differences in CHD4 protein levels between tumors and normal tissue have been recently reported, but do not point to a conclusive trend. For example, decreased expression of CHD4 in ovarian tumors correlates with decreased progression-free and overall survival.[102] In contrast, increased expression of CHD4 in hepatocellular carcinoma was found to be associated with poor prognoses.[86] Therefore, differences in CHD4 protein levels between normal and malignant cells may be tissue specific. In any case, these findings argue that a threshold level of CHD4 may be required for efficient DSB repair, implying that leukemia cells containing less endogenous CHD4 may be more vulnerable to CHD4 inhibition than their normal counterparts.

As combinations of anthracyclines and high-dose ara-C form the foundation of both AML induction and salvage therapy, inhibiting CHD4 might enhance the efficacy of current regimens without increasing the required doses of these agents. This would be of particular

interest for anthracycline based-regimens, as the maximum lifetime dose of anthracyclines is severely limited by a cumulative, dose-dependent cardiotoxicity,[9] although study of CHD4 inhibition in cardiac tissue is needed to corroborate this. Furthermore, the chromatin-relaxation effect of CHD4 inhibition may have additional implications for anthracycline-based therapy, as anthracyclines have been found to displace nucleosomes from transcription start sites of genes located in regions of relaxed chromatin which deregulates the transcriptome and drives apoptosis in AML cells[103]. Thus, inhibition of CHD4 may also potentiate DNA damage-independent mechanisms of anthracycline-mediated anti-leukemic activities.

Chapter 3: Depletion of CHD4 modulates expression of AML cell genes that regulate tumor formation in vivo and colony formation in vitro.

Rationale

CHD4 is a core component of the NuRD complex, which is best known for its ability to epigenetically regulate gene expression. As previously mentioned, within the context of cancer, NuRD is known to repress the expression of tumor suppressor genes.[48] Our lab previously determined that the inhibition of the NuRD component MBD2 can lead to the restored expression of some of these repressed tumor suppressor genes in a breast cancer model, which results in a severe decrease in tumor cell proliferation both *in vitro* and in mice xenografts.[49] Furthermore, studies in our lab found that inhibition of CHD4 potentially has a significantly larger effect on NuRD-dependent gene regulation when compared to inhibition of MBD2.[67] Therefore, we hypothesized that inhibition of CHD4 would decrease AML cell proliferation due to the restored expression of NuRD-depended repressed tumor suppressor genes in AML.

Results

Inhibition of CHD4 improves survival in mice. As seen in Figure 17 (and repeated experiments shown in Figure 22), mice engrafted with CHD4 depleted cells harbored significantly lower tumor burden than mice engrafted with control cells, despite injection with equivalent numbers of viable leukemic cells at the same time.

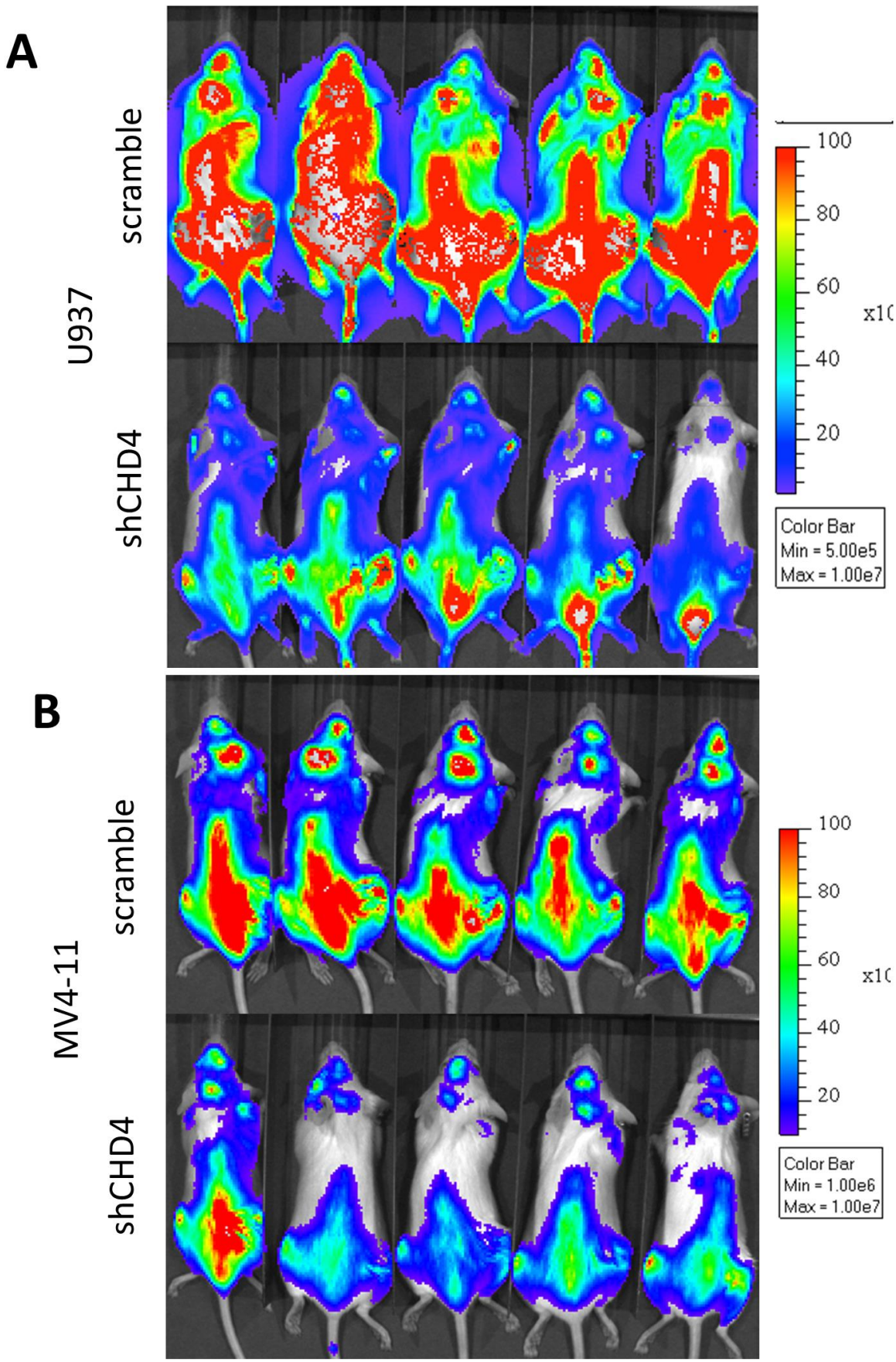
A
U937
scramble
shCHD4
100
80
60
40
20
x10
Color Bar
Min = 5.00e5
Max = 1.00e7
B
MV4-11
scramble
shCHD4
100
80
60
40
20
x10
Color Bar
Min = 1.00e6
Max = 1.00e7

Figure 22. Mice engrafted with CHD4 depleted AML cells harbored significantly lower tumor burden than controls. Despite injection with equivalent numbers of viable leukemic cells at the same time, mice engrafted with CHD4-depleted AML cells continuously harbored significantly lower tumor burdens than mice engrafted with control cells. Shown in this figure are the time points when mice engrafted control cells reached their humane endpoints. (A) Shown is day 16 post engraftment with $5x10^6$ U937 cells by tail-vein injection. For this replicate, mice engrafted with CHD4 depleted cells did not reach their humane endpoint until ~26 days post engraftment. (B) Shown is day 25 post engraftment with $5x10^6$ MV4-11 cells by tail-vein injection. For this replicate, mice engrafted with CHD4 depleted cells did not reach their humane endpoint until ~31 days post engraftment.

Given that depletion of other NuRD components has been shown to decrease the proliferation of tumor cells both *in* vitro and in *vivo*,[49] we first investigated if CHD4 depletion altered the proliferation rate of AML cells. CHD4 depletion did not significantly alter the *in vitro* (Figure 23) or *in vivo* (Figure 24) proliferation rate, nor did it alter the cell cycle distribution of the tested AML cell lines (Figure 25). Therefore, proliferative alterations are unlikely to account for the discrepancy in the tumor burden between mice engrafted with control versus CHD4-depleted cells.

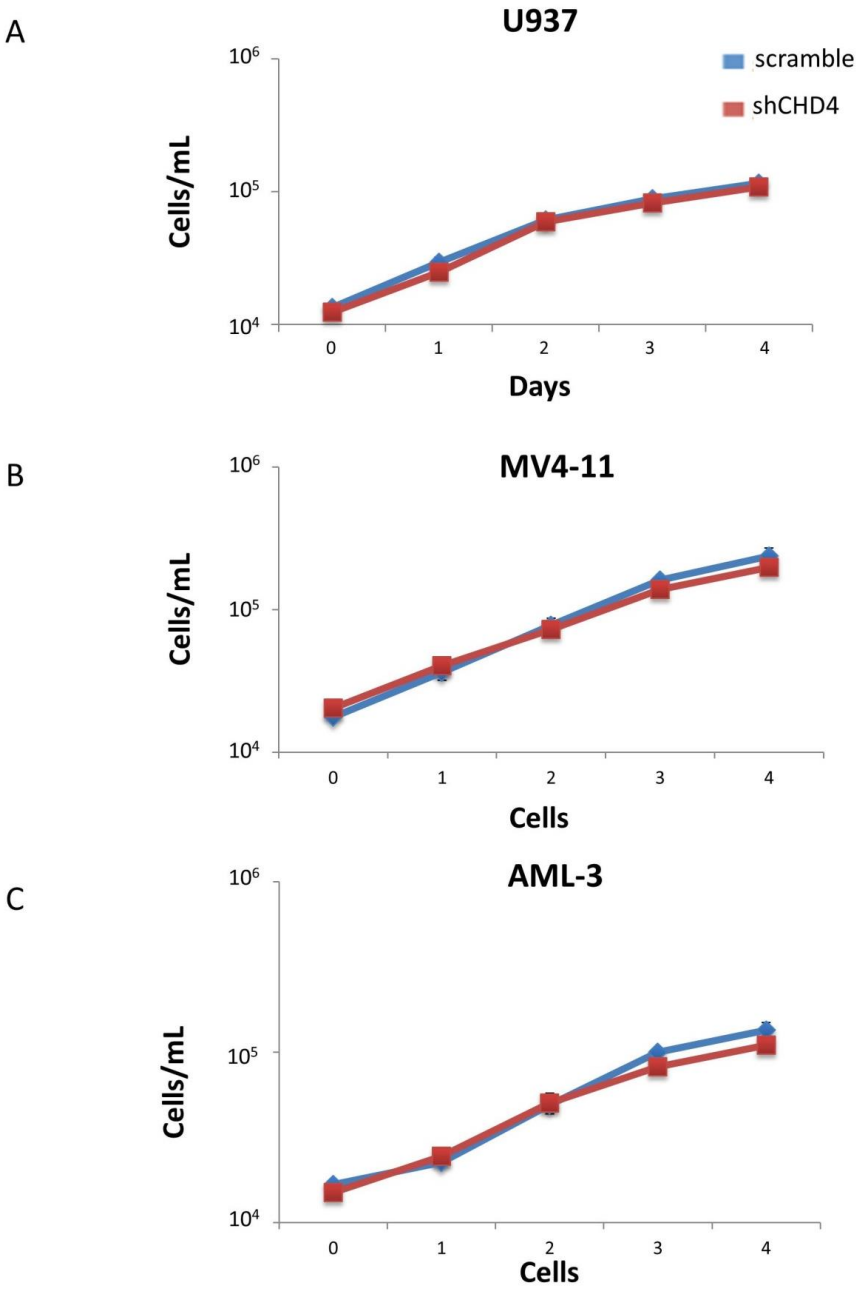

Figure 23. CHD4 depletion does not alter *in vitro* proliferation rate of AML cells. (A) U937, (B) MV4-11, and (C) AML-3 cells were seeded at a density of 150,000 cells/mL and the cell density was measured every 24 hours. CHD4 depletion did not alter the proliferation rate.

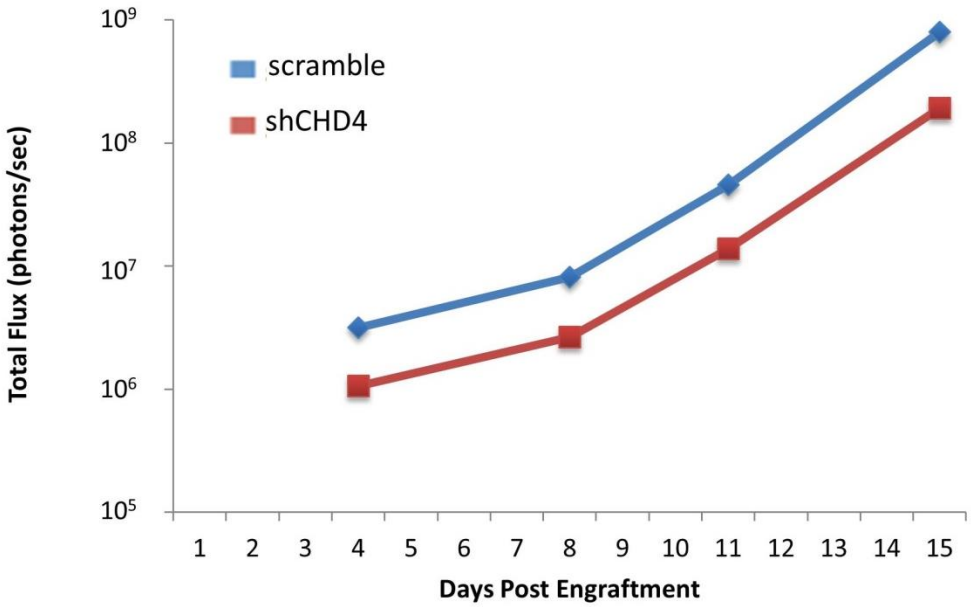

Figure 24. CHD4 depletion does not alter *in vivo* proliferation rate of U937 cells. The total radiance of untreated NSG mice engrafted with the same number of viable, luciferase-expressing U937 cells was measured over time. The radiance of mice engrafted with CHD4-depleted cells increased at a similar rate to that of mice engrafted with control cells, indicating that the *in vivo* growth rate of CHD4-depleted cells is similar to that of controls. However, the difference in the total flux between mice engrafted with CHD4-depleted cells and controls at early time points suggests that fewer CHD4-depleted cells are capable of engrafting.

A

U937

Scramble

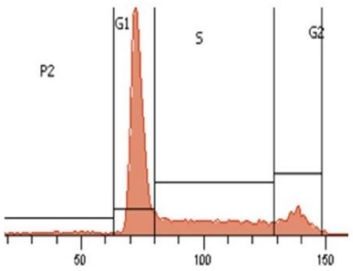

G1	53.8%
S	28.2%
G2	12.8%
P2	4.4%

shCHD4

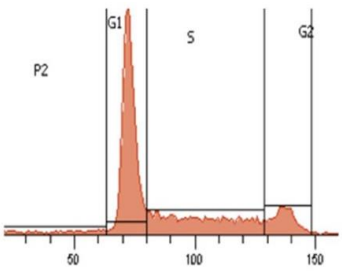

G1	51.2%
S	30.4%
G2	12.8%
P2	5.3%

B

MV4-11

Scramble

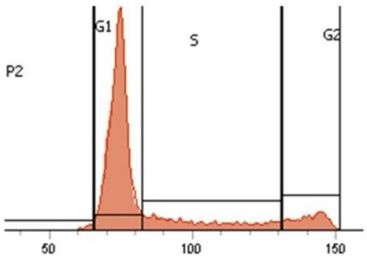

G1	66.7%
S	20.1%
G2	10.5%
P2	2.1%

shCHD4

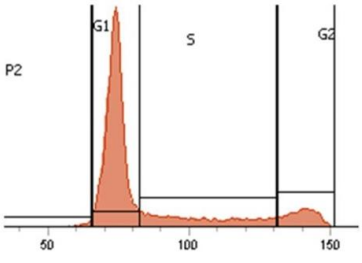

G1	66.1%
S	20.4%
G2	10.9%
P2	1.8%

C

AML-3

Scramble

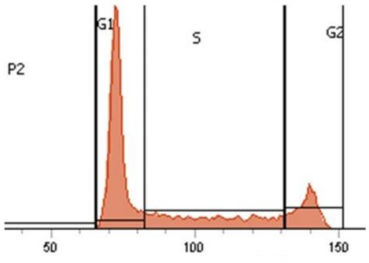

G1	54.3%
S	28.5%
G2	16.1%
P2	0.4%

shCHD4

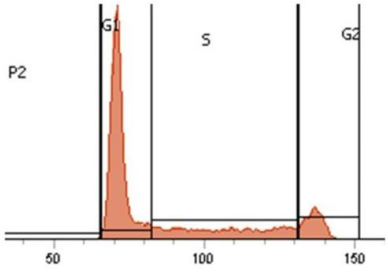

G1	58.1%
S	28.1%
G2	12.8%
P2	1.0%

Figure 25. CHD4 depletion does not alter the cell cycle distribution of AML cells. (A) U937, (B) MV4-11, and (C) AML-3 cells were stained with PI and analyzed using flow cytometry. CHD4 depletion did not significantly alter the cell cycle distribution of the cells.

An alternative explanation for the decrease in tumor burden is that CHD4 depletion reduces the tumor forming capacity of the leukemic cells. We performed soft agar colony forming assays, as leukemic cells capable of forming colonies in soft agar have been shown to possess the ability to initiate disease *in vivo*.[104] Indeed, CHD4 depletion sharply reduced the formation of AML colonies in soft agar (Figure 26, Figure 27), suggesting that CHD4 is required to maintain the full tumor forming ability of these cells. Of interest, we replicated the colony formation assays utilizing methylcellulose (Figure 28) and found similar results to the soft agar. Additionally, depletion of another NuRD component MBD2 resulted in a similar decrease of colony forming potential in the methylcellulose, albeit a lesser extent than what was achieved with the depletion of CHD4. This finding provides evidence that CHD4 may be acting through the NuRD complex to regulate colony formation.

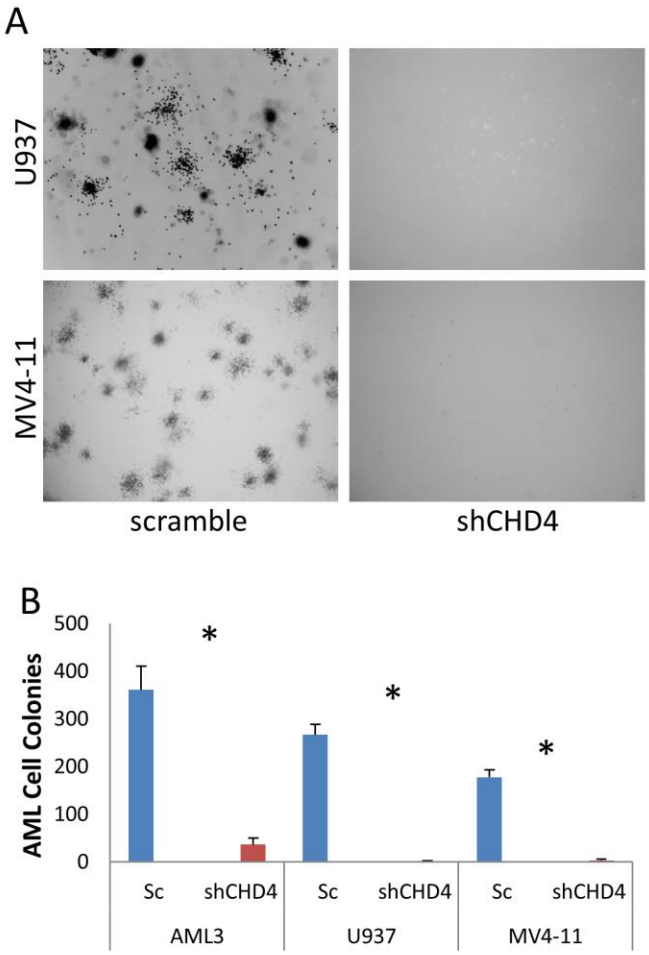

Figure 26. CHD4-depletion sharply decreases the colony formation potential of AML cells in soft agar. CHD4-depleted cells were inhibited in their ability to engraft into the NSG mice. CHD4-depletion severely reduced the ability of U937 and MV4-11 cell lines to form colonies in soft agar. (A) 20x representative images of colonies. (B) Quantitation of AML colonies (* indicates $p<0.05$, n=3)

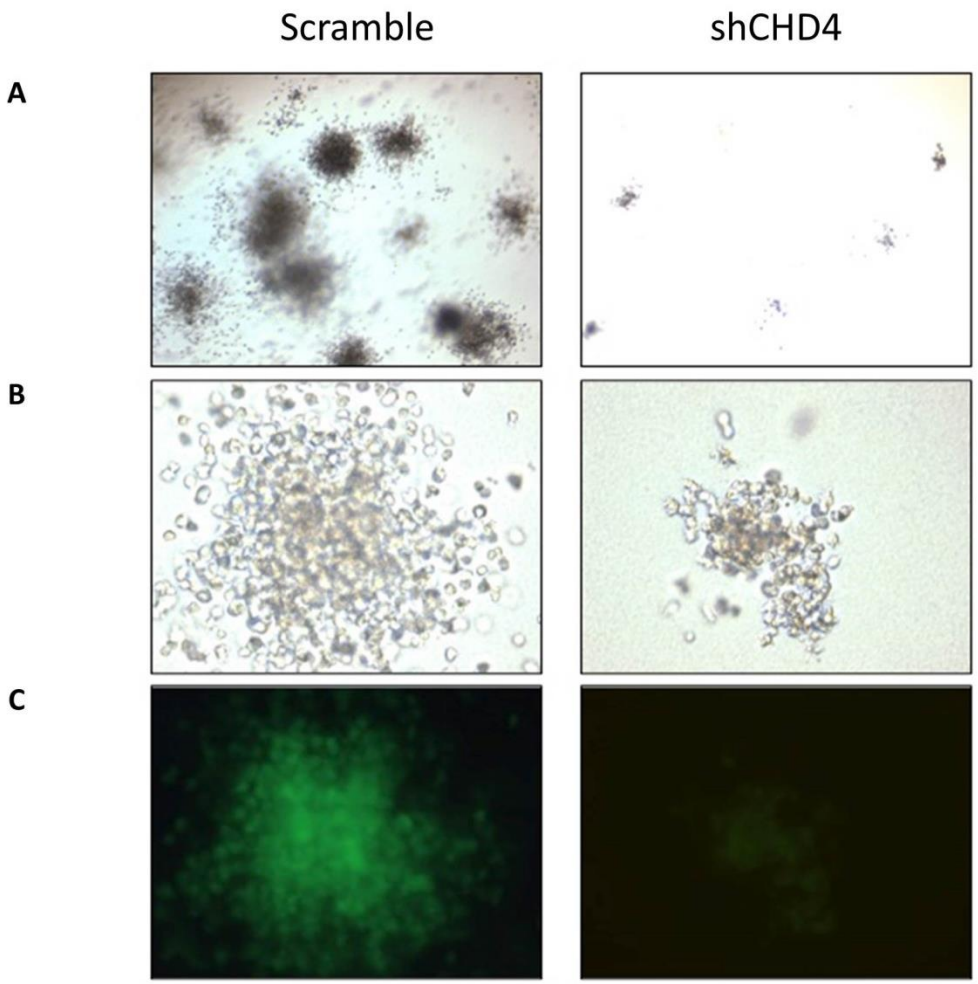

Figure 27. CHD4 depletion in AML3 cells restricts colony formation in soft agar. (A) 40x representative images of colony formation assay using AML3 cells. (B) 200x images of selected colonies shown in A. (C) 200x GFP fluorescent images of colonies shown in B. Since the vector used to express the shRNAs co-expressed GFP, the low expression of GFP in the few remaining colonies in the CHD4-depleted AML3 cells may indicate that the colonies formed due to insufficient CHD4 depletion.

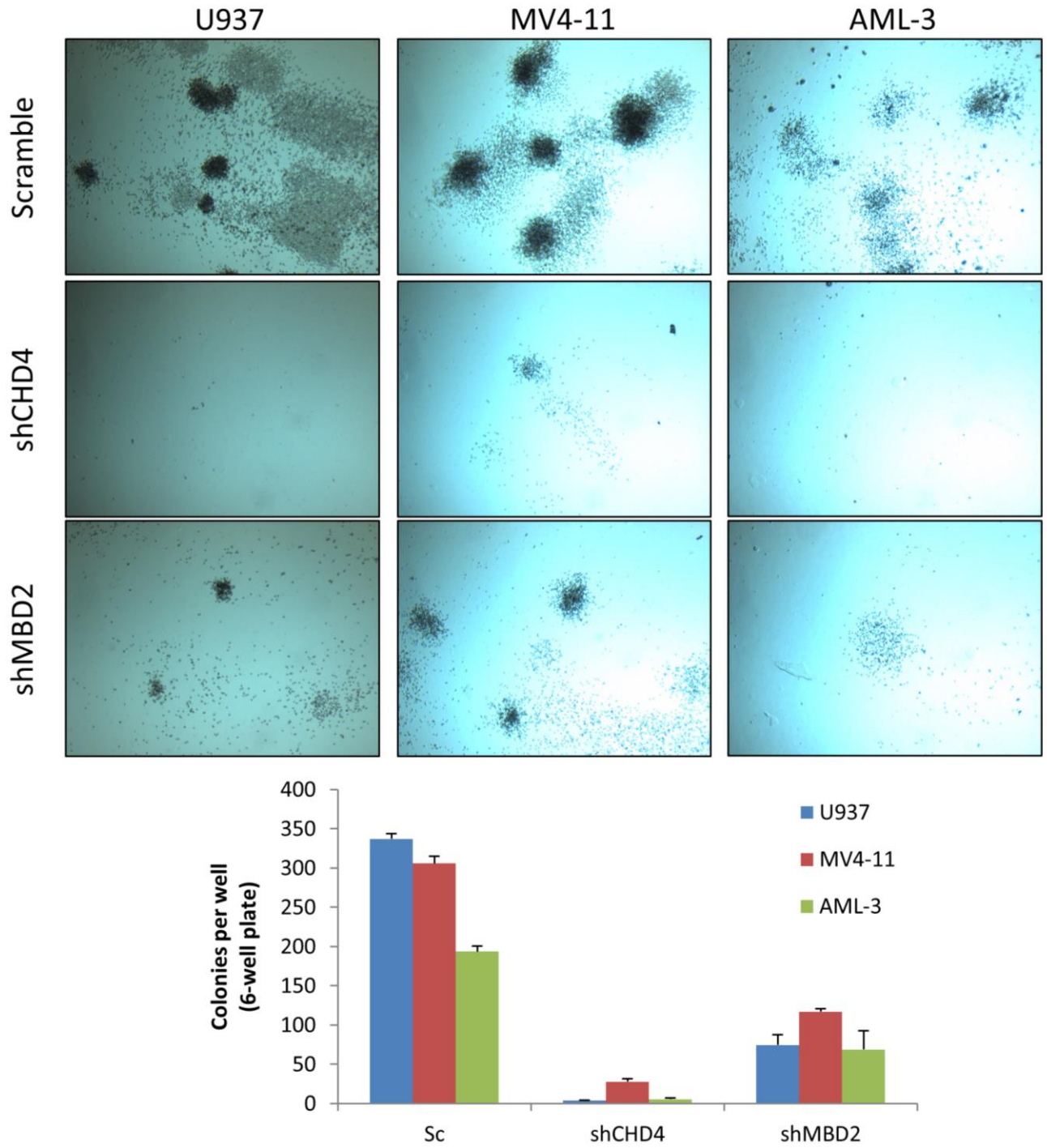

Figure 28. CHD4 depletion restricts colony formation in methylcellulose. We replicated the colony formation assays in methylcellulose and found, similar to the assays performed in soft agar, that CHD4 depletion decreases the number of colonies recovered. Additionally, we found that depletion of another NuRD component MBD2 resulted in a similar, albeit to a lesser extent. Shown are representative images of the colonies and their quantification.

CHD4 depletion alters the expression of genes involved in tumor formation. To gain insight into the molecular basis for this loss of colony forming potential, we reevaluated data from our previously mentioned microarray experiment. In addition to predicting an increase in cell death of leukemic cells, the IPA analysis indicated that CHD4 depletion results in a net decrease in the expression of genes previously reported to increase the colony-forming potential of tumor cells and concomitantly induces the expression of genes previously reported to decrease the colony forming potential of tumor cells (Figure 29). Taken together, the IPA analysis predicted a significant decrease in the colony formation potential of both U937 and MV4-11 cells.

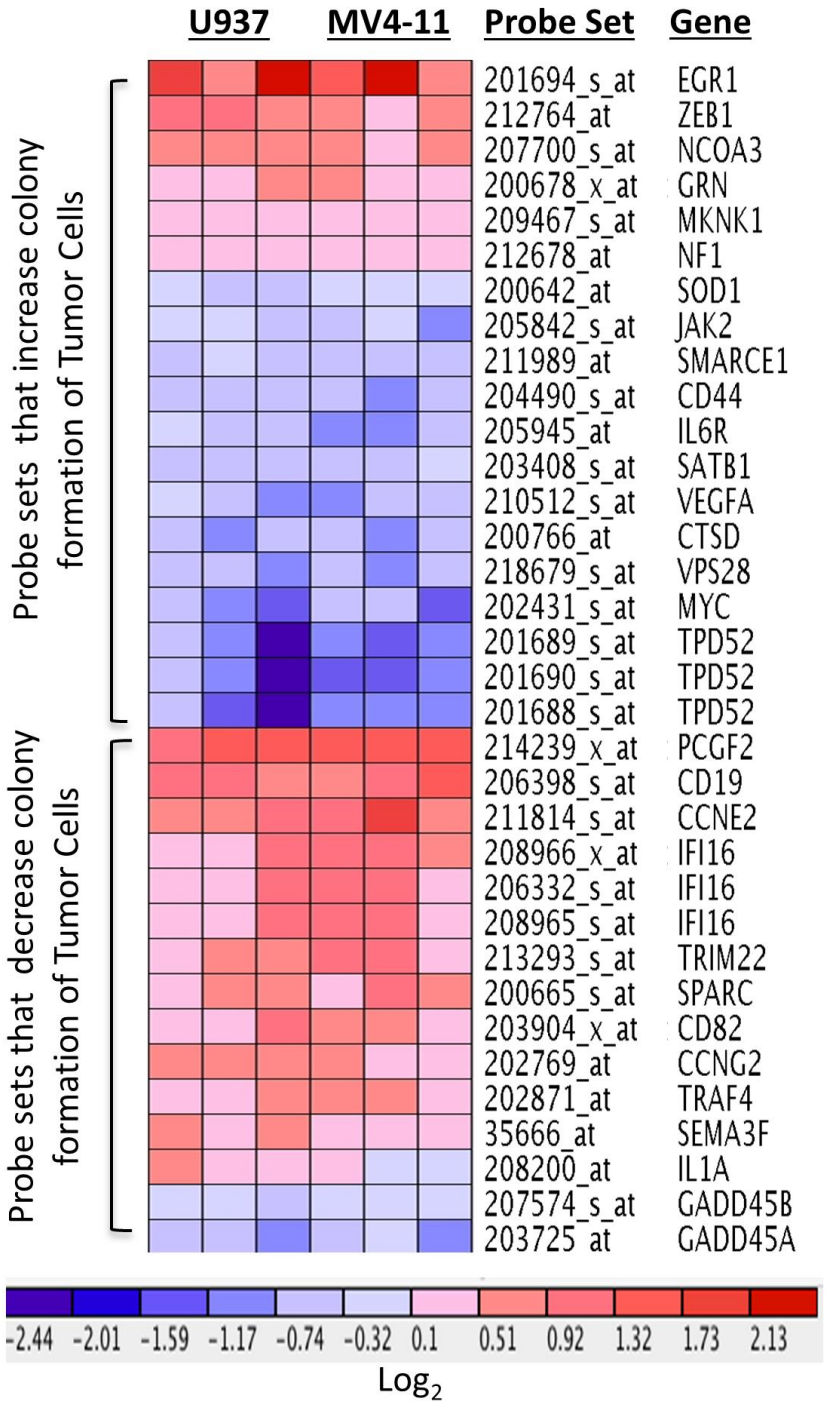

Figure 29. CHD4 depletion alters expression of genes involved in tumor formation. Microarray arrays were performed to determine the gene expression alterations associated with CHD4-depletion. The Ingenuity Pathway Analysis software was used to interpret the data and predicted a significant decrease in the colony forming potential in both U937 and MV4-11 (Activation Z-score of -2.044 and -2.002, respectively).

We then utilized quantitative PCR to validate the expression alterations of several genes whose differential expression has previously been shown to significantly alter the colony formation of AML and hematopoietic stem cells, including Myc and PCGF2.[105,106107] Consistent with the microarray data, Myc was found to be down regulated and PCGF2 was found to be upregulated in the CHD4-depleted AML cells (Figure 30). An additional 7 genes known to play a role in the pathogenesis of AML were also validated in CHD4-depleted AML cells (Figure 31).[2,108–114] In conjunction with the IPA analysis, these results indicate that transcriptional alterations induced by the depletion of CHD4 can at least partially explain the decrease in colony forming potential in AML cells.

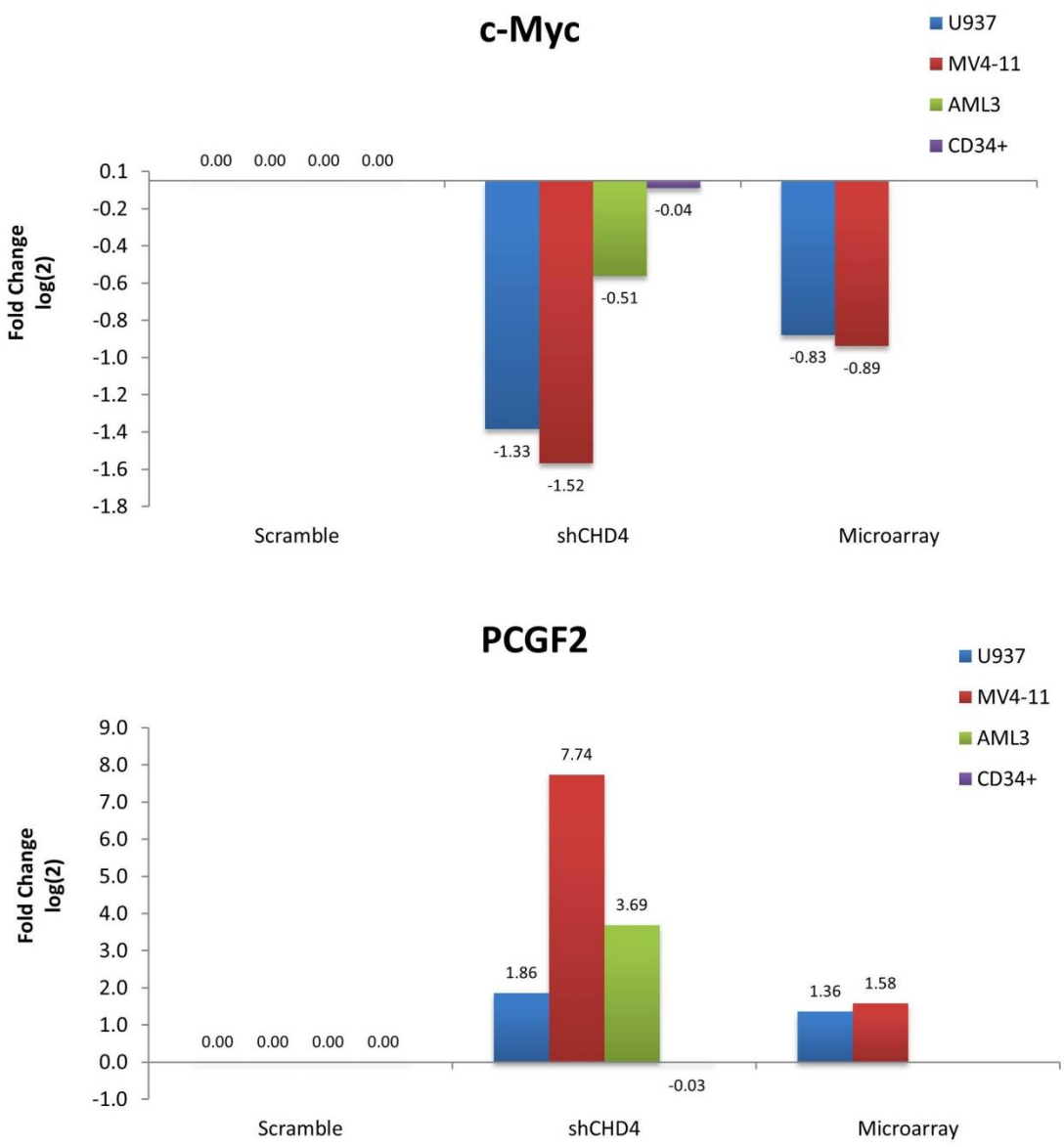

Figure 30. Quantitative PCR validation of c-Myc and PCGF2. Consistent with the microarray results, c-Myc was found to be down regulated and PCGF2 was found to be upregulated in the CHD4-depleted AML cells. However, CHD4 depletion in CD34+ hematopoietic progenitors did not significantly alter the expression of these genes. Values are expressed as fold change from control values in $\log_2$.

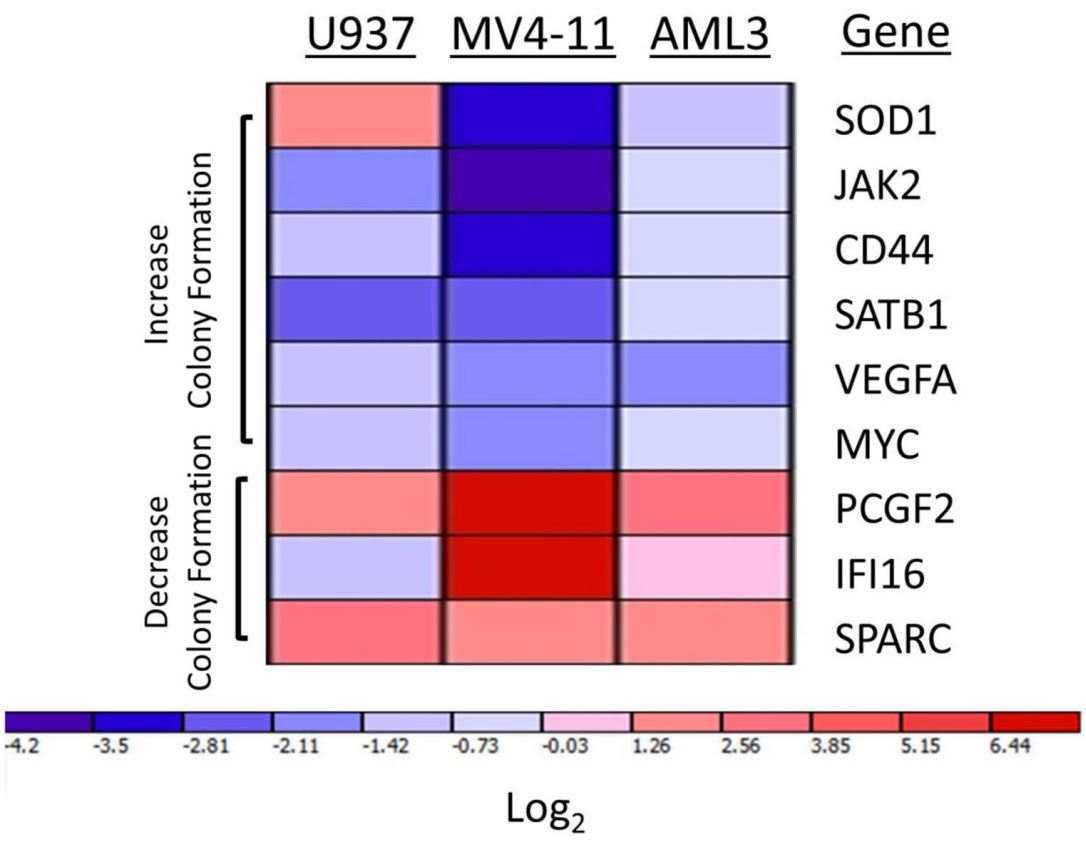

Figure 31. Microarray Validation. In addition to Myc and PCGF2, we validated 7 other genes included in the Ingenuity Pathway Analysis prediction by quantitative PCR. All 7 genes validated in MV4-11 and AML-3 cell lines, but only 5 validated in U937.

In contrast to the findings in AML cells, depletion of CHD4 did not significantly alter the colony forming potential of CD34+ cells isolated from normal donors (Figure 32). Consistent with this observation, the expression of neither Myc nor PCGF2 was significantly altered in the CHD4-depleted CD34+ cells (Figure 30).

A.

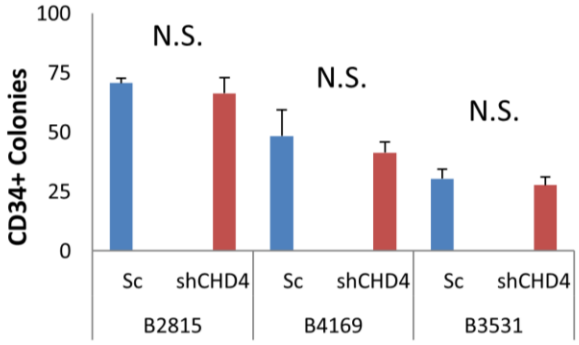

B.

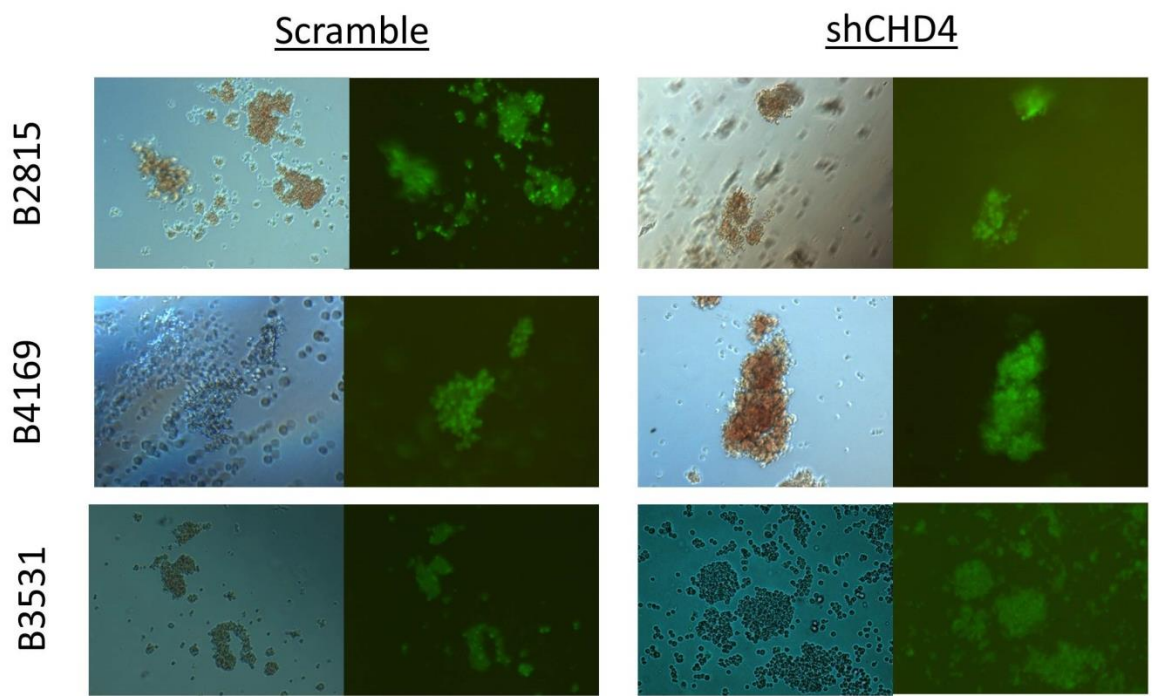

Figure 32. CHD4-depletion did not significantly alter the colony forming potential of CD34+ cells. (A) Depletion of CHD4 in CD34+ hematopoietic progenitors isolated from 3 normal donors did not result in a significant decrease in colony formation in methylcellulose. (B) Representative images of CD34+ colonies. 100X Images of colonies from CD34+ cells. Fluorescent images confirm that the colonies were indeed infected with the lentiviral vector containing the shRNA.

Discussion

In a clinically relevant mouse model of induction therapy, NSG mice engrafted with CHD4 depleted U937 cells displayed increased drug sensitivity and survival (Figure 17). An unexpected and important finding was that depletion of CHD4 significantly reduced the tumor burden of the xenografts, which resulted in an additional treatment-independent increase in survival.

Since our lab has previously shown that inhibition of the NuRD component MBD2 can sharply reduce breast cancer cell proliferation *in vitro* and xenograft formation *in vivo*,[49] we assessed the proliferative capacity of AML cells depleted of CHD4. In contrast to the breast cancer cells, we found that CHD4 depletion did not alter the *in vitro* or *in vivo* proliferative capacity of the 3 AML cells lines tested, nor did it alter the cell cycle distribution of these cells (Figure 23-25). Thus, we turned to investigating the tumor initiation properties of the CHD4 depleted cells. We observed that depletion of CHD4 sharply reduces the growth of AML colonies in soft agar (Figure 26, Figure 27) and methylcellulose (Figure 28), but not the growth of normal donor CD34+ hematopoietic progenitor colonies (Figure 32). This finding suggests that a minimal level of CHD4 is necessary for the maintenance of tumor forming behavior of leukemic cells and would lead us to hypothesize that a further depletion or knockout of CHD4 in the CD34+ cells would eventually result in a loss of colony formation potential of these cells.

We then investigated the molecular basis for the loss of colony formation using a microarray analysis (Figure 29). Based on the net gene expression changes induced by CHD4 depletion in U937 and MV4-11 cells, the Ingenuity Pathway Analysis software was able to successfully predict the observed reduction in colony formation. We then validated

a subset of the expression changes found in the prediction that have been previously associated with the pathogenesis of AML by means of quantitative PCR (Figure 30, Figure 31). Through this validation, we confirmed the majority of gene expression alterations found in the microarray. Although we focused our analysis on a subset of 9 genes, we do not believe that the alterations to these genes alone yield the observed reduction in colony formation. Rather, we believe that the observed phenotype is the result of the entirety of expression alterations induced by CHD4 depletion and that the subset of genes we focused on are merely the largest and easiest to detect alterations. Interestingly, we found that CHD4 depletion in CD34 cells did not result in the same gene expression changes to Myc and PCGF2 seen in the AML cells, which correlates with the observed colony forming assays.

AML cells that are capable of forming colonies have previously been defined as leukemic stem cells and are thought to be the cells that are capable of forming *de novo* and recurrent tumors *in vivo*.[104] Therefore, our findings suggest that a potential inhibitor of CHD4 would have a profound effect on inhibiting AML stem cells, although strong debate remains as to whether cell lines, such as the ones used in these studies, contain true, bonafide "leukemic stem cells". Future studies on the colony formation potential of primary AML cells depleted of CHD4 are needed to confirm our assertion. However, our finding that CHD4 depletion reduces colony and xenograft formation is consistent with evidence in the literature that implicates CHD4 and its associated NuRD complex in the maintenance of embryonic[115,116], myeloid[117], and tumor[85,86] stem cells. Although we attribute this decrease in colony formation to expression changes induced by CHD4 depletion, it should be noted that another group has reported that minimal amounts of DNA damage can impede

leukemic self-renewal and malignant hematopoiesis by inducing differentiation of leukemic stem cells.[118] Therefore, given that CHD4 plays a role in maintaining genomic integrity and the DSB repair pathway, the expression alterations from CHD4 depletion may not solely be responsible for the reduction in xenograft engraftment and colony formation.

Chapter 4: CHD4 as a therapeutic target in AML.

Rationale

We have identified that inhibition of CHD4 could increase the sensitivity of AML cells to standard genotoxic agents and reduce the tumor forming capacity of AML cells. Importantly, these effects are not seen in normal CD34+ hematopoietic progenitors. Based on this evidence, we believe that CHD4 is a promising therapeutic target for the management of AML.

Results

Depletion of CHD4 renders AML blasts more sensitive to the HDAC inhibitor Vorinostat. Since we have already established that CHD4 depletion sensitizes AML cells to the DNA-damaging agents DNR and araC, we next sought to determine if CHD4 depletion could sensitize AML cells to other agents. We decided to try the HDAC inhibitor Vorinostat (suberanilohydroxamic acid, SAHA) since CHD4 and HDAC 1/2 provide the chromatin remodeling activities of the NuRD complex. Consistent with our findings using DNR and araC, depletion of CHD4 does sensitize AML cells, but not normal CD34+ hematopoietic progenitors, to SAHA (Figure 33).

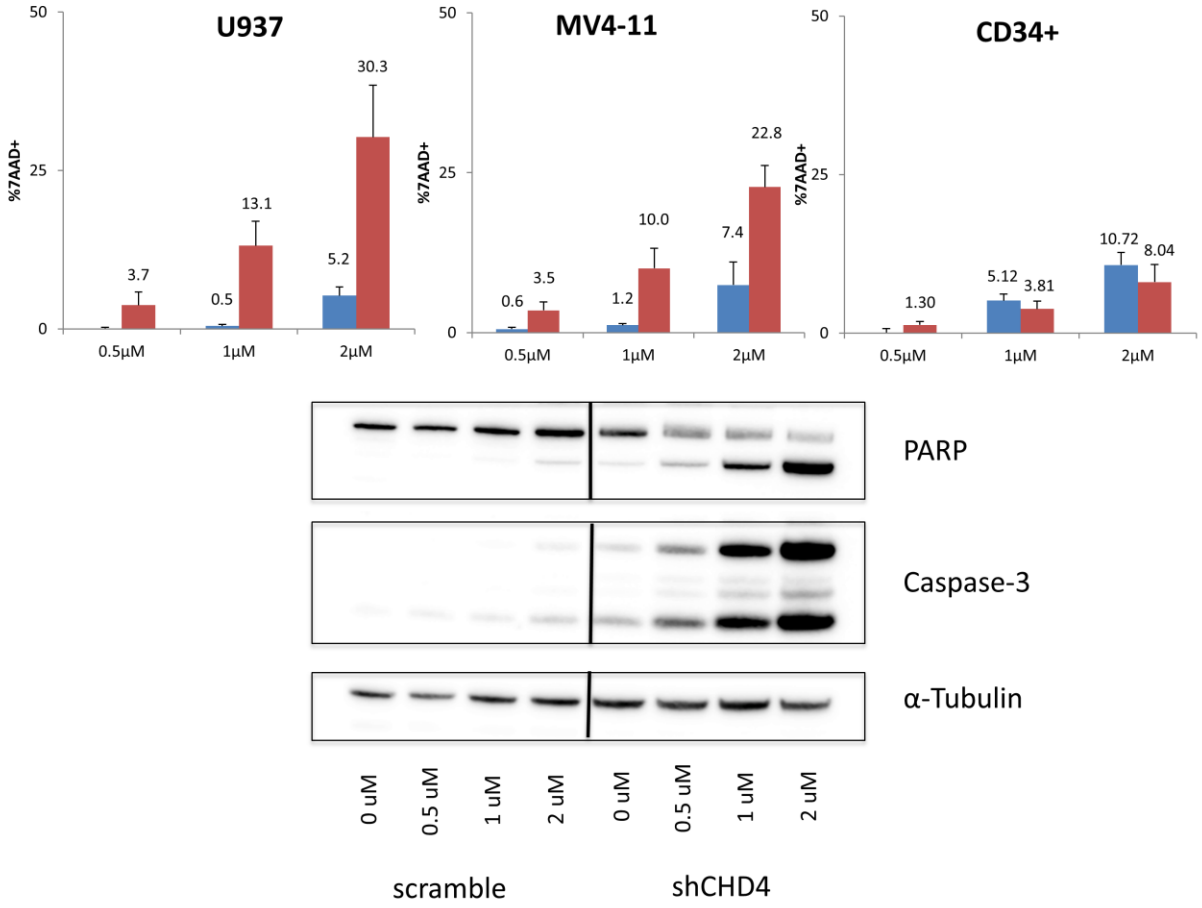

Figure 33. CHD4 inhibition sensitized AML, but not normal CD34+ cells to the HDAC inhibitor vorinostat. U937, MV4-11, and normal CD34+ hematopoietic progenitors were incubated with SAHA for 24 hours, after which a 7AAD stain was used to determine cell viability. CHD4 depletion (red) sensitized the AML cells to SAHA, but not the CD34+ cells. Shown are markers of apoptosis for U937 cells treated with SAHA.

Peptide inhibitor of CHD4. Previous studies determined that the transcriptional repression activity of the NuRD complex is dependent on the interaction of the tandem PHD domains of CHD4 to histone H3 tails on nucleosomes.[76] Functionally, the PHD domain of CHD4 was determined to allosterically regulate its own ATPase domain.[119] Therefore, a peptide inhibitor of CHD4 was designed to competitively inhibit the interaction of CHD4's PHD domains with the histone H3 tails (Figure 34A). This inhibitor consists of the first 12 amino acids of histone H3 with a trimethylation modification on K9, which was previously shown to increase the binding affinity.[76] To facilitate the entry of the peptide into cells, an F4R8 cell penetration tag (shown in grey) was added to the C terminus.[120] This F4R8 tag was made retro-inverso with D-isomers of amino acids to increase resistance to photolytic degradation.[121] To confirm that the peptide inhibitor binds to the PhD domains of CHD4, we generated a Heteronuclear Single Quantum Coherence (HSQC) spectrum by NMR on a purified sample of the second PHD domain of CHD4 (Figure 34B). We then titrated in our peptide inhibitor and tracked the peak shifts, until saturation was reached (Figure 34C) and calculated the binding affinity (K_D) of CHD4's PHD2 domain for our peptide to be ~16μM (Figure 34D).

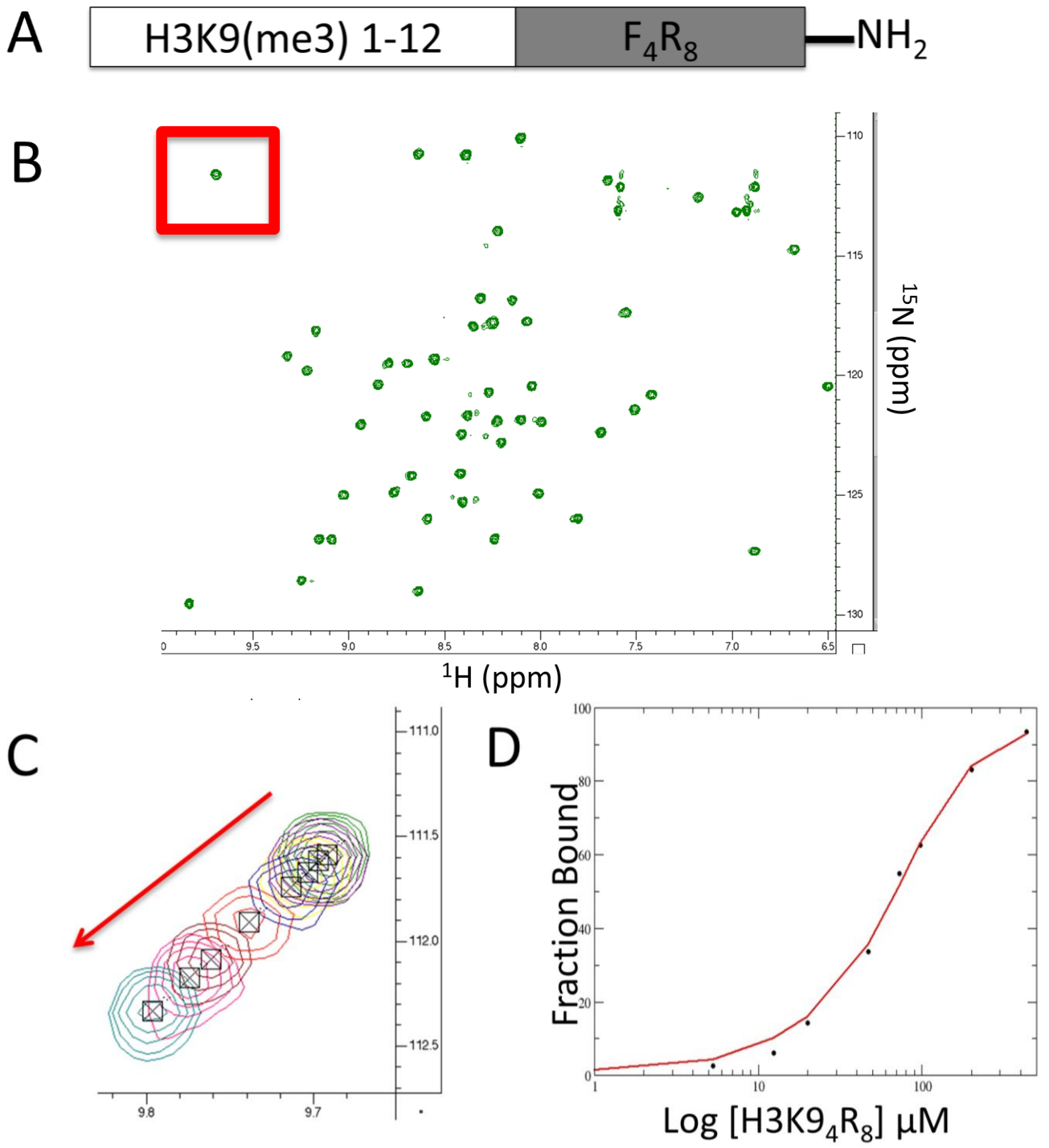

Figure 34. Peptide inhibitor of CHD4. CHD4 contains two tandem PHD finger domains that bind to Histone H3 tails. (A) Schematic of our retro-inverso peptide inhibitor. (B) HSQC spectra of PHD2 domain of CHD4. (C) Shown is the shift of the peak highlighted in red in the HSQC as the peptide was titrated in. Peaks traveled in the direction of the arrow. (D) The K_D of PHD2 for the peptide inhibitor was ~16µM.

Next, we wanted to confirm that the peptide inhibitor was able to gain entry into cells. The inhibitor was fluorescently labeled by adding a Hylite-488 fluorophore to the N-terminus. MDA-MB-435 cells were adhered to a glass bottom culture dish and treated with 10μM of fluorescently labeled inhibitor in serum containing media. Intracellular fluorescent intensity was monitored by time lapse confocal microscopy. Fluorescent images shown depict a representative of one of six fields observed immediately following (Figure 35A) and 30 minutes post treatment (Figure 35B). Similar to findings of Takayama et al., the influx of peptide into the cell tended to occur at specific locations, rather than across the entire plasma membrane. Additionally, we detected not only the presence of inhibitor within every cell observed, but also a presence within the nucleus. To confirm that the inhibitor could gain entry into hematopoietic cells, isolated CD34+ hematopoietic cells were incubated for 30 minutes with 10μM fluorescently labeled inhibitor in serum containing media. The cells were then washed repetitively with PBS and treated with trypsin to digest surface-bound peptide. Fluorescence microscopy was used to detect the presence of inhibitor within the cells (Figure 35C). CID cells, mouse hematopoietic cells that model human globin expression, were then treated with PBS control, 10μM control peptide, or 10μM inhibitor once a day for 48 hours to determine biological activity of the peptide. Expression of γ-globin, a gene known to be repressed by the NuRD complex, was determined to be higher in cells treated with the inhibitor compared to the control peptide (Figure 35D). Note, Figure 35D is a combination of results for the first 2 experiments performed; however, further replications were extremely inconsistent. Additionally, many proteins are capable of binding to H3K9me3 histone tails. Therefore, we are unsure if the reported increase in ϒ-globin was actually caused by the peptide inhibiting CHD4.

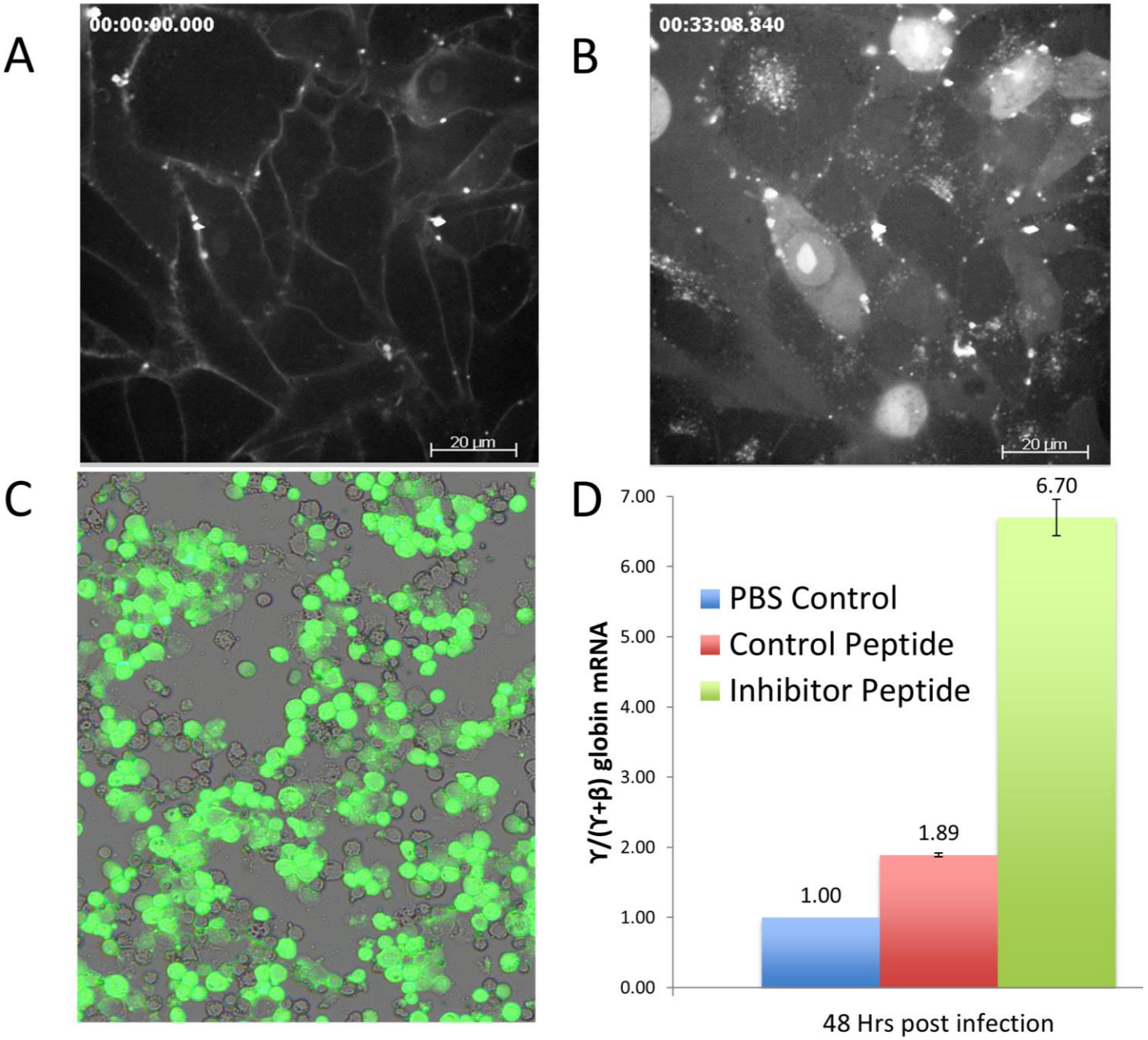

Figure 35. Peptide inhibitor of CHD4 inside cells. The inhibitor was labeled with a Hylite-488 fluorophore and placed onto MDA-MB-435 cells. Confocal microscopy was used to follow the peptide as it penetrated the cells. Shown are representative images immediately following the addition of the peptide to the cells (A) and 30 minutes later (B). Interestingly, the peptide penetrated the nucleus and nucleolus. (C) Human CD34+ cells were incubated with the peptide for 30 minutes and then treated with trypsin to demonstrate that the peptide would penetrate hematopoietic cells. (D) The peptide was placed onto CID cells where it induced the expression of Υ-globin, presumably by inhibiting CHD4/NuRD.

Discussion

While AML responses to single agent HDAC inhibitors have been modest at most, numerous preclinical studies are finding more synergy between HDAC inhibitors and other compounds, including inhibitors to Cyclin-dependent kinases, tyrosine kinases, cell cycle checkpoints, and the proteasome.[122] Therefore, we continued our work on CHD4-dependent sensitization of AML cells and found that CHD4 depletion also sensitizes AML cells to the HDAC inhibitor SAHA. We hypothesize that this sensitization to HDAC inhibitors may be induced by a further inhibition to the enzymatic functions of the NuRD complex, as CHD4 and HDAC 1 or 2 provide the known chromatin remodeling activity of NuRD. However, SAHA and other HDAC inhibitors have previously been reported to induce DSBs[123], indicating that a similar mechanism of sensitization as was found for DNR and araC could be responsible for the sensitization of SAHA. Further studies on the synergy between additional HDAC inhibitors and CHD4 inhibitors need to be performed. Regardless of the exact mechanism of sensitization, a potential CHD4 inhibitor could be used to potentiate the effects of HDAC inhibitors in AML.

Given the numerous domains required for the enzymatic function of CHD4, numerous opportunities and strategies exist for targeting CHD4. As a proof of principle, we developed a peptide that targets the PHD domains of CHD4. We showed that this peptide binds to the second PHD domain of CHD4 with a K_D of ~16μM and that the peptide can penetrate a cell membrane to gain access to the nucleus of tumor cells. We have not yet conclusively shown that this peptide can inhibit the function of CHD4, as nucleosome repositioning assays are required to demonstrate this, nor have we demonstrated any kind of specificity of our peptide for CHD4. However, future developments of CHD4 inhibitors

could take the form of peptides that target the PHD domains' interactions with histone tails, stabilize the chromo domains interaction with the ATPase-helicase domains, or even disrupt the interaction that CHD4 makes with the rest of the NuRD complex. Additionally, small molecule inhibitors could be screened to inhibit the ATPase-helicase domain directly.

Summary

The role of CHD4 in AML appears to be quite complex, as it exhibits a pro-oncogenic function through its role in tumor formation, but concurrently displays a tumor suppressor function in its facilitation of DSB repair. We attribute this apparent discrepancy to the diverse roles that CHD4 fulfills within a cell, including regulating gene expression and facilitating DNA repair. This exhibition of both pro-oncogenic and tumor-suppressor properties is shared with other chromatin modifiers such as HDAC1[124] and EZH2[125,126] and may reflect a general property of epigenetic regulators. Regardless, the data presented in these studies suggest that CHD4 represents a plausible, new therapeutic target in AML. Interestingly, this assertion was recently corroborated by a screening study performed in a mouse model of AML that identified the ATPase/helicase domain of CHD4 as a potential therapeutic target.[127]

Our work found that depletion of CHD4 sensitizes AML cells to DNA damage induced by the clinically used agents DNR and araC, both *in vitro* and *in vivo*. This sensitization is driven at least in part by the increased susceptibility of cells depleted of CHD4 to form DSBs and their impaired ability to repair such damage. Consistent with these findings, we observed that CHD4 depletion alters the important DSB repair pathways of ATM and Chk2. Additionally; we found that CHD4 depletion induces transcriptional alterations that may prime the cells for apoptosis before any treatment is administered. Therefore, we would expect a potential inhibitor of CHD4 to have a clear therapeutic benefit by enhancing the efficacy of current chemotherapeutic regimens without increasing the required doses of these agents. If true, a CHD4 inhibitor would be of particular interest for anthracycline based-regimens, which form the foundation of induction, consolidation, and salvage AML

therapies, as these regiments are severely limited by maximum lifetime doses of anthracyclines due to severe side-effects.

Unexpectedly, we also found that depletion of CHD4 significantly impedes the colony formation capacity and the subsequent xenograft engraftment of AML cells. We attribute this finding to the overall expression alterations induced by depletion of CHD4. Given that cells capable of forming colonies are thought to be the cells that are capable forming *de novo* and recurrent tumors *in vivo,*[104] a potential CHD4 inhibitor could also have broad implications for preventing tumor relapse.

Importantly, CHD4 depletion does not appear to sensitize normal CD34+ hematopoietic cells to DSB inducing agents, nor does it disrupt their colony forming potential. We attribute this discrepancy to the increased levels of endogenous CHD4 found in the CD34+ cells compared to AML cells. This difference in protein is important because it indicates that a potential inhibitor of CHD4 could have a "therapeutic window", in which a dose could be effective at achieving the desired effects in AML cells, while leaving the normal CD34+ cells in the bone marrow relatively untouched. This finding could have implications in terms of potential side-effects associated with a combination therapy of araC/DNR with a CHD4 inhibitor.

Given the numerous domains required for the enzymatic function of CHD4, numerous opportunities and strategies exist for targeting CHD4. Primarily, future developments of CHD4 inhibitors could take the form of peptides that target the PHD domains' interactions with histone tails, stabilize the chromo domains interaction with the ATPase-helicase domains, or even disrupt the interaction that CHD4 makes with the rest of

the NuRD complex. Additionally, small molecule inhibitors could be screened to inhibit the ATPase-helicase domain directly.

In conclusion, we have identified that CHD4 is a unique drug target in that a potential inhibitor would not only favorably alter the gene expression of tumor cells, but also would inhibit the DSB repair pathways of the cells. We therefore predict that an inhibitor to CHD4 could function through multiple mechanisms to yield an increase in patient survival.

Methods

Cells. Human AML U937 and MV4-11 cells were described previously.[128] OCI-AML3 cells were purchased from DSMZ (Braunschweig, Germany). Cells were cultured in RPMI-1640 (Gibco) supplemented with 10% Fetal Bovine Serum (Atlas), and 2% penicillin/streptomycin. Cell numbers were measured by a Cellometer Auto T4 (Nexcelom Bioscience).

Isolation of primary cells. This study was approved by the Virginia Commonwealth University Investigational Review Board and samples were collected with patient consent. Bone marrow was collected from AML patients with high disease load (>90% blasts in the marrow) and mononuclear cells were isolated by Ficoll-Hypaque gradient separation as described previously.[128] Normal CD34+ hematopoietic progenitor cells were isolated from de-identified apheresis units discarded by the VCU Bone Marrow Transplant unit as described previously.[67] All primary cells were cultured in StemSpan SFEM medium with 1× CC100 cytokine mix (StemCell Technologies) and 2% penicillin/streptomycin.

shRNA constructs were created as described previously.[67] Briefly, CHD4 target sequences (shCHD4-1: CGGTGAGATCATCCTGTGTGATA; shCHD4-2: GGACCTGAATGATGAGAAACAGA) and the Tip60 target sequence (CCTCAATCTCATCAACTACTA)[129] were cloned into a GFP-expressing pRRL.H1.shRNA vector and packaged into a lentivirus through calcium phosphate transfections in 293T cells. Infection efficiency was monitored by GFP on flow cytometry using a BD Caliper Flow

Cytometer. Cells were only used if the >90% of cells were GFP+ and the mean GFP intensity was between 100 and 500 units using the protocol described below.

Note: below 100 GFP units, the knockdown efficiency is too low and above 500 units, the cells would undergo apoptosis 7-9 days post infection due to over infection.

Note: all experiments began at least 6 days post infection with a lentivirus to give sufficient time for the protein knockdown and subsequent expression alterations to occur.

Flow Cytometry. GFP intensity was assessed on a BD Caliper Flow Cytometer at a flow rate of ~500 events per second with the following settings:

Parameter	Detector	Voltage	Amp	Mode
P1	FSC	E-1	6.72	lin
P2	SSC	287	3.12	lin
P3	FL1	339		log
P4	FL2	414		log
P5	FL3	535		log

Compensation:

FL1-LF2	0%
FL2-FL1	3.60%
FL2-FL3	0%
FL3-FL2	5%

All other flow cytometry was performed on a BD FACSCanto II Flow Cytometer.

Immunoblotting was performed as described previously.[130,131] Blots were imaged and quantitated using a Li-Cor Odyssey Fc Imager. Primary antibodies for the antigens studied were from several sources: H3K9ac, H3, H4K8ac, H4, cleaved-caspase 3, p-ATM (S1981), and ATM, all from Cell Signaling, CHD4 from Millipore, Poly(ADP-ribose)

Polymerase(PARP) from Biomol Research Laboratories, E2F1 from Santa Cruz, α-tubulin from Calbiochem.

Confocal Microscopy was performed on a Zeis 720 Meta microscope as previously described.[132] Primary antibodies used were against H3K9me3 and γ-H2A.X (Millipore). Images were quantified using the Velocity Image Analysis software (PerkinElmer).

1. To affix AML cells to the chamber slides (8 well, Nunc Lab-Tek II Chamber Slide w/cover, ThermoFisher)
    a. Add 250µL 1% Aqueous Alcian Blue (Electron Microscopy Sciences) and incubate at room temp for 30 min.
    b. Remove the Alcian Blue and rinse 4x with 500µL dH2O. Do not let the slides dry out.
    c. Harvest cells and wash 2X with PBS (to remove serum). Resuspend cells at $5x10^5$ cells/mL and add 200µL cells per well of Alcian Blue pretreated slide.
    d. Tape slides to a 96-well centrifuge adapter and spin at 500 RPM for 1 min (or slowest setting on centrifuge).
2. Wash wells 1x with PBS for 5 min
3. Fix the cells in 4% paraformaldehyde for 15 min.
4. Wash 2x with PBS for 5 min
5. Permeabilize the cells with 0.5% triton for 10 min
6. Wash 2x with PBS for 5 min
7. Block with 1% goat serum for 1 hr.
8. Add primary antibody and rock overnight at 4°C.
    Note: dilution for H3K9me3 antibody was 1:200
9. Wash 4x with PBS for 5 min
10. Add secondary antibody for 2.5 hours at room temp

11. Wash 4x with PBS for 5 min and protect from light.

Comet Assays were performed under neutral conditions using the Trevigen Comet Assay kit with modifications described below.

1. Prepare:

Lysis Solution

40mL of Trevigen lysis solution
4mL of DMSO
Cool to 4°C

Neutral Electrophoresis buffer

Prepare a 10X stock:

60.57g	Tris Base
204.12g	Sodium Acetate
450mL	dH2O

Adjust pH to 9.0 with glacial acetic acid. Adjust to final volume of 500mL. Sterile filter and store stock at room temp. Dilute 100mL 10X stock into 900mL dH2O to prep 1L of 1X working buffer and cool to 4°C.

DNA Precipitation Solution

Prepare a 10mL stock solution of 7.5M Ammonium Acetate

5.78g	NH_4Ac
10mL	dH2O

After the Ammonium Acetate dissolves, combine:

6.7 mL	7.5M NH_4Ac
43.3 mL	95%EtOH

SYBR Green Gold Solution

1µL	10,000X SYBR Gold in DMSO
30mL	TE Buffer, pH 7.5

TE buffer

10mM	Tris-HCl
1mM	EDTA
pH to 7.5	

Diluted solution is stable for several weeks at 4°C in the dark

2. Melt LMAgarose in a beaker of boiling water for 5 min, with the cap loosened, then cool in a 37°C water bath for 30 min. Warm CometSlides at 37°C for 30 min as well.

3. Harvest AML cells by centrifugation, wash 1x in ice cold CA^{++}/Mg^{++} free PBS, and then suspend cells at $1x10^5$ cell/mL in ice cold CA^{++}/Mg^{++} free PBS.

4. Combine 10µL of cells (diluted to $1x10^5$ cell/mL) with 90µL of 37°C LMAgaros, mix gently, and immediately pipet 50µL of mixture onto the prewarmed CometSlide. Spread the mixture out evenly on the sample area of the slide with the pipet tip.

4. Incubate slides on a level surface at 4°C in the dark for 30 min.

5. Incubate slides in 4°C Lysis solution for 1 hour (or overnight) at 4°C in the dark.

6. Equilibrate slides in 4°C 1X Neutral Electrophoresis buffer for 30 min at 4°C in the dark.

7. Place slides into the center of a DNA gel electrophoresis unit and align equidistant from electrodes. Insure each slide is facing the same direction. Add 4°C 1X Neutral Electrophoresis buffer, ensure buffer is not more than 0.5 cm above the slides. Apply voltage at 1V per cm of the electrophoresis unit (measured from electrode to electrode) for 1 hr.

8. Immerse slides in DNA Precipitation Solution for 30 min at room temp.

9. Immerse slides in 70% EtOH for 30 min at room temp.

10. Dry samples at 37°C for 15 minutes. Store slides in desiccant if necessary.

11. For analysis, stain each circle on the slides with 100µL of diluted SYBR Green Gold Solution for 30 min. Tap to remove excess solution and wash briefly in dH2O. Allow slides to dry completely at 37°C (~15 min) before using fluorescent microscopy to detect comets

    Note: Max excitation/emission of SYBR Green Gold is 496/522 nm

    Note: To facilitate analysis, you ideally only want 1-2 comets per image taken. Be sure to capture the ENTIRE tail and that all tails are oriented in the same direction on each image.

Comets were quantitated by the CASPLab Comet Assay software[133] with the following values:

Head Center Threshold	0.8
Use Comet Threshold	no
Tail Threshold	0.05
Head Threshold	0.15
Tail Cluster	Profile 1

Cell Sensitivity Assay. Cells were incubated with DNR (Sigma), ara-C (Sigma), or SAHA (Sigma) for 24 hours and stained with 7-Aminoactinomycin D (Sigma). Stain intensity was read by a BD FACSCanto Cell Analyzer to determine cell viability.

1. Prepare 7AAD
   Add 500µL DMSO to 1mg 7AAD. Make 25µL aliquots in black eppendorf tubes and store at -20°C. For working solutions, add 975µL PBS to the 25µL aliquot of 7AAD, store at 4°C for up to 2 weeks.

2. Add 4µL of working solution 7AAD to 1 mL of suspension cells (in 5mL flow tubes). Votex gently and incubate at 37°C for 15 min. Protect cells from light.

3. Staining was quantitated using a BD FACSCanto Flow Cytometer with the following settings:

Parameters	Type	Voltage	Log
FSC	A	170	off
SSC	A	286	on
Green	A	373	on
Orange	A	325	on
PE-Texas Red	A	400	on
488-670LP	A	400	on

Compensation

Fluorochrome	Value (%)
Orange - Green	40.00
PE-Texas Red - Green	8.00
488-670LP - Green	2.10
Green - orange	9.00
488-670LP - orange	100.00
PE-Texas Red - 488-670LP	16.00

Note: the 488-orange compensation is so high so as to remove the effects of DNR.

Cell Cycle Analysis was performed using the FxCyclePI/RNAse kit (ThermoFisher).

1. Harvest cells and wash in PBS

2. Resuspend $1x10^6$ cells into 1mL PBS.

3. Cool on ice and add 3mL cold (-20°C) 200 proof EtOH. Incubate for at least 1hr (can do over-night) at -20°C.

4. Pellet cells and remove buffer

5. Resuspend in 0.5mL of FxCyclePI/RNAse solution. Incubate for 30 min at room temp in the dark.

6. Analyze using 488/585 nm excitation/emission filter of flow.

***In vivo* studies** were approved by the VCU Institutional Animal Care and Use Committee and animals were treated humanely. Female NOD scid gamma mice (NSG, Jackson Laboratories) were engrafted intravenously via the tail vein with $5x10^6$ luciferase-expressing U937 cells. Tumor progression was monitored by the total radiance generated within each mouse upon subcutaneous administration of luciferin as measured by the IVIS 200 imaging system (Xenogen Corporation). Once tumor engraftment was confirmed, the mice were treated with a previously described model of the human "7+3" induction therapy.[88,89] Briefly, this regimen consisted of 3 consecutive days of Doxorubicin (100 mg/kg, Selleck Chemicals) and ara-C (33 mg/kg. Selleck Chemicals) given intravenously by tail-vein injection, followed by 2 additional days of ara-C (33 mg/kg) given by intra-peritoneal injection.

Colony Forming Assays were performed as previously described.[130] For AML cell lines, 5,000 cells were suspended in 1mL of 1x RPMI supplemented with 0.35% agarose (Difco), 10% FBS, and 2% penicillin/streptomycin and plated into a well of a 12-well plate. 5mL of water was placed in between the wells to prevent the agar from becoming too dry. Cells were allowed to grow for 14 days and colonies were identified as having >50 cells.

1. Melt 0.7% DNA grade agarose in microwave in sterile H2O. Place in a 40°C water bath for at least 30 min to cool. **It is important to insure that the agarose is not >40°C, otherwise the cells will be killed.**

2. Prepare 2mL aliquots of 2X RPMI + 20% FPS + 2X Pen/Strep in 15mL tubes for each condition. Warm to 37°C

3. Dilute cells of interest to $2x10^5$ cells/mL.

4. Add 2mL of the melted 0.7% agar and 100µL of diluted cells to a tube containing the 2X RMPI. Vortex gently to mix and plate 1mL into 3 wells of a 12 well plate.

5. Let the plate incubate at room temperature for 15 minutes to allow the agar to solidify, then add 5mL sterile H2O in between wells to prevent the agar from becoming too dry.

6. Incubate the plates for 10-14 days at 37°C. Count colonies that contain >50 cells.

Note: It is important to perform step 4 quickly, as the agar will begin to solidify soon after being removed from the 40°C bath.

For CD34+ cells, the Methocult H4434 Classic kit (Stem Cell Technologies) was used per manufacture's protocol. The soft-agar colony formation assays were replicated in the Methocult H4434 Classic kit as well for the AML cell lines.

Microarray analysis was performed using HG-U133Ax2 GeneChips (Affymetrix). Quality of the hybridization was assessed by examining the average background, scaling factor, percent of probe sets called present by the detection call algorithm, and the 3':5' ratio for GAPDH and ACTIN. Each GeneChip was independently normalized using quantile normalization and the robust multi-array average method was applied to probe set expression summaries.[134] For each probe set, a moderated t-test was used to make comparisons using the limma Bioconductor package[135,136] in the R programming environment.[137] The p-values were used in estimating the false discovery rate using the

Benjamini and Hochberg method[138] and probe sets having an FDR<0.05 were considered significant. Pathway analysis of the significant probe sets was performed using the Ingenuity Pathway Analysis software (Qiagen).

Quantitative PCR was performed on an Applied Biosystem 7500 Fast Real-Time PCR system. RNA was extracted in 1mL TRIzol (Life Technologies) and converted to cDNA with an iScript cDNA Synthesis Kit (Biorad).

RNA Extraction

1. Add 200µL of chloroform to 1mL of cells thoroughly dissolved in TRIzol. Shake for 15 sec and incubate at room temp for 2 min.

2. Centrifuge at 12,000g for 15 min at 4°C. Remove 500µL of the top layer and save in a new tube. To this top layer, add (in order):
   1µL glycogen
   0.4mL Isopropanol
   Invert 6x to mix and incubate for 10 min at room temp.

3. Centrifuge at 12,000g for 10 min at 4°C. Discard the supernatant after confirming presence of pellet.

4. Wash with 1mL of 4°C 75% EtOH and vortex gently.

5. Centrifuge at 7,500g for 5 min. Remove EtOH, zip spin tube and remove as much remaining EtOH, then air dry pellet for 5 min until it become slightly translucent. Add 20µL dH2O and incubate on ice for 10 min.

6. Quantitate RNA concentration on nanodrop and dilute to 200 ng/µL.

7. DNase treat the cells:
   10µL RNA
   0.5µL DNase I
   0.5µL Super RNase Inhibitor
   2µL DNase Buffer
   7µL ultra-pure H2O
   Incubate at 37°C for 30 min, heat inactivate at 97°C for 10 min.

8. Synthesize cDNA

5µL	DNase treated RNA
0.5µL	RTase
2µL	RT mix
2.5µL	ultra-pure H2O

9. Quantitative PCR

12.5µL	FastStart SYBR Green Reaction Mix (Rox)
7.5µL	primer mix (0.1µM Forward and Reverse)
5µL	cDNA

All primers were designed using the IDTdna website to have a Tm of 60°C. All results were normalized to GAPDH.

qPCR Primers

Gene	Forward	Reverse
CD44	TACATCCTCACATCCAACACC	GTGCCATCACGGTTAACAATAG
CHD4	AGTGCTGCAACCCATACCTCT	ATGCCCACCCTCCTTAAGGTTCTT
Chk2	GCGCCTGAAGTTCTTGTTTC	GTCCTATGCTCAGAGAAAGGTG
GAPDH	TCGACAGTCAGCCGCATCTTCTTT	ACCAAATCCGTTGACTCCGACCTT
IFI16	AAGTTCCGAGGTGATGCTG	CTTTCTTGATAGGGCTGGTCC
JAK2	AGATGGAAACTGTTCGCTCAG	TAGGCCTCTGTAATGTTGGTG
Myc	TTCGGGTAGTGGAAAACCAG	AGTAGAAATACGGCTGCACC
PCGF2	GACGAGCCACTGAAGGAATAC	GCTGGACACGGTACTTGAG
SATB1	CTTTAAAACACTCGGGCCATC	CCTTTCTCACCAGCACAAATTC
SOD1	TGGCCGATGTGTCTATTGAAG	GCGTTTCCTGTCTTTGTACTTTC
SPARC	ATGACAAGTACATCGCCCTG	GAGAATCCGGTACTGTGGAAG
VEGFA	CATCACCATGCAGATTATGCG	CCTTTCCCTTTCCTCGAACTG

Funding

This work was supported by NIH R01 CA 67708 (SG) and Leukemia and Lymphoma Society of America Grant #6472-15 (SG), NIH R01 DK 29902 (GDG), VCU Massey Cancer Center Support Grant NCI 5P30 CA016059, and VCU CCTR grant NIH ULITR000058.

Services and products in support of the research project were generated by the VCU Massey Cancer Center Flow Cytometry, Biostatistics, and Tissue and Data Acquisition and Analysis Core Shared Resources, supported, in part, with funding from NIH-NCI Cancer Center Support Grant P30 CA016059.

Microscopy was performed at the VCU - Dept. of Anatomy & Neurobiology Microscopy Facility, supported, in part, by funding from NIH-NINDS Center Core Grant 5 P30 NS047463 and, in part, by funding form NIH-NCI Cancer Center Support Grant P30 CA016059.

References

1. Doulatov, S., Notta, F., Laurenti, E. & Dick, J. E. Hematopoiesis: a human perspective. *Cell Stem Cell* **10,** 120–136 (2012).
2. Borghesi, L. Hematopoiesis in steady-state versus stress: self-renewal, lineage fate choice, and the conversion of danger signals into cytokine signals in hematopoietic stem cells. *J. Immunol. Baltim. Md 1950* **193,** 2053–2058 (2014).
3. Notta, F. *et al.* Isolation of single human hematopoietic stem cells capable of long-term multilineage engraftment. *Science* **333,** 218–221 (2011).
4. Byrd, J. C. *et al.* Pretreatment cytogenetic abnormalities are predictive of induction success, cumulative incidence of relapse, and overall survival in adult patients with de novo acute myeloid leukemia: results from Cancer and Leukemia Group B (CALGB 8461). *Blood* **100,** 4325–4336 (2002).
5. Cancer Genome Atlas Research Network. Genomic and epigenomic landscapes of adult de novo acute myeloid leukemia. *N. Engl. J. Med.* **368,** 2059–2074 (2013).
6. Tefferi, A. & Letendre, L. Going beyond 7 + 3 regimens in the treatment of adult acute myeloid leukemia. *J. Clin. Oncol. Off. J. Am. Soc. Clin. Oncol.* **30,** 2425–2428 (2012).
7. Löwenberg, B. *et al.* High-dose daunorubicin in older patients with acute myeloid leukemia. *N. Engl. J. Med.* **361,** 1235–1248 (2009).
8. Fernandez, H. F. *et al.* Anthracycline dose intensification in acute myeloid leukemia. *N. Engl. J. Med.* **361,** 1249–1259 (2009).
9. Volkova, M. & Russell, R. Anthracycline Cardiotoxicity: Prevalence, Pathogenesis and Treatment. *Curr. Cardiol. Rev.* **7,** 214–220 (2011).

10. Cassileth, P. A. *et al.* Maintenance chemotherapy prolongs remission duration in adult acute nonlymphocytic leukemia. *J. Clin. Oncol. Off. J. Am. Soc. Clin. Oncol.* **6,** 583–587 (1988).
11. Thol, F., Schlenk, R. F., Heuser, M. & Ganser, A. How I treat refractory and early relapsed acute myeloid leukemia. *Blood* **126,** 319–327 (2015).
12. Döhner, H. *et al.* Diagnosis and management of acute myeloid leukemia in adults: recommendations from an international expert panel, on behalf of the European LeukemiaNet. *Blood* **115,** 453–474 (2010).
13. Herzig, R. H., Lazarus, H. M., Wolff, S. N., Phillips, G. L. & Herzig, G. P. High-dose cytosine arabinoside therapy with and without anthracycline antibiotics for remission reinduction of acute nonlymphoblastic leukemia. *J. Clin. Oncol. Off. J. Am. Soc. Clin. Oncol.* **3,** 992–997 (1985).
14. Reese, N. D. & Schiller, G. J. High-dose cytarabine (HD araC) in the treatment of leukemias: a review. *Curr. Hematol. Malig. Rep.* **8,** 141–148 (2013).
15. Minotti, G., Menna, P., Salvatorelli, E., Cairo, G. & Gianni, L. Anthracyclines: Molecular Advances and Pharmacologic Developments in Antitumor Activity and Cardiotoxicity. *Pharmacol. Rev.* **56,** 185–229 (2004).
16. Xie, C. *et al.* Mechanisms of Synergistic Antileukemic Interactions between Valproic Acid and Cytarabine in Pediatric Acute Myeloid Leukemia. *Clin. Cancer Res.* **16,** 5499–5510 (2010).
17. Galmarini, C. M., Mackey, J. R. & Dumontet, C. Nucleoside analogues: mechanisms of drug resistance and reversal strategies. *Leukemia* **15,** 875–890 (2001).

18. Jekimovs, C. *et al.* Chemotherapeutic compounds targeting the DNA double-strand break repair pathways: the good, the bad, and the promising. *Front. Oncol.* **4,** 86 (2014).
19. Probst, A. V., Dunleavy, E. & Almouzni, G. Epigenetic inheritance during the cell cycle. *Nat. Rev. Mol. Cell Biol.* **10,** 192–206 (2009).
20. Herman, J. G. & Baylin, S. B. Gene silencing in cancer in association with promoter hypermethylation. *N. Engl. J. Med.* **349,** 2042–2054 (2003).
21. Dawson, M. A., Kouzarides, T. & Huntly, B. J. P. Targeting Epigenetic Readers in Cancer. *N. Engl. J. Med.* **367,** 647–657 (2012).
22. Li, B., Carey, M. & Workman, J. L. The Role of Chromatin during Transcription. *Cell* **128,** 707–719 (2007).
23. Stanley, F. K. T., Moore, S. & Goodarzi, A. A. CHD chromatin remodelling enzymes and the DNA damage response. *Mutat. Res.* **750,** 31–44 (2013).
24. O'Shaughnessy, A. & Hendrich, B. CHD4 in the DNA-damage response and cell cycle progression: not so NuRDy now. *Biochem. Soc. Trans.* **41,** 777–782 (2013).
25. Murga, M. *et al.* Global chromatin compaction limits the strength of the DNA damage response. *J. Cell Biol.* **178,** 1101–1108 (2007).
26. Price, B. D. & D'Andrea, A. D. Chromatin Remodeling at DNA Double-Strand Breaks. *Cell* **152,** 1344–1354 (2013).
27. Margueron, R. & Reinberg, D. Chromatin structure and the inheritance of epigenetic information. *Nat. Rev. Genet.* **11,** 285–296 (2010).
28. Luger, K., Dechassa, M. L. & Tremethick, D. J. New insights into nucleosome and chromatin structure: an ordered state or a disordered affair? *Nat. Rev. Mol. Cell Biol.* **13,** 436–447 (2012).

29. Jiang, C. & Pugh, B. F. Nucleosome positioning and gene regulation: advances through genomics. *Nat. Rev. Genet.* **10,** 161–172 (2009).
30. Voss, T. C. & Hager, G. L. Dynamic regulation of transcriptional states by chromatin and transcription factors. *Nat. Rev. Genet.* **15,** 69–81 (2014).
31. Breiling, A. & Lyko, F. Epigenetic regulatory functions of DNA modifications: 5-methylcytosine and beyond. *Epigenetics Chromatin* **8,** 24 (2015).
32. Takai, D. & Jones, P. A. Comprehensive analysis of CpG islands in human chromosomes 21 and 22. *Proc. Natl. Acad. Sci.* **99,** 3740–3745 (2002).
33. Svedruzić, Z. M. & Reich, N. O. The mechanism of target base attack in DNA cytosine carbon 5 methylation. *Biochemistry (Mosc.)* **43,** 11460–11473 (2004).
34. Singal, R. & Ginder, G. D. DNA methylation. *Blood* **93,** 4059–4070 (1999).
35. McCabe, M. T., Brandes, J. C. & Vertino, P. M. Cancer DNA methylation: molecular mechanisms and clinical implications. *Clin. Cancer Res. Off. J. Am. Assoc. Cancer Res.* **15,** 3927–3937 (2009).
36. Strahl, B. D. & Allis, C. D. The language of covalent histone modifications. *Nature* **403,** 41–45 (2000).
37. Bannister, A. J. & Kouzarides, T. Regulation of chromatin by histone modifications. *Cell Res.* **21,** 381–395 (2011).
38. Allfrey, V. G., Faulkner, R. & Mirsky, A. E. ACETYLATION AND METHYLATION OF HISTONES AND THEIR POSSIBLE ROLE IN THE REGULATION OF RNA SYNTHESIS. *Proc. Natl. Acad. Sci. U. S. A.* **51,** 786–794 (1964).
39. Virani, S., Colacino, J. A., Kim, J. H. & Rozek, L. S. Cancer Epigenetics: A Brief Review. *ILAR J.* **53,** 359–369 (2012).

40. Feinberg, A. P. & Vogelstein, B. Hypomethylation distinguishes genes of some human cancers from their normal counterparts. *Nature* **301,** 89–92 (1983).
41. Fraga, M. F. *et al.* A mouse skin multistage carcinogenesis model reflects the aberrant DNA methylation patterns of human tumors. *Cancer Res.* **64,** 5527–5534 (2004).
42. Esteller, M. Epigenetics in Cancer. *N. Engl. J. Med.* **358,** 1148–1159 (2008).
43. Fraga, M. F. *et al.* Loss of acetylation at Lys16 and trimethylation at Lys20 of histone H4 is a common hallmark of human cancer. *Nat. Genet.* **37,** 391–400 (2005).
44. Krusche, C. A. *et al.* Histone deacetylase-1 and -3 protein expression in human breast cancer: a tissue microarray analysis. *Breast Cancer Res. Treat.* **90,** 15–23 (2005).
45. Weichert, W. *et al.* Class I histone deacetylase expression has independent prognostic impact in human colorectal cancer: specific role of class I histone deacetylases in vitro and in vivo. *Clin. Cancer Res. Off. J. Am. Assoc. Cancer Res.* **14,** 1669–1677 (2008).
46. Fritzsche, F. R. *et al.* Class I histone deacetylases 1, 2 and 3 are highly expressed in renal cell cancer. *BMC Cancer* **8,** 381 (2008).
47. Singal, R., Wang, S. Z., Sargent, T., Zhu, S. Z. & Ginder, G. D. Methylation of promoter proximal-transcribed sequences of an embryonic globin gene inhibits transcription in primary erythroid cells and promotes formation of a cell type-specific methyl cytosine binding complex. *J. Biol. Chem.* **277,** 1897–1905 (2002).
48. Lai, A. Y. & Wade, P. A. Cancer biology and NuRD: a multifaceted chromatin remodelling complex. *Nat. Rev. Cancer* **11,** 588–596 (2011).
49. Mian, O. Y. *et al.* Methyl-binding domain protein 2-dependent proliferation and survival of breast cancer cells. *Mol. Cancer Res. MCR* **9,** 1152–1162 (2011).

50. Wade, P. A. Methyl CpG-binding proteins and transcriptional repression. *BioEssays News Rev. Mol. Cell. Dev. Biol.* **23,** 1131–1137 (2001).

51. Bird, A. P. & Wolffe, A. P. Methylation-induced repression--belts, braces, and chromatin. *Cell* **99,** 451–454 (1999).

52. Sansom, O. J., Maddison, K. & Clarke, A. R. Mechanisms of disease: methyl-binding domain proteins as potential therapeutic targets in cancer. *Nat. Clin. Pract. Oncol.* **4,** 305–315 (2007).

53. Ballestar, E. *et al.* Methyl-CpG binding proteins identify novel sites of epigenetic inactivation in human cancer. *EMBO J.* **22,** 6335–6345 (2003).

54. Chatagnon, A. *et al.* Preferential binding of the methyl-CpG binding domain protein 2 at methylated transcriptional start site regions. *Epigenetics* **6,** 1295–1307 (2011).

55. Fraga, M. F. *et al.* The affinity of different MBD proteins for a specific methylated locus depends on their intrinsic binding properties. *Nucleic Acids Res.* **31,** 1765–1774 (2003).

56. Polo, S. E., Kaidi, A., Baskcomb, L., Galanty, Y. & Jackson, S. P. Regulation of DNA-damage responses and cell-cycle progression by the chromatin remodelling factor CHD4. *EMBO J.* **29,** 3130–3139 (2010).

57. Larsen, D. H. *et al.* The chromatin-remodeling factor CHD4 coordinates signaling and repair after DNA damage. *J. Cell Biol.* **190,** 731–740 (2010).

58. Luijsterburg, M. S. *et al.* A new non-catalytic role for ubiquitin ligase RNF8 in unfolding higher-order chromatin structure. *EMBO J.* **31,** 2511–2527 (2012).

59. Klement, K. *et al.* Opposing ISWI- and CHD-class chromatin remodeling activities orchestrate heterochromatic DNA repair. *J. Cell Biol.* **207,** 717–733 (2014).

60. Fujita, N. *et al.* MTA3 and the Mi-2/NuRD complex regulate cell fate during B lymphocyte differentiation. *Cell* **119,** 75–86 (2004).

61. Guschin, D., Wade, P. A., Kikyo, N. & Wolffe, A. P. ATP-Dependent histone octamer mobilization and histone deacetylation mediated by the Mi-2 chromatin remodeling complex. *Biochemistry (Mosc.)* **39,** 5238–5245 (2000).

62. Ramírez, J., Dege, C., Kutateladze, T. G. & Hagman, J. MBD2 and Multiple Domains of CHD4 Are Required for Transcriptional Repression by Mi-2/NuRD Complexes. *Mol. Cell. Biol.* **32,** 5078–5088 (2012).

63. Hayakawa, T. & Nakayama, J.-I. Physiological roles of class I HDAC complex and histone demethylase. *J. Biomed. Biotechnol.* **2011,** 129383 (2011).

64. Cai, Y. *et al.* The NuRD complex cooperates with DNMTs to maintain silencing of key colorectal tumor suppressor genes. *Oncogene* **33,** 2157–2168 (2014).

65. Sansom, O. J. *et al.* Deficiency of Mbd2 suppresses intestinal tumorigenesis. *Nat. Genet.* **34,** 145–147 (2003).

66. Lopez-Serra, L. *et al.* Unmasking of epigenetically silenced candidate tumor suppressor genes by removal of methyl-CpG-binding domain proteins. *Oncogene* **27,** 3556–3566 (2008).

67. Amaya, M. *et al.* Mi2β-mediated silencing of the fetal γ-globin gene in adult erythroid cells. *Blood* **121,** 3493–3501 (2013).

68. Rupon, J. W., Wang, S. Z., Gaensler, K., Lloyd, J. & Ginder, G. D. Methyl binding domain protein 2 mediates γ-globin gene silencing in adult human βYAC transgenic mice. *Proc. Natl. Acad. Sci. U. S. A.* **103,** 6617–6622 (2006).

69. Gnanapragasam, M. N. *et al.* p66Alpha-MBD2 coiled-coil interaction and recruitment of Mi-2 are critical for globin gene silencing by the MBD2-NuRD complex. *Proc. Natl. Acad. Sci. U. S. A.* **108,** 7487–7492 (2011).

70. Tong, J. K., Hassig, C. A., Schnitzler, G. R., Kingston, R. E. & Schreiber, S. L. Chromatin deacetylation by an ATP-dependent nucleosome remodelling complex. *Nature* **395,** 917–921 (1998).

71. Wade, P. A., Jones, P. L., Vermaak, D. & Wolffe, A. P. A multiple subunit Mi-2 histone deacetylase from Xenopus laevis cofractionates with an associated Snf2 superfamily ATPase. *Curr. Biol. CB* **8,** 843–846 (1998).

72. Xue, Y. *et al.* NURD, a novel complex with both ATP-dependent chromatin-remodeling and histone deacetylase activities. *Mol. Cell* **2,** 851–861 (1998).

73. Zhang, Y., LeRoy, G., Seelig, H. P., Lane, W. S. & Reinberg, D. The dermatomyositis-specific autoantigen Mi2 is a component of a complex containing histone deacetylase and nucleosome remodeling activities. *Cell* **95,** 279–289 (1998).

74. Wang, H. B. & Zhang, Y. Mi2, an auto-antigen for dermatomyositis, is an ATP-dependent nucleosome remodeling factor. *Nucleic Acids Res.* **29,** 2517–2521 (2001).

75. Mansfield, R. E. *et al.* Plant homeodomain (PHD) fingers of CHD4 are histone H3-binding modules with preference for unmodified H3K4 and methylated H3K9. *J. Biol. Chem.* **286,** 11779–11791 (2011).

76. Musselman, C. A. *et al.* Bivalent recognition of nucleosomes by the tandem PHD fingers of the CHD4 ATPase is required for CHD4-mediated repression. *Proc. Natl. Acad. Sci. U. S. A.* **109,** 787–792 (2012).

77. Allen, H. F., Wade, P. A. & Kutateladze, T. G. The NuRD architecture. *Cell. Mol. Life Sci. CMLS* **70,** 3513–3524 (2013).

78. Watson, A. A. *et al.* The PHD and Chromo Domains Regulate the ATPase Activity of the Human Chromatin Remodeler CHD4. *J. Mol. Biol.* **422,** 3–17 (2012).

79. Williams, C. J. *et al.* The chromatin remodeler Mi-2beta is required for CD4 expression and T cell development. *Immunity* **20,** 719–733 (2004).

80. Reynolds, N., O'Shaughnessy, A. & Hendrich, B. Transcriptional repressors: multifaceted regulators of gene expression. *Dev. Camb. Engl.* **140,** 505–512 (2013).

81. Smeenk, G. *et al.* The NuRD chromatin-remodeling complex regulates signaling and repair of DNA damage. *J. Cell Biol.* **190,** 741–749 (2010).

82. Urquhart, A. J., Gatei, M., Richard, D. J. & Khanna, K. K. ATM mediated phosphorylation of CHD4 contributes to genome maintenance. *Genome Integr.* **2,** 1 (2011).

83. Pan, M.-R. *et al.* Chromodomain helicase DNA-binding protein 4 (CHD4) regulates homologous recombination DNA repair, and its deficiency sensitizes cells to poly(ADP-ribose) polymerase (PARP) inhibitor treatment. *J. Biol. Chem.* **287,** 6764–6772 (2012).

84. Sims, J. K. & Wade, P. A. Mi-2/NuRD complex function is required for normal S phase progression and assembly of pericentric heterochromatin. *Mol. Biol. Cell* **22,** 3094–3102 (2011).

85. Chudnovsky, Y. *et al.* ZFHX4 interacts with the NuRD core member CHD4 and regulates the glioblastoma tumor-initiating cell state. *Cell Rep.* **6,** 313–324 (2014).

86. Nio, K. *et al.* Defeating EpCAM(+) liver cancer stem cells by targeting chromatin remodeling enzyme CHD4 in human hepatocellular carcinoma. *J. Hepatol.* (2015). doi:10.1016/j.jhep.2015.06.009

87. Than Htun, M. Photophysical study on daunorubicin by fluorescence spectroscopy. *J. Lumin.* **129,** 344–348 (2009).

88. Zuber, J. *et al.* Mouse models of human AML accurately predict chemotherapy response. *Genes Dev.* **23,** 877–889 (2009).

89. Wunderlich, M. *et al.* AML cells are differentially sensitive to chemotherapy treatment in a human xenograft model. *Blood* **121,** e90–97 (2013).

90. Derheimer, F. A. & Kastan, M. B. Multiple roles of ATM in monitoring and maintaining DNA integrity. *FEBS Lett.* **584,** 3675–3681 (2010).

91. Kaidi, A. & Jackson, S. P. KAT5 tyrosine phosphorylation couples chromatin sensing to ATM signalling. *Nature* **498,** 70–74 (2013).

92. Shiloh, Y. & Ziv, Y. The ATM protein kinase: regulating the cellular response to genotoxic stress, and more. *Nat. Rev. Mol. Cell Biol.* **14,** 197–210 (2013).

93. Biswas, A. K. & Johnson, D. G. Transcriptional and nontranscriptional functions of E2F1 in response to DNA damage. *Cancer Res.* **72,** 13–17 (2012).

94. Zannini, L., Delia, D. & Buscemi, G. CHK2 kinase in the DNA damage response and beyond. *J. Mol. Cell Biol.* **6,** 442–457 (2014).

95. Schwarz, J. K., Lovly, C. M. & Piwnica-Worms, H. Regulation of the Chk2 protein kinase by oligomerization-mediated cis- and trans-phosphorylation. *Mol. Cancer Res. MCR* **1,** 598–609 (2003).

96. Zhang, P., Gao, W., Li, H., Reed, E. & Chen, F. Inducible degradation of checkpoint kinase 2 links to cisplatin-induced resistance in ovarian cancer cells. *Biochem. Biophys. Res. Commun.* **328,** 567–572 (2005).

97. Kass, E. M. *et al.* Stability of checkpoint kinase 2 is regulated via phosphorylation at serine 456. *J. Biol. Chem.* **282,** 30311–30321 (2007).

98. Pegoraro, G. *et al.* Ageing-related chromatin defects through loss of the NURD complex. *Nat. Cell Biol.* **11,** 1261–1267 (2009).

99. Falk, M., Lukasova, E., Gabrielova, B., Ondrej, V. & Kozubek, S. Chromatin dynamics during DSB repair. *Biochim. Biophys. Acta BBA - Mol. Cell Res.* **1773,** 1534–1545 (2007).

100. Nackerdien, Z., Michie, J. & Böhm, L. Chromatin decondensed by acetylation shows an elevated radiation response. *Radiat. Res.* **117,** 234–244 (1989).

101. Fritzsche, H. *et al.* Anthracycline antibiotics. Interaction with DNA and nucleosomes and inhibition of DNA synthesis. *Biochemistry (Mosc.)* **26,** 1996–2000 (1987).

102. Guillemette, S. *et al.* Resistance to therapy in BRCA2 mutant cells due to loss of the nucleosome remodeling factor CHD4. *Genes Dev.* **29,** 489–494 (2015).

103. Pang, B. *et al.* Drug-induced histone eviction from open chromatin contributes to the chemotherapeutic effects of doxorubicin. *Nat. Commun.* **4,** 1908 (2013).

104. Dick, J. E. Stem cell concepts renew cancer research. *Blood* **112,** 4793–4807 (2008).

105. Pan, X.-N. *et al.* Inhibition of c-Myc overcomes cytotoxic drug resistance in acute myeloid leukemia cells by promoting differentiation. *PloS One* **9,** e105381 (2014).

106. Kajiume, T., Ninomiya, Y., Ishihara, H., Kanno, R. & Kanno, M. Polycomb group gene mel-18 modulates the self-renewal activity and cell cycle status of hematopoietic stem cells. *Exp. Hematol.* **32,** 571–578 (2004).

107. Guo, W.-J. *et al.* Mel-18 Acts as a Tumor Suppressor by Repressing Bmi-1 Expression and Down-regulating Akt Activity in Breast Cancer Cells. *Cancer Res.* **67,** 5083–5089 (2007).

108. Er, T.-K. *et al.* Antioxidant status and superoxide anion radical generation in acute myeloid leukemia. *Clin. Biochem.* **40,** 1015–1019 (2007).

109. Cook, A. M. *et al.* Role of altered growth factor receptor-mediated JAK2 signaling in growth and maintenance of human acute myeloid leukemia stem cells. *Blood* **123,** 2826–2837 (2014).

110. Laranjeira, P. *et al.* Expression of CD44 and CD35 during normal and myelodysplastic erythropoiesis. *Leuk. Res.* **39,** 361–370 (2015).

111. Steidl, U. *et al.* A distal single nucleotide polymorphism alters long-range regulation of the PU.1 gene in acute myeloid leukemia. *J. Clin. Invest.* **117,** 2611–2620 (2007).

112. Weidenaar, A. C. *et al.* High acute myeloid leukemia derived VEGFA levels are associated with a specific vascular morphology in the leukemic bone marrow. *Cell. Oncol. Dordr.* **34,** 289–296 (2011).

113. Dawson, M. J. & Trapani, J. A. IFI 16 gene encodes a nuclear protein whose expression is induced by interferons in human myeloid leukaemia cell lines. *J. Cell. Biochem.* **57,** 39–51 (1995).

114. Siva, K. *et al.* SPARC is dispensable for murine hematopoiesis, despite its suspected pathophysiological role in 5q-myelodysplastic syndrome. *Leukemia* **26,** 2416–2419 (2012).

115. Reynolds, N. *et al.* NuRD suppresses pluripotency gene expression to promote transcriptional heterogeneity and lineage commitment. *Cell Stem Cell* **10,** 583–594 (2012).

116. Zhu, D., Fang, J., Li, Y. & Zhang, J. Mbd3, a Component of NuRD/Mi-2 Complex, Helps Maintain Pluripotency of Mouse Embryonic Stem Cells by Repressing Trophectoderm Differentiation. *PLoS ONE* **4,** e7684 (2009).

117. Yoshida, T. *et al.* The role of the chromatin remodeler Mi-2beta in hematopoietic stem cell self-renewal and multilineage differentiation. *Genes Dev.* **22,** 1174–1189 (2008).

118. Santos, M. A. *et al.* DNA-damage-induced differentiation of leukaemic cells as an anti-cancer barrier. *Nature* **514,** 107–111 (2014).

119. Morra, R., Lee, B. M., Shaw, H., Tuma, R. & Mancini, E. J. Concerted action of the PHD, chromo and motor domains regulates the human chromatin remodelling ATPase CHD4. *FEBS Lett.* **586,** 2513–2521 (2012).

120. Takayama, K. *et al.* Enhanced intracellular delivery using arginine-rich peptides by the addition of penetration accelerating sequences (Pas). *J. Control. Release Off. J. Control. Release Soc.* **138,** 128–133 (2009).

121. Cerchietti, L. C. *et al.* A peptomimetic inhibitor of BCL6 with potent antilymphoma effects in vitro and in vivo. *Blood* **113,** 3397–3405 (2009).

122. Bose, P. & Grant, S. Rational Combinations of Targeted Agents in AML. *J. Clin. Med.* **4,** 634–664 (2015).

123. Palmieri, D. *et al.* Vorinostat inhibits brain metastatic colonization in a model of triple-negative breast cancer and induces DNA double-strand breaks. *Clin. Cancer Res. Off. J. Am. Assoc. Cancer Res.* **15,** 6148–6157 (2009).

124. Santoro, F. *et al.* A dual role for Hdac1: oncosuppressor in tumorigenesis, oncogene in tumor maintenance. *Blood* **121,** 3459–3468 (2013).

125. Simon, C. *et al.* A key role for EZH2 and associated genes in mouse and human adult T-cell acute leukemia. *Genes Dev.* **26,** 651–656 (2012).

126. Karanikolas, B. D. W., Figueiredo, M. L. & Wu, L. Polycomb Group Protein EZH2 is an Oncogene that Promotes the Neoplastic Transformation of a Benign Prostatic Epithelial Cell Line. *Mol. Cancer Res. MCR* **7,** 1456–1465 (2009).

127. Shi, J. *et al.* Discovery of cancer drug targets by CRISPR-Cas9 screening of protein domains. *Nat. Biotechnol.* **33,** 661–667 (2015).

128. Rahmani, M. *et al.* Dual inhibition of Bcl-2 and Bcl-xL strikingly enhances PI3K inhibition-induced apoptosis in human myeloid leukemia cells through a GSK3- and Bim-dependent mechanism. *Cancer Res.* **73,** 1340–1351 (2013).

129. Li, Y. *et al.* 60-kDa Tat-interactive Protein (TIP60) Positively Regulates Th-inducing POK (ThPOK)-mediated Repression of Eomesodermin in Human CD4+ T Cells. *J. Biol. Chem.* **288,** 15537–15546 (2013).

130. Rahmani, M., Dai, Y. & Grant, S. The histone deacetylase inhibitor sodium butyrate interacts synergistically with phorbol myristate acetate (PMA) to induce mitochondrial damage and apoptosis in human myeloid leukemia cells through a tumor necrosis factor-alpha-mediated process. *Exp. Cell Res.* **277,** 31–47 (2002).

131. Rahmani, M., Davis, E. M., Bauer, C., Dent, P. & Grant, S. Apoptosis induced by the kinase inhibitor BAY 43-9006 in human leukemia cells involves down-regulation of Mcl-1 through inhibition of translation. *J. Biol. Chem.* **280,** 35217–35227 (2005).

132. Golding, S. E. *et al.* Extracellular signal-related kinase positively regulates ataxia telangiectasia mutated, homologous recombination repair, and the DNA damage response. *Cancer Res.* **67,** 1046–1053 (2007).

133. Końca, K. *et al.* A cross-platform public domain PC image-analysis program for the comet assay. *Mutat. Res.* **534,** 15–20 (2003).

134. Irizarry, R. A. *et al.* Summaries of Affymetrix GeneChip probe level data. *Nucleic Acids Res.* **31,** e15 (2003).

135. Smyth, G. K. Linear models and empirical bayes methods for assessing differential expression in microarray experiments. *Stat. Appl. Genet. Mol. Biol.* **3,** Article3 (2004).

136. Gentleman, R. C. *et al.* Bioconductor: open software development for computational biology and bioinformatics. *Genome Biol.* **5,** R80 (2004).

137. Anonymous. R: a language and environment for statistical computing. *GBIF.ORG* (2015). at <http://www.gbif.org/resources/2585>

138. Benjamini, Y. & Hochberg, Y. Controlling the False Discovery Rate: A Practical and Powerful Approach to Multiple Testing. *J. R. Stat. Soc. Ser. B Methodol.* **57,** 289–300 (1995).